Università degli Studi di Padova

Dipartimento di Scienze Biomediche Sperimentali

SCUOLA DI DOTTORATO DI RICERCA IN : BIOSCIENZE e BIOTECNOLOGIE

INDIRIZZO: BIOLOGIA CELLULARE

CICLO: XXIII

Drosophila *Marf is the evolutionary ancestor of mammalian Mfn2: a phylogenetic analysis*

Direttore della Scuola : Ch.mo Prof. Giuseppe Zanotti

Coordinatore d'indirizzo: Ch.mo Prof. Cesare Montecucco

Supervisore :Ch.mo Prof. Luca Scorrano

Dottorando : Valentina Debattisti

SOMMARIO

1. Riassunto dell'attività svolta

I mitocondri sono organelli essenziali per l'omeostasi cellulare. La loro funzione primaria è di produrre energia : la respirazione mitocondriale fornisce la maggior parte di ATP necessaria per le reazioni endoergoniche. Inoltre, essi regolano i livelli e i transienti di calcio citosolico e hanno un ruolo cruciale nei processi di apoptosi, invecchiamento e stress ossidativo (Jouaville et al., 1995; Wang, 2001). Il 20% della superficie mitocondriale è in stretto contatto con il reticolo endoplasmico (RE). Questa disposizione è importante per la generazione di microdomini ad alta concentrazione di calcio necessari in certe condizioni per l'attivazione dell'uniporto mitocondriale del Ca^{2+}. I siti di stretto contatto tra il RE e i mitocondri formano le cosiddette "membrane associate ai mitocondri" (MAMs), che sono cruciali per il trasporto di lipidi e Ca^{2+} tra i due organelli e hanno un ruolo anche nel processo di morte cellulare (Rizzuto et al., 1998). Sebbene i meccanismi molecolari alla base di questa stretta vicinanza tra il RE e i mitocondri siano in larga parte ignoti, si ritiene che tale interazione possa essere regolata da cambiamenti morfologici dei due organelli (Pitt set al., 1999; Simmen et al., 2005).
La forma del reticolo mitocondriale è determinata dall'equilibrio tra eventi di fusione e fissione, controllati da una famiglia di "proteine di morfologia mitocondriale". In cellule di mammifero, la fusione mitocondriale è controllata dalle proteine mitofusina-1 (MFN1) e mitofusina-2 (MFN2) nella membrana esterna e da OPA1 nella membrana mitocondriale interna (Olichon et al., 2002). Nel nostro laboratorio è stato dimostrato che OPA1 promuove la fusione dei mitocondri solo in presenza di mitofusina 1 (Cipolat et al., 2004). La fissione richiede il passaggio aggiuntivo della traslocazione della proteina Drp1 dal citosol ai mitocondri, dove si ancora a hFis1, il suo adattatore molecolare nella OMM. L'oligomerizzazione di Drp1 fornisce la forza meccanica per costringere le membrane mitocondriali fino alla frammentazione dell'organello (Hinshaw et al., 1999; Smirnova et al., 2001). La traslocazione di Drp1 ai mitocondri dipende dalla sua defosforilazione ad opera della fosfatasi calcineurina e di altre fosfatasi (Cereghetti et al., 2008).
Le mitofusine sono GTPasi appartenenti alla famiglia delle dinamine che controllano la fusione e la morfologia dei mitocondri. In passato, la presenza di due mitofusine nei mammmiferi ha sollevato la questione sulla loro divergenza funzionale. Oggi molti

risultati supportano l'idea che Mfn1 e 2 non abbiano funzioni ridondanti. Mfn2 ha ruoli che Mfn1 non esercita, come il controllo dei processi di ossidazione mediati dai mitocondri (Bach et al., 2005) e la funzione anti-proliferativa (Chen et al., 2004). Inoltre, mentre la fusione mitocondriale indotta dalla proteina della membrana interna OPA1 richiede Mfn1, (Cipolat et al., 2004), Mfn2 sembra essere coinvolta nella regolazione della giustapposizione reticolo endoplasmatico (RE)-mitocondri (de Brito e Scorrano, 2008a). MFN2 è stata associata inoltre alla neuropatia di Charcot-Marie-Tooth di tipo IIa (CMTIIa) (Züchner et al., 2004b). Sia Mfn1 e Mfn2 sono essenziali per lo sviluppo embrionale e topi deficienti in entrambi muoiono prematuramente, ma (Chen et al, 2003) embrioni *Mfn2-/-* mostrano anche difetti di placentazione. Tuttavia, l'ablazione post-placentazione di una singola Mfn nel topo porta a due fenotipi completamente diversi: i topi *Mfn1*$^{-/-}$ sono vitali, mentre topi *Mfn2*$^{-/-}$ muoiono tra P1 e P17 come conseguenza della massiccia degenerazione cerebellare (Chen et al. , 2007). Non è chiaro se i diversi fenotipi osservati *in vivo* e *in vitro* possano essere attribuiti a differenze funzionali o semplicemente ai diversi schemi di espressione delle due Mfn. Inoltre, tutti i vertebrati possiedono due Mfn, mentre solo una Mfn viene riscontrata nella maggior parte degli invertebrati, con l'eccezione di *D.melanogaster*.

Il moscerino della frutta possiede due mitofusine, ‘Fuzzy onion’ (Fzo) e Mitochondrial Assembly Regulatory Factor (Marf). Fzo è stato il primo mediatore della fusione mitocondriale individuato (Hales e Fuller, 1997). In spermatociti Fzo media la fusione dei mitocondri in due giganti organelli che formano una struttura chiamata Nebenkern, la quale serve a dare energia al flagello degli spermatidi. Nel mutante di fzo i mitocondri non riescono a fondersi e si avvolgono l'un l'altro come molti organelli frammentati, dando l'impressione di 'cipolle increspate' se osservate al microscopio elettronico. Anche se Fzo è in grado di promuovere l'allungamento mitocondriale, è espresso solo negli spermatidi. Ciò ha sollevato la questione di come la fusione dei mitocondri potesse venire regolata in altri tessuti del moscerino della frutta. Nel 2002 il secondo omologo delle mitofusine Marf è stato identificato in *D.melanogaster* (Hwa et al., 2002). A differenza di Fzo, DMarf è espressa ubiquitariamente e condivide il 64% di omologia con entrambe le mitofusine dei mammiferi. Quindi, Marf può essere considerato la singola mitofusina "funzionale" e *Drosophila melanogaster* è dunque un organismo modello utile per studiare la filogenesi di MFN nei vertebrati superiori. Le domande a cui abbiamo cercato di dare risposta in questa tesi sono le seguenti:

questo organismo modello rappresenta il punto di svolta evolutiva da uno a due mitofusine? Quale Mfn è funzionalmente più vicina a DMarf?

Al fine di rispondere a queste domande, abbiamo innanzitutto cercato di capire in quale estensione DMarf potesse complementare le mitofusine dei mammiferi. Per ottenere una visione più ampia dal punto di vista filogenetico, abbiamo esteso la nostra analisi alle mitofusine 1 e 2 del vertebrato *Xenopus laevis* (XMfn1 e XMfn2) e all'omologo di mitofusina di lievito *S.cerevisae* (Fzo1p). L'espressione di Fzo1p, DMarf, XMfn1 e XMfn2, induce allungamento dei mitocondri in *Mfn1*$^{-/-}$ o *Mfn2*$^{-/-}$ MEF, recuperando il fenotipo di frammentazione causato dalla mancanza delle singole Mfn e indicando che esse possono sostituire entrambe le Mfn.

A differenza di *Mfn1*$^{-/-}$ MEF, *Mfn2*$^{-/-}$ MEF mostrano una morfologia del reticolo endoplasmico alterata (de Brito e Scorrano, 2008b). Questo difetto è recuperato solo dopo l'espressione di hMfn2 o di una variante hMfn2 specificamente localizzata al RE (hMfn2^{YFFT}), indipendentemente dalla forma mitocondriale. Mfn2 infatti è parzialmente localizzata nel RE e si trova arricchita nelle MAMs. Per capire se DMarf potesse complementare Mfn2 anche nella regolazione della morfologia del RE, abbiamo co-trasfettato *Mfn2-/-* MEFs con Dmarf con il tag V5 e una proteina fluorescente gialla localizzata nel RE (ERYFP). DMarf riesce a recuperare la morfologia del RE in *Mfn2-/-*, mostrando quindi una più forte conservazione funzionale con Mfn2.

Abbiamo poi rivolto la nostra attenzione ad un analisi *in vivo* della funzione di DMarf in *Drosophila*. DMarf è essenziale per la vitalità, poichè il silenziamento ubiquitario o specificatamente a carico del sistema nervoso o del tessuto muscolare della proteina è letale. In larve DMarf-RNAi i mitocondri si aggregano nelle regioni perinucleari dei corpi cellulari neuronali e dei tessuti muscolari. Inoltre, giunzioni neuromuscolari degli individui DMarf-RNAi risultano gravemente depauperati dei mitocondri rispetto alle larve di controllo. Dato che mitofusina-2 regola la morfologia del reticolo endoplasmico e il suo avvicinamento ai mitocondri, abbiamo studiato l'effetto del silenziamento di Dmarf sull'architettura del RE, la quale è risultata essere seriamente compromessa nei tessuti muscolari mostrando perdita dell'organizzazione del RE lungo i sarcomeri in seguito al silenziamento della proteina.

Per studiare l'effetto della sovraespressione di hMfn in *Drosophila*, abbiamo caratterizzato le linee transgeniche esprimenti hMfn1, hMfn2 e hMfn2R94Q, una delle mutazioni più frequenti associate al CMT2A (Züchner et al., 2004a).

Aggregazione dei mitocondri in corpi cellulari neuronali e nel muscolo e organelli di forma allungata o aggregati all'interno di assoni sono stati osservati in seguito a sovraespressione di tutte le hMfns. Tuttavia, l'analisi delle giunzioni neuromuscolari ha rivelato una grande differenza tra le espressioni hMfn1, hMfn2 e hMfn2R94Q: mentre le giunzioni di individui sovraesprimenti hMfn2 e hMfn2R94Q erano depauperate dei mitocondri, l'espressione di hMfn1 non ha modificato la distribuzione degli organelli nel sistema nervoso e mitocondri erano mantenuti all'interno delle giunzioni. L'organizzazione del RE nel muscolo non è stata influenzata dall'espressione di hMfns wild-type; la morfologia del RE è invece alterata in tessuti muscolari di individui esprimenti hMfn2R94Q, mettendo in luce un aspetto non ancora indagato nello studio della patogenesi di Charcot-Marie-Tooth e suggerendo l'alterazione della morfologia del RE come uno dei plausibili fattori che possono contribuire alla patogenesi della malattia.

Dato che DMarf è stato in grado di complementare sia entrambe le Mfn nella morfologia mitocondriale e sia Mfn2 nella regolazione della morfologia del RE, abbiamo cercato di capire in che misura hMfn1 e -2 potessero complementare DMarf in *Drosophila*. L'espressione simultanea dei transgeni MFN2 e *DMarf*-RNAi nel sistema nervoso o nel tessuto muscolare provocano parziale sopravvivenza fino all'età adulta, mentre Mfn1 o Mfn2R94Q non sono riusciti a recuperare il fenotipo letale del DMarf-RNAi. Tuttavia, gli aggregati mitocondriali erano ancora presenti nei corpi delle cellule neuronali e nei tessuti muscolari e le giunzioni neuromuscolari di individui esprimenti contemporaneamente DMarf-RNAi e hMfn2 prive di mitocondri. Quindi, anche se MFN2 recupera la letalità dovuta al silenziamento di DMarf, questo non può essere attribuito a un recupero della morfologia e della distribuzione mitocondriale. Abbiamo quindi valutato il recupero dell'organizzazione del RE in individui esprimenti simultaneamente Dmarf-RNAi e hMfn. HMfn1 non ha avuto alcun effetto sull' alterazione del RE causata da Dmarf-RNAi. Al contrario, hMfn2 espressione ha recuperato l'architettura del RE nel muscolo sia quando espressa ubiquitariamente o solo nel tessuto muscolare.

In conclusione, in questa tesi abbiamo dimostrato che l' espressione di Fzo1p, DMarf, XMfn1 e XMfn2 è in grado di recuperare la morfologia mitocondriale in *Mfn1* $^{-/-}$ e *Mfn2* $^{-/-}$ MEF. Inoltre DMarf complementa specificamente la morfologia del RE in *Mfn2* $^{-/-}$ MEF. Quindi, il ruolo delle mitofusine nella regolazione della dinamica mitocondriale è conservato tra vertebrati e invertebrati. Tuttavia, esperimenti *in vivo*

dimostrano che Mfn2, ma non Mfn1 recupera il fenotipo letale dovuto al silenziamento di DMarf in *Drosophila melanogaster*. Il recupero di DMarf-RNAi da parte di hMfn2 sembra correlare con la correzione dell' organizzazione del RE, mentre la morfologia mitocondriale e la distribuzione non sono vengono ripristinati. Possiamo quindi ipotizzare che Marf sia funzionalmente più vicina ai Mfn2 rispetto a Mfn1, la quale potrebbe essere comparsa più tardi nel corso dell'evoluzione dei mammiferi. Infine, altri fattori,oltre l'alterazione della morfologia e distribuzione mitocondriale nel sistema nervoso potrebbero spiegare la letalità causata dal silenziamento di DMarf e essere quindi coinvolti nella patogenesi della CMT2A.

2. Summary

Mitochondria are essential organelles for cellular homeostasis. Their main function is to produce energy: mitochondrial respiration provides most of the ATP required for endoergonic reactions. Furthermore, they regulate levels and transients of cytosolic Ca^{2+} and are crucially involved in apoptosis, aging and oxidative stress (Dimmer and Scorrano, 2006). As much as 20% of the mitochondrial surface is in close contact with the endoplasmic reticulum (ER). This organization is important for the generation of high Ca^{2+} microdomains required to activate mitochondrial Ca^{2+} uptake under certain conditions (Rizzuto et al., 1998a). The sites where ER and mitochondria are juxtaposed form the so called mitochondria-associated membranes (MAMs), crucial for lipid and Ca^{2+} traffic between the two organelles and are also involved in cell death (de Brito and Scorrano, 2010). Molecular mechanisms responsible for this ER-mitochondria juxtaposition are largely unknown, but it is thought that structural changes of either organelle could regulate the interaction (Pitts et al., 1999; Simmen et al., 2005).

The shape of mitochondria is determined by the equilibrium between fusion and fission processes, controlled by a family of “mitochondria-shaping proteins”. In mammalian cells, mitochondrial fusion depends on mitofusin 1 and 2 (Mfn1 and 2) in the outer mitochondrial membrane and on the inner membrane protein optic atrophy 1 (Opa1) (Liesa et al., 2009). Fission requires the additional step of translocation of dynamin-related protein 1 (Drp1) from the cytosol to mitochondria where it presumably docks on the protein fission-1 (hFis1), its adaptor in the outer membrane. Oligomerization of Drp1 is believed to provide the mechanical force to constrict mitochondrial membranes and to fragment the organelle (Hinshaw, 1999b; Smirnova et al., 2001). Translocation of Drp1 to mitochondria depends on its dephosphorylation by calcineurin and other phosphatases (Cereghetti et al., 2008).

Mitofusins are dynamin-related GTPases which control mitochondrial fusion and morphology. In the past, the presence of two mammalian mitofusins raised the question of their functional divergence. Nowadays many findings support the idea that Mfn1 and 2 do not display redundant functions. Mfn2 has roles which are not shared by Mfn1, such as the control of mitochondrial oxidation (Bach et al., 2005b) and anti-proliferative function (Chen et al., 2004a). Moreover, while mitochondrial fusion mediated by the inner mitochondrial membrane GTPase OPA1 requires Mfn1

(Cipolat et al., 2004b), Mfn2 appears to be involved in the regulation of endoplasmic reticulum (ER)-mitochondria tethering (de Brito and Scorrano, 2008a). MFN2 has also been involved in several diseases including the peripheral Charcot-Marie-Tooth type IIa (CMTIIa) neuropathy (Zuchner et al., 2004a). Both Mfn1 and Mfn2 are essential for embryonic development and mice deficient in either gene die in mid-gestation, but *Mfn2-/-* embryos display also deficient placentation (Chen et al., 2003h).. However, post-placentation ablation of either Mfn in the mouse leads to two completely different phenotypes: Mfn1-/- mice are viable, while Mfn2-/- ones day between P1 and P17 as a consequence of massive cerebellar degeneration (Chen et al., 2007b). It is unclear whether the different phenotypes observed in vivo and in vitro can be ascribed to functional differences or simply to different expression patterns of the two Mfns . In addition, it should be noted that all vertebrates possess two Mfn, whereas only one Mfn is retrieved in almost all invertebrates reigns, with the exception of *D.melanogaster*.

The fruitfly possesses 2 mitofusins, Fuzzy onion (Fzo) and Mitochondrial Assembly Regulatory Factor (Marf). Fzo was the first identified mediator of mitochondrial fusion (Hales and Fuller, 1997a). In spermatocytes Fzo mediates the fusion of mitochondria into two giant organelles that form a structure called Nebenkern, which is required to give energy to the flagellum of the spermatid. In fzo mutant flies, mitochondria fail to fuse and wrap each other as many fragmented organelles, giving the impression of ‘fuzzy onions’ when viewed at the electron microscopy. Altough Fzo was able to promote mitochondrial elongation, it was expressed restrictely to spermatids. This raised the question of how mitochondrial fusion was regulated in other tissues of the fruitfly. In 2002 the second mitofusin homologue Marf was identified in *D.melanogaster* (Hwa et al., 2002). Unlike Fzo, DMarf is expressed ubiquitously and shares 64% of homology with both mammalian mitofusins. Thus, Marf can be likely considered the single “functional” invertebrate Mfn and *Drosophila melanogaster* is therefore a useful model organism to investigate phylogenesis of higher vertebrate Mfns. In this thesis we set to answer to the following questions: does this model organism represent the evolutionary turning point from one to two mitofusins? Which Mfn is functionally closer to DMarf?

To answer to these questions, we first tried to understand in which extension DMarf could complement mammalian mitofusins. To obtain a wider phylogenetic view, we extended our analysis on mitofusins 1 and 2 from the vertebrate *Xenopus laevis*

(XMfn1 and XMfn2) and on mitofusin homologue from the yeast *S.cerevisae* (Fzo1p). The expression of Fzo1p, DMarf, XMfn1 and XMfn2, induced mitochondrial elongation in Mfn1$^{-/-}$ or Mfn2$^{-/-}$ MEFs, rescuing the fragmented phenotype caused by the absence of the Mfns and indicating that they can substitute for both Mfns.

Unlike Mfn1$^{-/-}$ MEFs, Mfn2$^{-/-}$ MEFs have altered ER morphology (de Brito and Scorrano, 2008b). This defect is recovered only after expression of hMfn2 or by an ER-targeted variant of hMfn2 (hMfn2^{YFFT}), independently from mitochondrial shape. In fact Mfn2 is partially localized on ER and is enriched in MAMs. To investigate whether DMarf could complement Mfn2 also in ER shape regulation, we cotransfected Mfn2$^{-/-}$ MEFs with DMarf-V5 and ER-targeted yellow fluorescent protein (ERYFP). DMarf was able to rescue ER shape in Mfn2-/-, thus displaying a functional overlap with Mfn2.

We then turned our attention to an *in vivo* analysis of DMarf function in *Drosophila*. DMarf was essential for viability as shown by ubiquitous, neuronal and muscle specific downregulation of the protein, which were all lethal. In larvae depleted of DMarf mitochondria clumped in the perinuclear regions of neuronal cell bodies and muscle tissues. In addition, neuromuscular junctions (NMJs) of DMarf-RNAi individuals were severely depleted of mitochondria compared to control larvae. Given that Mitofusin-2 regulates ER morphology and tethering to mitochondria, we also investigated the effect of DMarf knockdown on ER architecture which was seriously compromised upon DMarf knockdown in muscle tissues, with loss of the sarcomeric organization of the ER.

To investigate the effect of overexpression of hMfns in *Drosophila,* we characterized transgenic lines expressing hMfn1, hMfn2 and hMfn2^{R94Q}, one of the most frequent mutations associated with CMT2A (Zuchner et al., 2004b). Aggregation of mitochondria in neuronal cell bodies and muscle and elongated or clumped organelles inside axons were observed upon overexpression of all hMfns. However, NMJs analysis revealed a major difference between hMfn1, hMfn2 and hMfn2^{R94Q} expressions: while NMJs of hMfn2 and hMfn2^{R94Q} overexpressing individuals were depleted of mitochondria, hMfn1 expression did not alter organelles distribution in the nervous system and mitochondria were retained inside junctions. Muscle ER organization was not affected in wild-type hMfns expressing larvae; interestingly, ER morphology was found altered in muscle tissues only of hMfn2^{R94Q} individuals, showing an aspect never investigated in the study of Charcot-Marie-Tooth

pathogenesis and suggesting ER morphology alteration as one of the putative factors contributing to the pathobiology of the disease.

Given that DMarf was able to complement both mfns in mitochondrial morphology and Mfn2 in ER shape regulation, we tried to understand to which extent hMfn1 and -2 could surrogate Marf in *Drosophila*. Simultaneous expression of Mfn2 and Marf-RNAi transgenes in the nervous system or in muscle resulted in partial survival to adulthood,. while Mfn1 or $Mfn2^{R94Q}$ were unable to recover the DMarf-RNAi and the flies died as pupae,. However, mitochondrial clusters were still present in neuronal cell bodies and muscle and mitochondria were lacking in NMJs of individuals simultaneously expressing DMarf-RNAi and hMfn2. Thus, although Mfn2 rescued DMarf depletion lethality, this could not be ascribed to a recovery of mitochondrial morphology and distribution. We therefore assessed recovery of ER organization in individuals simultaneously expressing DMarf-RNAi and hMfns. HMfn1 had no effect on ER alteration caused by DMarf knockdown. On the contrary, hMfn2 expression recovered muscle ER architecture both when expressed ubiquitously or only in the muscle .

In conclusions, in this Thesis we demonstrate that Fzo1p, DMarf, XMfn1 and XMfn2 expression could rescue mitochondrial morphology in *Mfn1* -/- and *Mfn2*-/- MEFs. Moreover DMarf specifically complements ER shape in *Mfn2*-/- MEFs. Thus, mitofusins role in regulation of mitochondrial dynamics is conserved between vertebrates and invertebrates. On the other hand, *in vivo* experiments show that Mfn2, but not Mfn1 rescues the lethal phenotype of DMarf knock-down in *Drosophila melanogaster*. the rescue of DMarf-RNAi by hMfn2 seemed correlate with the correction of ER organization, whereas mitochondrial morphology and distribution were not restored. We can therefore speculate that Marf is functionally closer to Mfn2 than Mfn1, which may have diverged later during mammalian evolution. Finally, factors other than the disruption of mitochondrial distribution and morphology in the nervous system could explain the lethal phenotype of DMarf knockdown and in perspective be involved in the pathogenesis of CMT2a

3. Introduction

Eukaryotic cells are surrounded by a plasma membrane (PM) and contain extensive internal membranes that enclose specific compartments, the organelles, and separate them from the rest of the cytoplasm, the region of the cell lying outside the nucleus. Most eukaryotic cells contain many mitochondria, which occupy up to 25% of the cytoplasmic volume.

Mitochondria are the main site of ATP production. In addition to converting cellular energy, they are involved in a range of other processes, such as signalling, cellular differentiation and death, as well as in the control of the cell cycle and cell growth. Finally, mitochondria have been implicated in several human diseases, including degenerative disorders and cancer and may play a role in the aging process.

Mitochondria are complex organelles and their elaborate structure is very important for their function. In certain cell types they are organized in networks of interconnected mitochondria. Ultrastructurally, the inner membrane (IM) can be further subdivided in an inner boundary membrane and in the cristae compartment, bag-like folds of the IM connected to it via narrow tubular junctions. The ultrastructure and the reticular organization of the organelle are determined by mitochondria-shaping proteins that impinge on the equilibrium between fusion and fission processes.

3.1 Mitochondrial shape and dynamics

Mitochondria were described for the first time in 1857 by the anatomist Rudolf Albrecht von Koelliker who called them “sarcosome”. In the 1950s Sjöstrand and Palade led pioneering work on electron microscopy of mitochondria. They both recognized that mitochondria have two very different membranes, an outer (OMM) and a highly convoluted inner (IMM) membrane. It was proposed that mitochondria posses two soluble compartments: the intermembrane space (IMS), between the OM and the IM, and the matrix, the central electrondense space. Palade’s model evolved into that currently depicted in textbooks in which the inner mitochondrial membrane is one continuous closed surface with a complex morphology, folded in ridges called cristae (Figure 1A). This model, sometimes called the baffle model, depicts the

cristae with broad openings to the intermembrane space on one side of the mitochondrion and protruding across the matrix nearly to the other side (Palade, 1952; Palade, 1952).

Mitochondrial shape in living cells is very heterogeneous and can range from small spheres to interconnected tubules (Bereiter-Hahn and Voth, 1994a) (Figure 1 A, B, D). For example, mitochondria of rat cardiac muscle and diaphragm skeletal muscle appear as isolated ellipses or tubules in embryonic stages but then reorganize into reticular networks in the adult (Bakeeva et al., 1981; Bakeeva et al., 1972). The different shapes of mitochondria were already noticed in early times by cytologists who observed this organelle under the light microscope. Noticing that mitochondrial morphology was heterogeneous, they accordingly christened this organelle 'mitochondrion', a combination of the Greek words for 'thread" and "grain'. The morphological plasticity of mitochondria results from the ability of this organelle to undergo fusion and fission. Real-time imaging reveals that individual mitochondrial tubules continually move back and forth along their long axes on radial tracks. Occasionally, two mitochondrial tubules encounter each other and fuse, end to end or head to site (Bereiter-Hahn and Voth, 1994b); (Chen et al., 2003g). On the other hand, these tubules can also undergo fission events, giving rise to two or more mitochondrial units. It is important to note that mitochondrial fusion and fission are complicated processes, being mitochondria bound by two membranes. Thus, any mechanism of fusion and fission should take into account that the coordinate fusion-division of four lipid bilayers is required to complete the process.

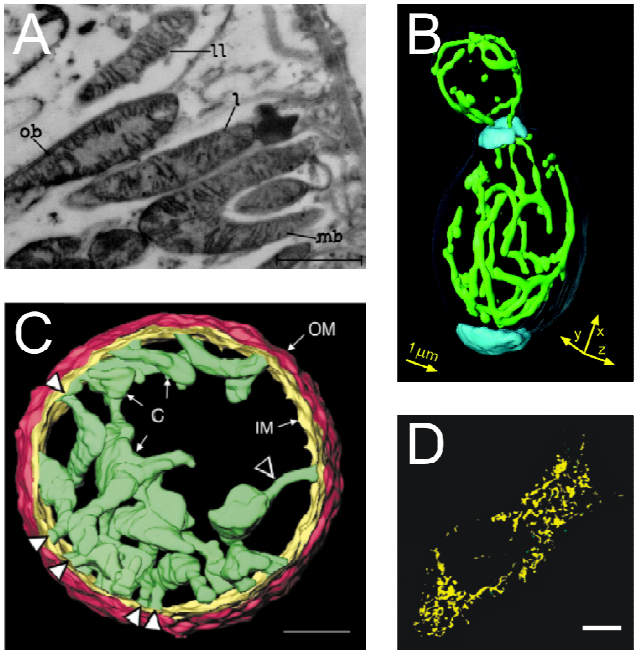

Figure 1 – **The many shapes of mitochondria**. (**A**) Mitochondria of various shapes in the epithelium of a proximal convoluted tubule of the rat kidney (Magnification 27,400X; 1) (**B**) Surface rendered 3D stack of the mitochondrial network of *S. cerevisiae* expressing GFP-targeted to the mitochondrial matrix. Adapted from (Egner et al., 2002). (**C**) Three-dimensional reconstructions of isolated

rat liver mitochondria obtained by high-voltage (1000 kV) electron microscopic tomography using two-axis tilting. OM: outer membrane, IM: inner membrane, C: selected cristae; arrowheads point to narrow tubular regions that connect cristae to periphery and to each other. Bar, 0.4 μm. Adapted from (Mannella, 2000). (**D**) Morphology of a mouse embryonic fibroblast transfected with mitochondrially targeted red fluorescent protein. Bar, 15μm. Adapted from (Frezza et al., 2006a)

3.1.1 Mitochondria shaping proteins

3.1.1.1 Proteins involved in mitochondrial fusion

Fzo/mitofusin -1,-2

The first mediator of mitochondrial fusion identified was the *D. melanogaster* Fuzzy onion protein (Fzo1), an evolutionarily conserved, large transmembrane GTPase localized in the outer mitochondrial membrane. In *Drosophila* the Fzo gene is activated during spermatogenesis and mutations in the gene are responsible for sterility in the male fly (Hales and Fuller, 1997b). Fzo1 mediates the formation of two giant mitochondria wrapped one around the other. The resulting structure resembles an onion slice, is called Nebenkern and is required to produce energy for the flagellum of the spermatid. In *fzo* mutant flies mitochondria fail to fuse and wrap each other as many fragmented organelles, which resemble ‘fuzzy onions’. *Drosophila* possesses another mitofusin homologue, the ‘mitochondrial assembly regulatory factor’ (Marf) which is expressed ubiquitously in males and females. Muscle tissues specific knock-down of DMarf induces fragmentation and alteration of ultrastructure of mitochondria (Deng et al., 2008c).

The *S. cerevisiae* orthologue of Fzo1 mediates mitochondrial fusion events during mitotic growth and mating and is required for long-term maintenance of mitochondrial DNA (Hermann et al., 1998; Rapaport et al., 1998). Fzo1p has two homologues in mammals, MFN1 and MFN2 (Santel and Fuller, 2001), which both control mitochondrial fusion. MFN1 and -2 display high (81%) homology and similar

topologies, both residing in the OM (Chen et al., 2003f; Rojo et al., 2002b; Santel et al., 2003). They possess an N-terminal GTPase domain, two transmembrane domains spanning the outer mitochondrial membrane and two coiled coil motifs crucial for protein–protein interaction (Santel and Fuller, 2001).

MFN1 and MFN2 act in *trans* on opposing membranes by bridging mitochondria, maintaining a distance of 95 Angstrom between the two membranes (Koshiba et al., 2004d). However, MFN2 seems to have a different role from MFN1. First, it has been shown that MFN1 has a higher GTPase activity than MFN2, although its affinity for GTP is lower (Ishihara et al., 2004c). In agreement with this, MFN1 exhibits a higher capacity to induce fusion (Ishihara et al., 2004b). The differential role played by the two mitofusins during mitochondrial fusion was first demonstrated by directly measuring mitochondrial fusion rates in *Mfn1*-/- and *Mfn2*-/- cells. These experiments substantiated that cells containing only MFN1 retain more fusion activity than those that contain only MFN2 (Chen et al. 189-200). Extending these cell biological observations, genetic ablation of the two genes in the mouse does not result in the same phenotype: *Mfn1*-/- mice die in midgestation, whereas *Mfn2*-/- embryos display deficient placentation (Chen et al., 2003e).

A recent work from our lab demonstrated that MFN2 is localized not only on the outer mitochondrial membrane but also on ER and it is enriched at the ER-mitochondria interface. Besides controlling ER morphology, MFN2 on ER forms homotypic and heterotypic complexes with MFN1 and MFN2 on the outer mitochondrial membrane and it controls the tethering between the two organelles. The regulation of this juxtaposition is crucial for the mitochondrial Ca^{2+} uptake upon Ca^{2+} release from ER stores (de Brito and Scorrano, 2008c).

Mgm1p/ Msp1p/Opa1

Optic atrophy 1 (OPA1) is a dynamin-related protein located in the IMM. Mgm1p, the yeast homologue of OPA1, has been identified in a genetic screen for nuclear genes required for the maintenance of mtDNA in the budding yeast *S. cerevisiae* (Jones and Fangman, 1992a; Jones and Fangman, 1992b). Years later, Pelloquin and colleagues isolated Msp1p, the *S. pombe* orthologue (Pelloquin et al., 1999). The human gene of Opa1 was identified in 2000 by two independent groups (Alexander et al., 2000; Delettre et al., 2000; Delettre et al., 2000). Albeit Mgm1p and Opa1

display a sequence identity of only approximately 20%, they maintain a highly conserved secondary structure, consisting of a N-terminal mitochondrial targeting sequence (MTS) composed of scattered positively charged amino acid residues, two consecutive hydrophobic segments, a GTPase domain, a middle domain, and a C-terminal coiled-coil domain that may correspond to GTPase effector domain GED (Satoh et al., 2003). The pleckstrin homology and proline-rich domains, found in classical dynamins, are missing. The functional analysis of Mgm1p and Msp1 reveals that both proteins are required for the maintenance of fusion-competent mitochondria in *S. cerevisiae* and *pombe* (Wong and Scott, 2004). The high degree of secondary structure conservation suggests that the function of OPA1 is conserved in mammals. On the other hand, it was less clear whether OPA1 played a role in fission, or in fusion of mitochondria, since high levels of OPA1 can drive fragmentation of the mitochondrial reticulum (Griparic et al., 2004a; Misaka et al., 2002; Olichon et al., 2003b). However, in our laboratory it has been shown that a linear relationship between OPA1 levels and mitochondrial fusion exists, as overexpression of OPA1 enhances fusion, while its downregulation by siRNA represses it in mouse embryonic fibroblasts.

3.1.1.2 Proteins involved in mitochondrial fission

Dnm1p/Dlp1/Drp1

The two proteins fission 1 (FIS1) and dynamin-related-protein 1 (DRP1) regulate mitochondrial fission in mammals. The dynamin-like-protein (Dlp) 1p in yeast, DRP-1 in *C. elegans*, and DLP1/DRP1 in mammals are homologues. DRP1 exists largely in a cytosolic pool, but a fraction is found in spots on mitochondria at sites of costriction (Labrousse et al., 1999; Smirnova et al., 2001). DRP1 contains a dynamin-like-central domain and a C-terminal GTPase effector domain (GED), in addition to its N-terminal GTPase. DRP1 can oligomerize, *in vitro*, into ring-like structures and intermolecular oligomerization is observed at membrane constriction sites. Given these similarities with dynamin, DRP1 has been proposed to couple GTP hydrolysis with mitochondrial membrane constriction and fission (Hinshaw, 1999a).

Fis1p/hFis1

Fis1p is a 17-kDa integral protein of the outer mitochondrial membrane (James et al., 2003). Its N-terminal domain is exposed to the cytoplasm and forms a tetratricopeptide (TPR)-like fold (Stojanovski et al., 2004; Suzuki et al., 2003). The C-terminal domain of FIS1 possesses a predicted TM domain and a short stretch of amino acids facing the IMS. FIS1 is thought to recruit DRP1 to punctuate structures on mitochondria during mitochondrial fusion. It is therefore considered the limiting factor in the fission reaction (Stojanovski, 2004). Moreover it has been shown that hFis1 is a bifunctional protein which independently regulates fission and apoptosis (Alirol et al., 2006).

Mff

Mff is a novel component of the mammalian mitochondrial fission machinery. Mff is a tail-anchored membrane protein located in the outer mitochondrial membrane and on peroxisomes. The hydrophobic carboxy-terminal segment serves as a membrane anchor, while the amino-terminal conserved repeats and the coiled coil domain might be involved in the interaction with other proteins. The silencing of Mff by siRNA inhibits mitochondrial fragmentation and leads to the appearance of an elongated mitochondrial network, similar to that obtained by silencing of Fis1 and DRP1. The topological and functional similarities between Mff and FIS1 suggests that they act in the same pathway, but the fact that they are not found in the same complex suggests that they fulfill different functions in the process of mitochondrial and peroxisomal fragmentation (Gandre-Babbe and van der Bliek, 2008).

Endophilin b1

Endophilin B1, a member of the endophilin family of fatty acid acyl transferases that participate in endocytosis, has been shown to play a role in mitochondrial fission (Karbowski et al., 2004). During endocytosis, endophilin 1 builds complexes with dynamin I, the dynamin responsible for the severing of the neck of the nascent endocytic vesicle, and provides the required lipid modification (Schmidt et al., 1999b). Endophilin B1 partially colocalizes and cofractionates with mitochondria and its downregulation by siRNA leads to changes in mitochondrial shape, as well as the

formation of OM-bound structures resembling those formed by vesicles in neuronal terminals after inactivation of endophilin 1.

Members of the endophilin family, which are all Bin-Amphiphysin-Rvs(BAR)-domain proteins (like for example amphiphysin and endophilin 1), are supposed to participate in the regulation of membrane curvature, a process required for membrane scission during dynamin-mediated endocytosis (Gallop et al., 2006a). However, the mechanism by which BAR-domain proteins and related components regulate membrane scission has recently been questioned. First, it has been proposed that BAR-domain proteins have an acyl transferase activity that promotes membrane fission by altering membrane curvature from positive to negative (Schmidt et al., 1999a). Later studies by the laboratory of H. McMahon demonstrated that BAR-domain proteins have no fatty acyl transferase activity as previously believed (Gallop and McMahon, 2005). The amphipathic helices of BAR domains alter membrane curvature by inserting into the phospholipids bilayers and not by displaying a fatty acyl transferase activity (Gallop et al., 2006b). Similarly, endophilin B1 seems to participate in the control of the morphology of OM by altering membrane curvature. Whether this is a direct effect, or it requires the recruitment of other proteins, such as phospholipase D and/or other mitochondria-shaping proteins, remains to be elucidated.

Mtp18

MTP18, a nuclear-encoded mitochondrial membrane protein, is suggested to be a component required for mitochondrial fission in mammalian cells (Tondera et al., 2004; Tondera et al., 2005). MTP18 is supposed to be an intramitochondrial protein exposed to the IMS, however it is still not clear whether MTP18 is an OM or IM protein. Interestingly MTP18 is a downstream effector of phosphatidyl-inositol 3-kinase (PI3-K) signalling. It has been reported that overexpression of MTP18 leads to mitochondrial fragmentation. On the other hand, after downregulation of MTP18 levels by siRNA, mitochondria appear filamentous. Thus, MTP18 could be a regulator of mitochondrial shape that responds to activation of PI3-K, coupling morphology of the reticulum to cellular cues.

3.1.2 Mechanisms of mitochondrial fusion and fission

Several important characteristics of mitochondria make their fusion mechanism particularly intriguing. First, unlike almost all other intracellular fusion events, neither SNAREs nor the AAA-ATPase NSF have been implicated in the fusion reaction. Indeed, there are specific, dedicated mitochondrial fusion molecules, suggesting that the machinery evolved independently and is uniquely tailored for this organelle. Second, mitochondria have two membranes: therefore, the fusion of four sets of lipid bilayers must be coordinated. Third, unlike viral fusion and most SNARE-mediated fusion, mitochondrial fusion is homotypic. Finally, mitochondrial fusion it is likely to be influenced by cellular energetic demands, apoptotic stimuli and developmental cues. Taken together, these characteristics suggest that mitochondria fuse through a novel mechanism that reflects their unique endosymbiontic origin and double membrane architecture.

Why do mitochondria continually fuse and divide? Recent studies show that these processes have important consequences for the morphology, function and distribution of mitochondria. First, fusion and fission control the shape, length and number of mitochondria. The balance between these opposing processes regulates mitochondrial morphology. Second, fusion and fission allow mitochondria to exchange lipid membranes and intramitochondrial content. Such exchange is probably crucial for maintaining the health of a mitochondrial population. When mitochondrial fusion is abolished, a large fraction of the mitochondrial population loses nucleoids (Chen et al., 2007a). In addition to mtDNA, other components, such as substrates, metabolites or specific lipids, can be restored in defective mitochondria by fusion. Third, the shape of mitochondria affects the ability of cells to distribute their mitochondria to specific subcellular locations. This function is especially important in highly polarized cells, such as neurons. Mitochondrial fusion and fission affect the mitochondrial distribution in dendrites. In hippocampal neurons, mitochondria accumulate at dendritic spines following neuronal stimulation. Inhibition of mitochondrial fission causes elongation of the mitochondria and decreases the abundance of dendritic mitochondria and the density of dendritic spines. Conversely, increased fission facilitates the mobilization of dendritic mitochondria and leads to an increased spine number (Li et al., 2004a). Mitochondrial dynamics appear to be

important for proper mitochondrial redistribution in lymphocytes during chemotaxis (Campello et al., 2006). Finally, mitochondrial fission facilitates apoptosis by regulating the release of intermembrane-space proteins into the cytosol. Moreover mitochondria actively participate in the regulation of Ca^{2+} signalling by taking up and releasing Ca^{2+} in response to physiological, inositol triphosphate coupled agonists. This process relies on the relative position of mitochondria in the cytosol, as well as on their juxtaposition to the ER, required for the production of microdomains of high [Ca^{2+}], essential for the activation of the low affinity mitochondrial Ca^{2+} uniporter (Rizzuto et al., 2000). It is therefore conceivable that changes in mitochondrial shape influence mitochondrial participation in the Ca^{2+} game. This hypothesis is substantiated by the finding that excessive fission by Drp1 blocks propagation of Ca^{2+} waves (Szabadkai et al., 2004), while Fis1 reduces refilling of ER Ca^{2+} stores, probably by impairing capacitative Ca^{2+} entry from the plasma membrane (Frieden et al., 2004). Surprisingly, Fis1 promotes higher degrees of fragmentation than Drp1, yet its effect on the propagation of mitochondrial Ca^{2+} waves is apparently much lower. A possibility is that Drp1 has a specific but yet not characterized function on mitochondrial Ca^{2+} propagation, in addition to its effect on mitochondrial morphology.

3.1.2.1 Regulation of fission

Mitochondrial fission in mammalian cells seems to follow the same mechanism described in yeast. Like in yeast, it has been shown that DRP1 is recruited to spots on mitochondria and it seems that constriction of the membranes takes place via interaction with FIS1, since it has been shown that recombinant DRP1 and recombinant FIS1 can interact in vitro (Yoon et al., 2003; Youn et al., 1999). However, this association has never been shown *in vivo* and reduction of FIS1 levels by siRNA does not disrupt DRP1 localization to mitochondria (Lee et al., 2004b). While this could argue against the possibility that Fis1 acts as the mitochondrial receptor for DRP1, it should be considered that the residual level of FIS1 could till be sufficient to recruit DRP1 to mitochondria. A growing number of studies is contributing to the characterization of the signals that induce the recruitment of DRP1 to mitochondria and the turnover of the protein. Dephosphorilation of serine 637 was shown to be one of this signals (Cereghetti, 2008). DRP1 forms a complex with calcineurin and cyclophilin A in the cytosol. When calcineurin is activated by a

mitochondrial depolarization-dependent increase of cytosolic Ca^{2+}, it dephosphorylates DRP1, which translocates to mitochondria and induces fission of the organelle.

3.1.2.2 Regulation of fusion

Fusion of mammalian and yeast mitochondria is thought to occur in a similar way. The mammalian orthologues of Fzo1p, MFN1 and MFN2, are believed to dock two juxtaposed mitochondria via their coiled coil domains (Koshiba et al., 2004c). In the case of MFNs, two molecules on opposing membranes can bind in trans to bridge mitochondria, maintaining a distance of 95 Å between the two membranes (Koshiba et al., 2004b). But how is OMM fusion coordinated with IMM fusion? In yeast a multimolecular complex of Mgm1p, Ugo1p and Fzo1p apparently coordinates fusion of the two membranes. On the other hand, a mammalian orthologue of Ugo1p has not yet been identified and it is unclear whether OPA1 and MFN1 direclty interact to promote mitochondrial fusion.

Studies in intact cells showed that in higher eukaryotes an intact IMM potential is required for mitochondrial fusion, which conversely appears to be independent of a functional cytoskeleton (Legros et al., 2002). Taking advantage of the yeast model, mitochondrial fusion has been recently recapitulated *in vitro*. This approach dissected the fusion process into two mechanistically distinct, resolvable steps: OMM fusion and IMM fusion. OMM fusion requires homotypic trans-interactions of the Fzo1p, the proton gradient component of the inner membrane electrical potential, and low levels of GTP hydrolysis. Fusion of the IMM requires the electrical component of the inner membrane potential and high levels of GTP hydrolysis. However, time-lapse analysis of mitochondrial fusion in yeast and mammalian cells, *in vivo*, clearly shows that fusion of the OMM and IMM is temporally linked. These observations indicate that individual fusion machineries exist in each membrane and that they can communicate *in vivo*, resulting in coupled outer and inner membrane fusion (Meeusen et al., 2004).

3.1.3 Mitochondrial dynamics and disease

3.1.3.1 Opa1 and ADOA

Mutations of OPA1 are associated with autosomal dominant optic atrophy (ADOA), also known as type I Kjer disease, the most common form of inherited optic neuropathy, with an estimated prevalence of 1:50000 (Alexander et al., 2000; Delettre et al., 2000; Delettre et al., 2000). Linkage analysis has revealed that OPA1, mapping to 3q28-q29, is the major locus (Votruba et al., 1997a) and a positional cloning approach similarly identified this gene as being responsible for OPA1-type DOA (Alexander, 2000).

The clinical features of ADOA are the decrease in visual acuity, tritanopia (dyschromatopsia characterized by confusion in the blue-yellow hues), sensitivity loss in the central visual fields, and pallor of the optic nerve (Ferre et al., 2005d)(Votruba et al., 1997b) . Classic DOA usually begins before 10 years of age, with a large variability in the severity of clinical expression, which may range from non-penetrant unaffected cases up to very severe, early onset cases, even within the same family carrying the same molecular defect (Carelli et al., 2004; Ferre et al., 2005c). Histopathology studies have shown diffuse atrophy of the ganglion cell layer that predominates in the central retina and loss of myelin and nerve tissue within the optic nerve (Kjer et al., 1996).

Most of the mutations associated with ADOA cluster in the GTPase and in the coiled coil domain of Opa1 (Ferre et al., 2005b). Almost 50% of mutations in the OPA1 gene described to date are predicted to lead to a truncated protein and suggest that haploinsufficiency is the cause of the disease (Ferre et al., 2005a; Marchbank et al., 2002; Pesch et al., 2001). Nearly 40% of mutations occurs in the GTPase domain and may cause a dominant negative effect, impairing the mechanoenzymatic activity of the protein complexes. This possibility is reinforced by the fact that two mouse models of Opa1 mutation (a GTPase missense and a nonsense, truncative mutation) display minimal retinal defects in the heterozygous status (Alavi et al., 2007; Davies et al., 2007).

It remains unclear why Opa1-ADOA manifests with an apparently restricted clinical ocular phenotype, comprising retinal ganglion cells (RGC) loss. Opa1 is ubiquitously expressed throughout the body: in the heart, skeletal muscle, liver, testis, and most abundantly in the brain and retina. In the human retina, Opa1 is present in the cells of the RGC layer, nerve fibre layer, the photoreceptor layer, and the inner and outer

plexiform layers (IPL & OPL). A plausible hypothesis as to why RGC neurons may be more vulnerable to OPA1 inactivation could be a particular susceptibility to mitochondrial membrane disorders inducing mitochondrial dysfunction or mislocalization. Indeed, reports describe altered mitochondrial ATP synthesis and respiration in OPA1-inactivated cells (Amati-Bonneau et al., 2005b; Chen et al., 2005). Moreover, recent studies show the effect of mitochondrial morphology regulation on mitochondrial distribution in neurons and their contribution to dendrite formation and synaptic plasticity (Li et al., 2004b). This could be of particular importance in RGC neurons that display a specific distribution of mitochondria in the cell body, myelinated and unmyelinated axons (Andrews et al., 1999; Bristow et al., 2002; Wang et al., 2003). Additionally, the defects in ADOA can be ascribed to the loss of the crucial control exerted by OPA1 on the structural organization of the cristae and apoptosis (Arnoult et al., 2005; Frezza et al., 2006b; Griparic et al., 2004b; Lee et al., 2004a; Olichon et al., 2003a). It is worthy to note that miss-sense point mutations in the highly conserved GTPase domain are responsible for a syndromic form of DOA associated with sensori-neural deafness, ataxia, axonal sensory-motor polyneuropathy, chronic progressive external ophthalmoplegia and mitochondrial myopathy (Amati-Bonneau et al., 2005a). Moreover, increasing evidence show a subclinical involvement of non-neuronal tissues, characterized by defects in mitochondrial dynamics (Delettre et al., 2000; Spinazzi et al., 2008), function (Lodi et al., 2004) and mtDNA content, thus revealing an unrecognized role of the Opa1 protein in mtDNA stability.

3.1.3.2 Mfn2 and Charcot-Marie Tooth type 2A

In 2004, work by Zuchner et al. mapped the mutations responsible for Charcot-Marie-Tooth 2A (CMT2A), and identified MFN2 as being the gene responsible for the disorder. CMT is one of the most common inherited disorders in humans, with an estimated prevalence of one in 2500 individuals. CMT neuropathies can be divided into 2 main groups, type 1 and type 2. In CMT1, nerve conduction velocities are considerably reduced. In CMT2, the nerve conduction velocities are normal but conduction amplitudes are decreased, due to the loss of nerve fibres (Zuchner et al., 2004c).

CMT2A is a neurodegenerative disorder characterized by the loss of sensory and motor axons at early stages of the disease and resulting in the degeneration of the neurons themselves during a later stage of the disease. The clinical symptoms of CMT are distal weakness of the lower limbs, sensory loss, decreased reflexes and foot deformities. Other symptoms include cranial nerve involvement, scoliosis, vocal cord paresis and glaucoma (Lawson et al., 2005b). Mutations in MFN2 account for around 20% of CMT2 cases, making this the most prevalent axonal form of CMT. Most MFN2 mutations in CMT2A cluster within the GTPase and the RAS-binding domains and are missense mutations (Kijima et al., 2005; Lawson et al., 2005a; Zuchner et al., 2004d). Recently, a *de novo* truncation mutation in MFN2 has been associated to CMT2 and optic atrophy (also known as hereditary motor and sensory neuropathy VI, HMSN VI) (Zuchner and Vance, 2006).

3.1.3.3 Mfn2 and type 2 diabetes mellitus

Many studies confirmed a correlation between Mfn2 levels and different physiological and pathophysiological conditions linked to metabolism, such as obesity, diabetes, insulin resistance exercise and weight loss. Indeed, conditions characterized by a defective mitochondrial oxidation, such as obesity and type 2 diabetes mellitus are associated with reduced *MFN2* gene expression (Bach et al., 2003c; Bach et al., 2005a); and, inversely, acute exercise or weight loss, which enhance mitochondrial oxidation, are related to increases in Mfn2 (Mingrone et al., 2005; Cartoni et al., 2005b). Furthermore, it was shown that the transcription factors PGC-1α and ERRα activate Mfn2 synthesis in muscle cells after acute physical exercise (Cartoni et al., 2005a; Garnier et al., 2005). A recent report indicates that insulin stimulates the production of Mfn2, which in turn inactivates RAS, blocking the downstream MEK-dependent signalling pathway. At the same time, insulin activates a PI3-K signalling pathway that leads to an increase in mitochondrial respiration (Pawlikowska et al., 2007)

3.1.3.4 Drp1

To date just one clinical case involving mutations in the gene coding for DRP1 has been described (Waterham et al., 2007). The patient showed microcephaly,

abnormal brain development and optic atrophy at birth and he died at 1 month of age. The elevated lactate concentrations in blood and cerebrospinal fluid suggested a compromised function of mitochondria and accumulation of cerotic acid in plasma suggested a defect in peroxisomal beta-oxidation. The disorder is caused by a heterozygous mutation (A395D) in the middle domain of DRP1, that acts in a dominant-negative manner, likely interfering with DRP1 homo-oligomerization. Consistently with the role of DRP1 in the regulation of mitochondrial and peroxisomal shape (Koch et al., 2003; Koch et al., 2004; Li and Gould, 2003), fibroblasts form the patient display abnormally elongated mitochondria and peroxisomes. Several of the observed abnormalities were similar to CMT neuropathy (e.g., truncal hypotonia and lack of tendon reflexes) and ADOA (e.g., optic atrophy) but the clinical course was more severe, suggesting that defects in mitochondrial fission have more severe consequences that alterations in fusion and that the clinical presentation can be exacerbated by the additional defect in peroxisomal fission.

3.1.4 Functional divergence between MFNs

Messenger ribonucleic acid (mRNA) and protein expression levels of MFN1 and MFN2 in mouse vary between tissues. MFN1 is predominantly expressed in heart, liver, pancreas, adrenal glands and testis (Eura et al., 2003; Santel and Fuller, 2001). MFN2 is abundant in heart, skeletal muscle, brain, adrenal glands and brown adipose tissue (Bach et al., 2003b). The existence of two MFNs in mammalian cells raised the question as whether they play similar, separate or dependent biological functions.

3.1.4.1 Protein structure

Human Mfn2 (757 amino acids) is 63% identical and 77% similar to human Mfn1 (741 amino acids). They share almost the same conserved functional domains: a GTPase domain and a coiled coil domain (HR2) located at the N-terminus of the proteins, protruding towards the cytosol; a bipartite transmembrane domain and a coiled coil domain (HR1) in the C-terminus (Koshiba et al., 2004a; Rojo et al., 2002a;

Santel, 2006). The coiled coil is a widespread helical structural motif functioning as oligomerization domain (Oakley and Hollenbeck, 2001).
Despite their highly similarity, the two mitofusins display some structural divergences. MFN2 possesses a p21ras-binding domain at its N-terminal, which is not retrieved in MFN1 (Chen et al., 2003d). Moreover, in silico analysis of MFN2 reveals that this protein also has a proline-rich-domain between aminoacids 576 and 590, which is poorly conserved in MFN1 and in Fzo1p. Proline-rich domains are involved in the binding to other proteins (Kay et al., 2000).

3.1.4.2 Role in fusion

As already mentioned, both Mfns participate in the regulation of mitochondrial fusion in mammalian cells. As shown by mitochondrial morphology observations, both *Mfn1*-/- and *Mfn2*-/- mouse embryonic fibroblasts display a fragmented mitochondrial network. However the two mitochondrial phenotypes are remarkably different: loss of MFN1 leads to a greater degree of fragmentation, resulting in either very short mitochondrial tubules or very small spheres that are uniform in size and unable to fuse; in contrast, *Mfn2*-/- fibroblasts exhibit mitochondrial spheres and tubules of varying sizes. Moreover, PEG cell fusion assay indicate that *Mfn1*-/- mitochondria in most polykaryons stay separate and do not intermix. In contrast, mitochondria of fused *Mfn2*-/- polykaryons are distributed throughout the cell (Chen et al., 2003c). Finally, a genetic approach demonstrated that MFN1 is necessary for the mitochondrial fusion mediated by OPA1 (Cipolat et al., 2004a) , while MFN2 seem to be dispensable for this process. This can be partially explained by the differential GTPase activity, which is greater in MFN1. However, MFN2 has a greater affinity for GTP (Ishihara et al., 2004a; Neuspiel et al., 2005). In summary, both MFNs mediate mitochondrial fusion, but in a different extent. Moreover, MFN2 has roles which are not shared by MFN1 (de Brito, 2008d) such as the control of mitochondrial oxidation (Bach, 2005b), anti-proliferative function (Chen, 2004b) and regulation of endoplasmic reticulum (ER)-mitochondria tethering (de Brito and Scorrano, 2008d).

3.1.4.3 Role in development

Both MFN1 and MFN2 are essential for embryonic development and loss of either MFN1 or MFN2 results in mid-gestational lethality (Chen et al., 2003b). *Mfn1*-/- embryos die at embryonic day (E) 10.5. However, by E12.5, most mutant embryos are resorbed. It is also noteworthy that by E8.5 most mutant embryos are smaller than their wt counterparts. In *Mfn2*-/-, normal numbers of live homozygous mutant embryos are recovered up to E9.5. However, after E10.5 embryos start to be resorbed. The live mutant embryos at E9.5 and E10.5 are slightly smaller than the wt ones, but otherwise well developed and show no obvious malformation. Another observation indicates that these two proteins possess a distinct function during embryonic development: while lethality in *Mfn2*-/- embryos results from an improper development of the placenta, *Mfn1*-/- giant cells develop normally (Chen et al., 2003a). During midgestation, placenta has a trilaminar structure, with the trophoblast forming the outermost layer. Trophoblast giant cells are polyploid cells able to invade the uterine lining, secrete hormones that support pregnancy and recruit blood vessels. However, in *Mfn2*-/- mice, the trophoblast giant cell layer is sparse and incomplete, resulting in placental insufficiency. Moreover, trophoblast cells present a fragmented mitochondrial network (Chen et al., 2003; Chan, 2006).

Meox2-Cre/Mfn1^{loxP} mice where Mfn1 is deleted only after embryonic stage E7 can develop to adulthood with no obvious defects (Chen et al., 2007c). In contrast, Meox2-Cre/Mfn2^{loxP} mice show premature death and severe defects in movement and balance, supported by the loss of Purkinje cells of the cerebellum and indicating a key role for Mfn2 in neurons. Also in *Zebrafish,* global *mfn2*-knockdown embryos present motor impairment, in addition to morphological defects and in motor axons and muscles abnormalities (Vettori et al., 2011). Taken together, these *in vivo* findings findings support the idea that both mitofusins are essential for development and underlie the nonredundant functions of MFN1 and MFN2.

3.1.4.4 Role in apoptosis

MFNs seem to play different roles also in apoptosis. Recent works show that early in the course of cell death, MFN1 mediated fusion is suppressed and the concomitant overexpression of both mitofusins protects from apoptosis induced by intrinsic stimuli like BID and etoposide (Sugioka et al., 2004). It has also been reported that MFN2 is present at mitochondrial fission sites during apoptosis, together with DRP1 and BAX

(Karbowski et al., 2002; Karbowski et al., 2006). MFN2 and its constitutively active mutant MFN2^{RasG12V} inhibit BAX activation, cytochrome *c* release and cell death progression (Neuspiel et al., 2005). Finally, BAX and BAK interact with MFN2, but not MFN1 in a high molecular weight complex. In sum, data gathered until now do not show a prominent role for MFN1 during apoptosis. This idea is reinforced by data, showing that *Mfn1*-/- cells are as susceptible as their wt counterparts to apoptosis and that OPA1 protects from apoptosis independently of MFN1 (Frezza et al., 2006).

3.1.4.5 Roles of MFN2 not shared with MFN1

In contrast to MFN1, MFN2 has been related to several cellular functions such as oxidative metabolism, cell cycle, mitochondrial axonal transport and ER-mitochondria calcium signalling.

Oxidative metabolism

Initial studies by the group of Antonio Zorzano reported altered glucose oxidation upon changes in Mfn2 expression in *in vivo* and *in vitro* models (Bach et al., 2003a; Pich et al., 2005). Mfn2 loss-of-function was reported to reduce oxygen consumption, oxidation of glucose, pyruvate and fatty acids. Other studies confirmed a correlation between Mfn2 levels and different physiological and pathophysiological conditions linked to metabolism, which we had already discuss above.

Cell cycle

In vascular smooth muscle cells (VSMC) with genetic hypertension MFN2 was named hyperplasia suppressor gene (HSG) due to its potential role as regulator of VSMC proliferation (Chen et al., 2004b); MFN2 is downregulated in proliferating VSMCs, and overexpression of Mfn2 in VSMCs blocks cell cycle by inhibiting the downstream RAS signalling pathway. In this model MFN2 leads to inactivation of the ERK1/2 cascade and to cell cycle arrest in G0/G1, independently of its mitochondrial localization. Moreover, MFN2 expression levels regulate VSMC proliferation *in vivo* in response to arterial injury, and VSMC proliferation in an animal model of artherosclerosis results in the suppression of MFN2 expression.

These observations implicate that dysregulation of MFN2 is a main contributor in proliferative cardiovascular disorders and suggest a possible contribution for MFN2 in proliferation disorders, such as cancer.

Mitochondrial axonal transport

Expression of disease alleles of Mfn2 were reported to cause defects in mitochondria distribution in motor neurons of transgenic mice (Detmer, 2008). Recently it was reported that in *Mfn2-/-* neurons mitochondria movement is impaired: *Mfn2-/-* mitochondria seem to stop frequently or to move at slow rate in both anterograde and retrograde directions (Misko, 2010b). However this defect is rescued by expression of either Mfn1 or Mfn2, so it seem that both mitofusins may influence mitochondrial transport, and there is still not evidence that this function is not related to their main role in controlling the morphology of the organelles.

ER-mitochondria tethering

Lack of *Mfn2* resulted in alterations of the ER morphology, as shown by a recent paper from our lab (de Brito and Scorrano, 2008e). MFN2 is selectively enriched in mitochondria-associated-membranes (MAMs), patches of ER membranes tethered to mitochondria, where multiple lipid biosynthetic enzymes that shuttle their products to the outer mitochondrial membrane also reside. In this context, endoplasmic reticulum resident MFN2 acts in trans with MFN1 and MFN2 localized on outer membranes of mitochondria, mediating the tethering between the two organelles. ER-mitochondria apposition is necessary for correct calcium signalling in the cell. Lack of Mfn2 results in an increase of ER calcium content and decrease rate of mitochondria calcium uptake. This raised the possibility that alteration of calcium homeostasis can be the cause of some specific phenotypes caused by depletion of Mfn2 (de Brito and Scorrano, 2008f).

3.2 ER-mitochondria interaction

The analysis of a wide variety of plant and animal tissues revealed close relationships between mitochondria and ER already in the late Sixties (Ruby et al., 1969). The frequency and appearance of these contacts led some researchers to propose that the OMM was an extension of the ER (Bracker and Grove, 1971). In

1973 Lewis and Tata demonstrated that mitochondria are enmeshed or entangled by the ER and that this association might have a functional relevance (Lewis and Tata, 1973). Electron microscopy recently confirmed that ER tubules surround mitochondria within about 200 nm of distance (Wang, 2000).
As much as 20% of the mitochondrial surface is in direct contact with the ER (Rizzuto et al., 1998b) underscoring the existence of a functional role of this association between the ER and mitochondria (Rizzuto et al., 1998c); it is now well documented that ER and mitochondria cooperate with each other in the control of physiological functions like metabolism, calcium signalling and apoptosis.
This crucial biological functions take physically place in ER-contiguous membranes tightly associated with the mitochondria which were christened mitochondria associated membranes (MAMs) by Jean Vance, who investigated for the first time their role in the exchange of phospholipids (Vance, 1990). Several studies proposed that MAMs associate with contact sites between IMM and OMM (Ardail et al., 1991; Ardail et al., 1993; Gaigg et al., 1995). Evidence supports the hypothesis that this reciprocal organelle-docking depends on the expression on both membranes of complementary proteins that link the two organelles together, possibly at specific sites (Pizzo and Pozzan, 2007).

3.2.1 MAMs as sites of phospholipids exchange

The distribution of enzymes responsible of phospholipids synthesis and conversion between ER and mitochondria suggests the existance of a constistent exchange of lipids between the two organelles. For example cholesterol is synthesized by enzymes which are located in the ER membranes, but the conversion of this phospholipid to pregnenolone takes place in on mitochondria, where cytochrome P450 scc resides (Thomson, 2003). Many other enzymes, which are involved in phospholipids metabolism, were reported to be enriched on MAMs: phosphatidylserine synthase-1 and -2 (Voelker, 2003) diacylglycerol acyltransferase and acylcoenzymeA (Rusinol et al., 1994), fatty acid CoA ligase 4 (FACL4). Altogether, strong evidences support the idea that mitochondria-ER interactions play a key role in controlling the metabolism of different cases of lipids and reinforce the hypothesis that exchange of phospholipids between membranes of different organelles may occur through the direct contact between the donor and the acceptor

membrane without the involvement of an intermediate partner like proteins or vescicles.

3.2.2 Role of MAMs in Ca^{2+} exchange

The involvement of ER and mitochondria in the maintenance of the cytosolic calcium concentration ($[Ca^{2+}]_{cyt}$) is fundamental for cell signalling and survival. $[Ca^{2+}]_{cyt}$ can increase after influx from the extracellular space or release from ER through inositol 1,4,5-trisphosphate receptors (IP_3Rs) channels. These form clusters throughout the ER membrane and their distribution can vary, depending on cell differentiation state and stimulation degree.

Mitochondria are $[Ca^{2+}]_{cyt}$ sensors and act as Ca^{2+} buffer. The $[Ca^{2+}]_m$ uptake occurs through an uniporter channel, localized in the IMM, and it depends on the mitochondrial membrane potential generated by the electrochemical gradient across the IMM, and is influenced by the organelle morphology. Ca2+ uptake can stimulate ATP production, steroid hormone biosynthesis (Jouaville et al., 1999) and transport of metabolites, or inhibit exocytosis in adrenal cells. Furthermore, it can induce or inhibit the IP_3Rs-mediated ER Ca^{2+} ($[Ca^{2+}]_{ER}$) release. On the other hand $[Ca^{2+}]_m$ overload can lead to permeability transition pore (PTP) opening, mitochondrial swelling, depolarization or activation of many types of cell death (Petit et al., 1998). Cite Bernardi phys review

$[Ca^{2+}]_{ER}$ is transferred from ER to a distinct subpopulation of mitochondria in close apposition with it (Filippin et al., 2003). Mitochondrial uniporter channel has a low affinity for Ca^{2+}, but the presence of high calcium microdomains in the proximity of IP_3Rs, that are partly enriched in ER-mitochondria contact sites, can explain the fast $[Ca^{2+}]_m$ uptake (Rizzuto et al., 1993).

Several factors can regulate this Ca^{2+} exchange. The voltage-dependent anion channel (VDAC), present in the OMM and enriched in MAMs (Rapizzi et al., 2002), when overexpressed, can accelerate the $[Ca^{2+}]_m$ entrance (Drummond et al., 2000). On the other hand, the ablation of type-3 IP_3Rs, that are specifically localized in MAMs, reduces the IP3-mediated $[Ca^{2+}]_m$ uptake in CHO cells (Mendes et al., 2005). Moreover the binding of VDAC1 to type-1 IP_3Rs through the fraction of the mitochondrial chaperone grp75 associated with the OMM, as well as the

overexpression of the cytosolic fraction of grp75, enhances the $[Ca^{2+}]_m$ uptake (Szabadkai et al., 2006).

3.2.3 MAMs as linkage between dependent ER-mitochondria Ca2+ exchange and apoptosis

Given that the regulation of physical distance between ER and mitochondria influences the amount of exchanged Ca^{2+}, this can impact on Ca^{2+}-dependent pathways (Csordas et al., 2006), like mitochondria-dependent cell death. Indeed, several reports show that increasing ER-mitochondria proximity facilitates the $[Ca^{2+}]_m$ uptake and consequently the activation of apoptosis, while the loosening of this strict interrelashionship has a prosurvival effect. The ablation of IP_3Rs in DT40 cells protects against apoptosis (Boehning et al., 2003), and their phosphorylation by the protein kinase Akt reduces their Ca^{2+}-release potential and has a pro-survival effect (Khan et al., 2006). These data confirm the essential role of these channels in mediating $[Ca^{2+}]_{ER}$ release and the consequent $[Ca^{2+}]_m$ uptake-dependent cell death. Several other factors are involved in the regulation of ER-mitochondria Ca^{2+} exchange-mediated apoptosis. For example, VDAC overexpression favors the $[Ca^{2+}]_m$ uptake in apoptosis-sensitive cells (Voehringer et al., 2000). Further, VDAC promotes PTP opening and cytochrome *c* (cyt *c*) release upon oxidative stress (Madesh and Hajnoczky, 2001). On the other hand, free cyt *c* in the cytosol can bind to the IP_3Rs, stimulating $[Ca^{2+}]_{ER}$ release. A recent study shows that the ablation of a specific isoform of the promyelocytic leukemia (PML) tumor suppressor, enriched in MAMs, has a pro-survival effect, caused by a reduction of IP3Rs-mediated $[Ca^{2+}]_{ER}$ release (Giorgi et al., 2010).

$[Ca^{2+}]_m$ can activate DRP1. The activation of DRP-1 and the induction of apoptosis can be mediated by caspase-8 cleavage of BAP31, an integral protein of the ER, forming a p20 fragment, or by caspase-8-dependent activation of tBID, that stimulates mitochondrial cyt *c* release. BIK, a pro-apoptotic Bcl-2 protein localized in the ER, can stimulate the ER Ca^{2+} release-dependent activation of DRP-1, or it can activate with NOXA the Bax-dependent release of cyt *c* from mitochondria (Germain et al., 2005).

The close relationship between Ca^{2+} exchange between ER and mitochondria and cell death involves also some Bcl-2 family proteins, key players in the regulation of

apoptosis, localized on mitochondria or ER. Indeed, some Bcl-2 members can regulate the opening of VDAC (Vander Heiden et al., 2001), while the anti-apoptotic protein Bcl-2 can control the phosphorylation state of type-1 IP_3Rs (Oakes et al., 2005) and the pro-apoptotic factor tBID promotes the IP3-mediated $[Ca^{2+}]_m$ uptake (Csordas et al., 2002).

Moreover, the overexpression of anti-apoptotic or the reduction of pro-apoptotic Bcl-2 proteins reduce $[Ca^{2+}]_{ER}$ and consequently the $[Ca^{2+}]_m$ uptake, inhibiting Ca^{2+}-dependent apoptosis (Scorrano et al., 2003).

3.3 *Drosophila melanogaster*: a model organism

Drosophila melanogaster is emerging as one of the most effective tools for analyzing the function of human disease genes, including those responsible for developmental and neurological disorders, cancer, cardiovascular disease, metabolic and storage diseases, and genes required for the function of the visual, auditory and immune systems. Although apparently different, humans and flies are very similar in crucial aspects. Key molecular pathways required for the development of a complex animal, such as patterning of the primary body axes, organogenesis, wiring of a complex nervous system and control of cell proliferation are highly conserved between flies and vertebrates. Similar developmental mechanisms act throughout bilaterally symmetric Metazoa to accomplish several important processes that include: specifying segment identity along the anterior-posterior axis; subdividing the ectoderm into neural versus non-neural domains along the dorsal-ventral axis; defining the primary axes from the body wall, organizing complex structures such as eyes, heart and liver; guiding the initial outgrowth of axons with respect to the midline of the nervous system; and, potentially, controlling basic behavior such as sleep or substance abuse.

Genes controlling these basic developmental processes are highly conserved between *Drosophila* and humans, supporting the potential role of flies as a model for studying human diseases. In 2001 a Blast analysis of 929 human disease genes listed in the Online Mendelian Inheritance in Man (OMIM) was performed against the fly data base (Reiter et al., 2001). This analysis revealed that 75% (defined by matches with expectation values (E-VALUE) ≤ 10^{-10}) of all human disease genes have related sequences in *D.melanogaster*; nowadays this percentage may have

increased as a consequence of the renewal of the annotation of human disease genes and of the fly database.

3.3.1 Advantages of *Drosophila melanogaster*

Beyond the strong conservation of gene sequences and developmental pathways with humans, *Drosophila* has also several experimental advantages, which support its scientific value as a model for studying human diseases: flies have a short life cycle (fig. 2), which takes about 15 days from the lay of the egg to the adult eclosion from the pupa; their maintenance has low costs as compared to mammalian models; they are small and easy to handle and allow the generation of large numbers of individuals that can be used for sophisticated genetic screens. If the altered expression of a human disease gene generates abnormal clearly visible phenotypes (such as defect in the structure of the eyes or wings malformations) in the fly, that can be used in conjunction with the rich genetic toolbox that have been developed in the last 90 year in the *Drosophila* research field to identify pathways that contribute to the pathology. This approach is unbiased, i.e., it is completely independent upon prior assumptions about mechanisms underlying the disease.

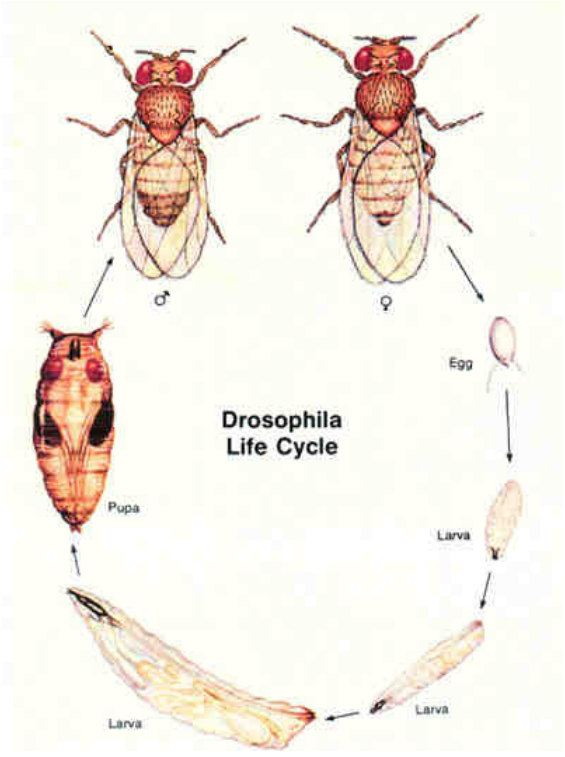

Figure 2 - Life cycle of *Drosophila melanogaster*
The eggs, which are about 0.5 millimetres long, hatch after 12–15 hours (at 25 ℃ or 77 ℉). The resulting grow for about 4 days (at 25 ℃) while molting twice (into 2nd- and 3rd-instar larvae), at about 24 and 48 h after hatching. Then the larvae encapsulate in the puparium and undergo a four-day-long metamorphosis (at 25 ℃), after which the adults eclose (emerge).

3.3.2 Creating models for human disease in *Drosophila*

Two main approaches can be used in *D.melanogaster* to create a model for human disease. First, 'forward-genetic' approaches can be applied. Usually, mutagenizing agents or transposable elements are used to generate a large-scale number of mutant flies. Screenings for the desired disease phenotype (for example, brain degeneration in the case of neurodegenerative disorders) are set up. Once the desired mutant flies have been selected, one can proceed to the identification of mutant genes, presumably involved in the generation of the phenotype of interest. Human homologues of the identified *Drosophila* gene products are plausible candidates for involvement in the disease that is being investigated. Many disease models were developed through this approach (Barinaga, 1999).

Alternately, when the disease genetic agent is known, 'reverse genetics' can be applied. Overexpression of dominant negative mutation or downregulation of a gene product may be used to screen for genetic interactors, after identification of a "scorable" phenotype (such as alteration of organization of cells in the eye). This approach is accomplished thanks to The Vienna Drosophila RNAi Center (VDRC), a joint initiative of the Institute of Molecular Biotechnology (IMBA) and the Research Institute of Molecular Pathology (IMP), which developed a Drosophila transgenic RNAi library. Moreover, the use of the binary system GAL4/UAS (Fig.3) is a major tool in reverse genetics, because it allows the ectopic expression of a transgene in a specific tissue or cell type. Geneticists created genetic varieties of fruit flies, called *GAL4 lines*, each of which expresses the yeast transcriptional activator GAL4 in some subset of the fly's tissues.

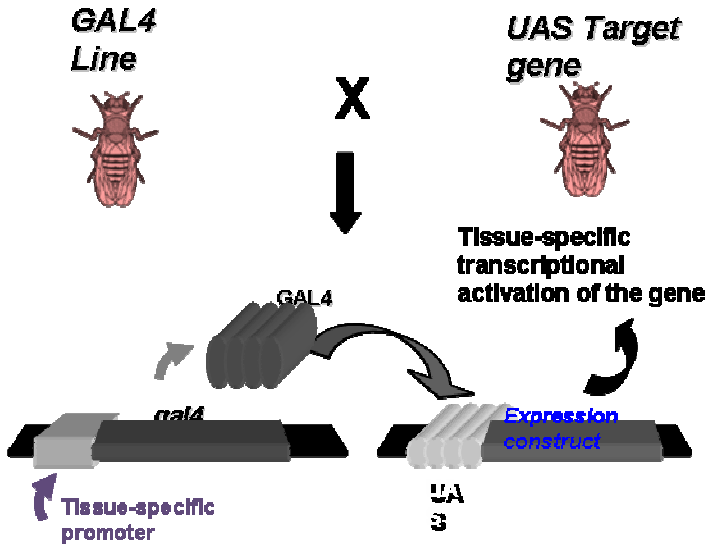

Figure 3 - GAL4/UAS system. Two transgenic fly lines are created. In the first (UAS–human-transgene fly), the human disease-related transgene is placed downstream of a UAS activation domain that consists of GAL4-binding sites. GAL4 is a yeast transcriptional activator; in the absence of ectopically expressed GAL4, the transgene is inactive in these transgenic flies. The transgene is activated by crossing these flies to transgenic flies that express GAL4 (enhancer-trap GAL4 fly), also known as the 'drivers'.

Likewise, *reporter lines* have been created, strains of flies with the special UAS region next to a desired gene. This is often GFP, a green fluorescent protein, or RFP, a red protein. Many of these lines are available at the Bloomington *Drosophila* Stock Center.

Homologous recombination is also used to generate *null*-mutant flies. This technique is mainly achieved by the use of the yeast FLP recombinase, which catalyzes recombinations between two FRT (FLP recombination target) sites (Rong and Golic, 2000).

3.3.4 Mitochondrial dynamics in *D.melanogaster*

As described above, the first mitofusin identified was found in the fruitfly. Fzo is expressed only in primary spermatids, and disappeared just at the end of meiosis and in the early stage spermatids (Hwa et al., 2002). During meiosis the small and numerous mitochondria of spermatocytes associate and aggregate behind the nucleus and fuse into two giant mitochondria that form the Nebenkern, which resembles an onion slice of concentric layers when viewed in cross section by transmission electron microscopy. In *fzo* mutant spermatids, mitochondria fail to fuse and wrap each other separately forming a structure resembling 'fuzzy onions'. This defect in mitochondria fusion results in male sterility. Thus, Fzo seems specifically

required for spermatids differentiation, and its expression is regulated by *Drosophila cannonball (can)* gene, involved in the control of mechanisms that coordinate the onset of testes development (White-Cooper et al., 1998)

On the contrary, DMarf mRNA levels are not changed in *can* mutant spermatids. In the embryos, DMarf transcripts are detectable in the pre-blastoderm, as a result of maternal contribute (Hwa et al., 2002). In the zygote, its mRNA is found since stage 8, and spreads in anterior and posterior midgut primordial and mesoderm after stage 11. It is also detectable in the developing gut, in midgut and in traces in somatic and pharyngeal muscle. The broader pattern of expression of DMarf let *Drosophila* scientists speculate a more widespread involvement of the protein in the mitochondrial fusion machinery.

In fact, recent studies on interaction between Parkinson's disease genes and mitochondrial dynamics demonstrated a major function for DMarf in mitochondrial fusion in muscle tissue (Deng et al., 2008b). Different independent groups found that loss of fusion machinery, Opa1 or Marf alone, partially rescued parkin or PINK phenotypes (Deng et al., 2008a) (Park et al., 2009; Poole et al., 2008; Yang et al., 2008). Single overexpression of either of the two proteins did not rescue PINK mutant phenotype (Park, 2009). Moreover DMarf is supposed to be ubiquitinated by Parkin (Ziviani et al., 2010).

Recently a study on the role of mitochondrial fusion in *D.melanogaster* heart revealed that depletion of either *Marf* or *Opa*-1 causes also heart dilation with severe contractile impairment. Marf-depleted cardiomyocytes have fragmented and clustered mitochondria, which result in a distortion of the myofibrillar architecture. A more severe cardiomyopathy was described in *Opa1-RNAi* flies, suggesting that additional mechanisms participate in the generation of the phenotype. Our knowledge of the function of the Opa1 *Drosophila* homologue came from the investigation of the effects of its heterozygous mutation in eye, heart and muscle. *Opa1*-depleted eyes were morphologically altered in pigmentation and showed visual dysfunction, which seems to correlate with an increase in ROS production. Heterozygous mutation of *Opa1* results also in decreased heart rates and increased arrhytmias that were not affected by antioxidant treatment (Shahrestani et al., 2009).

Not only fusion, but also the fission machinery plays a major role during spermatogenesis, as confirmed by studies on *Drp1* mutant spermatids. In wild-type spermatids, after the two giant mitochondria formation promoted by Fzo, the

Nebenkern unfurls and changes shape as a consequence of mitochondria fission and dispersion. *Drp1*^{KG03815} spermatocytes contain abnormally clustered mitochondria that fail to segregate properly during meiosis and to unfurl during spermatid elongation (Aldridge et al., 2007). This phenotype is consistent with the possibility that active Drp1-mediated fission is required to balance fusion and to separate the mitochondrial aggregate into individual organelles seen in mature primary spermatocytes.

Clusters of mitochondria unable to divide were also detected in photoreceptors soma of *Drp1* mutant flies (Verstreken et al., 2005). On the contrary, absence of Drp1 activity results in less mitochondria in synaptic buttons. *Drp1* mutants fail to maintain normal neurotransmission during intense stimulation and show alteration in the mobility of reserve vescicles pool of neuromuscular junctions.

4.Results

Marf, the single mitofusin of *D. melanogaster,* is selectively complemented by Mitofusin 2.

Valentina Debattisti[1,2,], Diana Pendin[3], Maria Giovanna Rossetto[3], Andrea Daga[3] and Luca Scorrano[1,2,4]

[1]*Dulbecco-Telethon Institute*

[2]*Venetian Institute of Molecular Medicine, Via Orus 2, 35129 Padova, Italy*

[3]*Eugenio Medea Scientific Institute, Conegliano 31015, Italy*

[4]*Department of Cell Physiology and Medicine, University of Geneva, 1 Rue M. Servet, 1211 Geneve, Switzerland*

Running title: Complementation of fruitfly Marf by mitofusin 2

Character counts: 43895

Address correspondence to Luca Scorrano. Email: luca.scorrano@unige.ch or to Andrea Daga. Email:daga@unipd.it.

Summary

Two outer membrane mitofusins (Mfn) mediate fusion of mammalian mitochondria, while lower eukaryotes possess only one homologue. Despite the involvement of the two mammalian Mfns in different cellular processes, it is still unclear if they are functionally interchangeable and what is the ancestral Mfn. Here we show that human Mfn2, but not Mfn1 complements *D. melanogaster* lacking the single mitofusin Marf. Ubiquitous, neuron and muscle specific ablation of Marf was lethal, altering mitochondria and endoplasmic reticulum (ER). A similar phenotype characterized flies overexpressing human Mfns and a Mfn2 mutant associated with the peripheral neuropathy Charcot-Marie-Tooth IIa. However, only Mfn2 rescued the developmental and functional defects in flies lacking Marf. While both Mfns corrected mitochondrial morphology, ER shape was recovered only by Mfn2. Thus, our data identify Mfn2 as the closest functional homologue of the single fruitfly mitofusin and substantiate *in vivo* the functional difference between the two mammalian Mfns.

Introduction

Mitochondria are metabolic and signalling hubs of the cell. Emerging evidence support an intimate relationship between their multifaceted functions and their morphology and ultrastructure: their critical roles in energy conversion, Ca2+ signalling, amplification of cell death, cell cycle progression all depend on the morphology of the organelle (Campello and Scorrano, 2010). Shape and ultrastructure of mitochondria are finely tuned by a growing family of proteins, conserved among eukaryotes, originally discovered in yeast (Westermann, 2010), that impinge on the fusion-fission balance of the organelle and whose mutations in humans are associated with a number of genetic diseases (Liesa et al., 2009).

While mammalian mitochondrial fission appears to be mediated by a single protein, dynamin related protein 1 that translocates from the cytoplasm to mitochondria, assembles into oligomers and fragments the organelle (Smirnova et al., 2001), fusion is more complicated and requires the coordinated interplay of at least three proteins. Mitofusins (Mfns) are large integral OM GTPases which control mitochondrial fusion and morphology (Santel and Fuller, 2001;Santel et al., 2003), together with the inner mitochondrial membrane dynamin-related protein Opa1 (Olichon et al., 2002). Mammals possess two Mfns (Mfn1 and 2) which are 63 % identical but do not seem to display redundant functions. The control of mitochondrial oxidation (Bach et al., 2005) and the anti-proliferative effect (Chen et al., 2004) by Mfn2 are not shared by Mfn1. Moreover, while mitochondrial fusion mediated by the inner mitochondrial membrane Opa1 requires Mfn1 (Cipolat et al., 2004), Mfn2 is enriched in subdomains of the outer membrane of mitochondria in close apposition to the endoplasmic reticulum (ER) and directly links mitochondria to the ER (de Brito and Scorrano, 2008b). Finally, mutations in MFN2 are associated with the peripheral Charcot-Marie-Tooth type IIa (CMTIIa) neuropathy (Zuchner et al., 2004). Both Mfns

are essential for embryonic development and mice deficient in either gene die in mid-gestation, but *Mfn2-/-* embryos display also deficient placentation (Chen et al., 2003). Interestingly, all vertebrates possess two mitofusins, whereas only one is retrieved in almost all invertebrates reigns.

The *S. cerevisiae* orthologue of mitofusins *fuzzy onions* (Fzo1p) mediates mitochondrial fusion events during mitotic growth and mating and is required for long-term maintenance of mitochondrial DNA (Hermann et al., 1998;Rapaport et al., 1998). In *C.elegans* a null-mutation of *Fzo-1* results in slow growth, reduced brood sizes, and high percentages of embryonic lethality (Breckenridge et al., 2008). The nematode mitofusin was discovered through its sequence homology to the *Drosophila fzo* gene, the first identified mediator of mitochondrial fusion (Hales and Fuller, 1997). In spermatocytes *Fzo* mediates the fusion of mitochondria into two giant organelles that form a structure called Nebenkern, which is required to give energy to the flagellum of the spermatid. In *fzo* mutant flies, mitochondria fail to fuse and wrap each other as many fragmented organelles, giving the impression of 'fuzzy onions' when viewed at the electron microscopy. Another Mfn homologue has been identified in *D.melanogaster*. This second homologue, christened *mitochondrial assembly regulatory factor (Marf)* has a broader pattern of expression compared to Fzo, which is expressed only in spermatocytes. Moreover, while Fzo displays 35% of identity with human Mfns, identity between DMarf and both human Mfns is higher, reaching 47% and making it a natural candidate to participate in mitochondrial morphogenesis in tissues other than the spermatocytes (Hwa et al., 2002). The first evidence that DMarf can regulate mitochondrial dynamics regulation came from studies on the role of Mfns in the mitochondrial quality control pathway controlled by PINK1/parkin (Deng et al., 2008). DMarf was found to be upregulated in PINK or parkin mutant flies and to be ubiquitinated by Parkin (Ziviani et al., 2010). Ubiquitous

ablation of DMarf is lethal, with all flies dying before pupation; selective ablation in the heart impairs mitochondrial morphology and cardiac function, which are recovered by both human Mfns, albeit complementation by Mfn2 appears more efficient (Dorn et al., 2011). Thus, the questions of whether the two mammalian Mfns are functionally interchangeable and the functional divergence observed in mammals as well as the different phenotypes caused by their ablation in the mouse are simply linked to their different expression pattern, as previously suggested (Chen et al., 2007) remain unanswered. Moreover, the phylogenetic relationship between the two Mfns of higher metazoans and the single one retried in the invertebrates is similarly unclear. We therefore decided to use *Drosophila* as a tool to address the function of its Mfn and to explore the phylogenesis of mammalian Mfns. Our data indicate that while all eukaryotic Mfn tested can complement the functions of the two mouse Mfns, only Mfn2 is able to correct developmentally and functionally the ablation of DMarf that impairs not only mitochondrial, but also endoplasmic reticulum morphology. Thus, our analysis confirms that Mfn2 has a broader spectrum of action than Mfn1 also *in vivo* and places it phylogenetically closer to the Mfn of the lower metazoan *Drosophila*.

Results and discussion

Correction of mitochondrial morphology in *Mfn1* and *Mfn2*$^{-/-}$ cells by lower eukaryotic Mfns.

Our knowledge of the emergence of two vertebrate Mfns from the single one found in invertebrates is scarce, despite the importance of Mfns in several cellular processes, from metabolism, to apoptosis, to tethering to other organelles (de Brito and Scorrano, 2008a). Moreover, the association between mutations in Mfn2 and CMTIIa further substantiates its importance in human biology (Zuchner et al., 2004). At the same time, in vivo models to test and evaluate pathogenesis and potential therapeutic strategies of CMTIIa are required. To start to address the problem of phylogenesis of Mfns we explored if mitochondrial fragmentation observed in cells lacking the mouse Mfns could be complemented by one vertebrate (*Xenopus laevis*) and two invertebrate (*D.melanogaster* and *S.cerevisae*) Mfns. A ClustalW analysis indicated that *Xenopus* Mfn1 (XMfn1) shares 84% of homology with hMfn1 (Fig S1A), whereas *Xenopus* Mfn2 (XMfn2) has a similarity of 93% to hMfn2 (Fig S1B). *Drosophila* Marf (DMarf) shares the same percentage (64) of sequence homology with both mammalian Mfns, whereas as expected sequence similarity resulted slightly lower in the case of *S. cerevisae* Fzo1p (46% of homology with hMfn1 and 50% of homology with hMfn2) (Fig. S1). Co-expression of Fzo1p, DMarf, XMfn1 and XMfn2 with a mitochondrially targeted yellow fluorescent protein (mtYFP) in mouse embryonic fibroblasts (MEFs) lacking *Mfn1* or *Mfn2* resulted in comparable expression levels of among the Mfns from the three organisms and in both cell lines (Fig. 1A). All the Mfns tested could rescue the fragmented *Mfn1*$^{-/-}$ or *Mfn2*$^{-/-}$ mitochondria (Fig. 1B and quantification in C,D). It should be noted that both visual

inspection and quantification revealed that hMfn1 was more powerful in *Mfn1*$^{-/-}$ MEFs, whereas hMfn2 was more effective in *Mfn2*$^{-/-}$ cells, as previously reported (Chen *et al.*, 2003). Interestingly, this differential potency was shared by the *Xenopus* Mfns, while Mfns from *D. melanogaster* and *S. cerevisiae* were equally efficient in *Mfn1* an *2*$^{-/-}$ cells. Thus, Fzo1p, DMarf, XMfn1 and XMfn2 can complement either mouse *Mfns*, demonstrating that the pro-fusion activity is conserved along evolution.

DMarf recovers ER morphology in *Mfn2*$^{-/-}$ MEFs.

The altered ER morphology that characterizes *Mfn2*$^{-/-}$ MEFs is recovered by hMfn2 or by an ER-targeted variant of hMfn2 (hMfn2^{YFFT}), independently from the correction of mitochondrial shape, but not by hMfn1. In fact, Mfn2 is partially localized on ER and is enriched in mitochondrial-associated-membranes (MAMs), patches of ER membranes tethered to mitochondria (de Brito and Scorrano, 2008b). We therefore wished to address whether DMarf, the single OM fusion protein closest in evolution to mammalian Mfns, could similarly complement ER morphology. Upon co-transfection of *Mfn2*$^{-/-}$ MEFs with DMarf-V5 and an ER-targeted yellow fluorescent protein (ERYFP) the three-dimensional (3D) reconstruction and volume rendering of confocal stacks of ERYFP showed that DMarf was able to recover ER morphology as efficiently as hMfn2, as shown by morphometric analysis (Fig. 1E). Importantly, DMarf is mainly localized on mitochondrial membranes, but it is also retrieved like hMfn2 at the points of contact between ER and mitochondria (Fig. S2) (de Brito and Scorrano, 2008b). Thus, the fruitly Mfn can correct the multiple, ER and mitochondrial defects of *Mfn2*$^{-/-}$ cells.

Loss of Dmarf in vivo is lethal, altering mitochondrial morphology and distribution

Constitutive ablation of mammalian Mfns in the mouse affects placentation and intrauterine development (Chen et al., 2003). Interestingly, conditional post-placentation deletion of either Mfns highlights important differences between the two: while mice lacking Mfn1 have no overt phenotype, *Mfn2*$^{-/-}$ mice develop a spontaneous Purkinje cell degeneration leading to death between postnatal days 1 and 17 (Chen et al., 2007). These results raised the question of whether mammalian Mfns function in a tissue specific manner to mediate mitochondrial fusion, or whether the functional difference that has been outlined in cellular models occurs also *in vivo*. DMarf function *in vivo* has been partially characterized in adult muscle tissues and dopaminergic neurons (Deng et al., 2008;Park et al., 2009), as well as in cardiomyocytes (Dorn et al., 2011). However, a comprehensive analysis of the effect of ablation of DMarf in multiple tissues has not been performed yet. Therefore, we made use of UAS-*DMarf*-RNAi transgenic flies, where the expression of the transgene (the RNAi in this case) can be controlled in space and time using the Gal4-UAS system REF. Effective knockdown of *DMarf* in S2 cells was confirmed by immunoblotting using a specific anti-DMarf antibody (Fig. 2A) and resulted in mitochondrial fragmentation (Fig. 2B), indicating that *Drosophila* DMarf has a major function in the regulation of mitochondrial morphology. Immunoblotting confirmed that the same RNAi was effective in the ablation of DMarf *in vivo* (Fig. S3A), allowing us to explore its function *in vivo* using the UAS tool described above. Ubiquitous, nervous system and muscle specific downregulation of DMarf was lethal; the distribution among developmental stages of the DMarf-deficient individuals showed that when DMarf was ablated in the muscle the phenotype was less severe (Fig. 2C). All DMarf-depleted larvae were small and sluggish (data not shown). To gain insight into the morphological details accompanying this lethal phenotype, we analysed mitochondrial shape at larval stage by crossing the *DMarf*-RNAi conditional flies with

UAS-mitochondrial green fluorescent protein (mtGFP) reporter lines. Confocal imaging of the ventral ganglion showed clustered mitochondria appeared in *DMarf*-RNAi neuronal cell bodies (Fig. 2D, upper magnified panel). Axons projecting out from the ganglion had small or clumped mitochondria (Fig. 2D, lower panel). This resulted in a severe depletion of the organelles inside neuromuscular junctions (NMJs) of muscle 6 and 7 (Fig. 2E and F). Muscles were also affected: smaller than in wild-type larvae, they also displayed altered mitochondrial architecture along the sarcomere, with marked clusterization of the organelles in perinuclear regions (Fig. 2E). The decreased muscle size could be a consequence of the primary mitochondrial defect, or of the "functional" denervation caused by the lack of mitochondria in the synapses. The impaired mitochondrial neuronal trafficking has been reported in mice as well as cell lines expressing lower levels of Mfn2, or pathogenic versions of the protein (Baloh *et al.*, 2007;Detmer *et al.*, 2008;Cartoni *et al.*, 2010). Our data further corroborate that intact mitochondrial fusion/fission is required to maintain axonal transport of the organelle and suggest that transport could be altered as a consequence of the abnormal clumping of mitochondria in cell bodies.

Since both neurons and muscle are affected by ubiquitous deletion of DMarf, we wished to separate their relative contribution to the lethal phenotype, by expressing *DMarf*-RNAi in each tissue separately under the control of the Elav-Gal4 and Mef2-Gal4 driver lines. Downregulation in both tissues was lethal; however Mef2-driven depletion allowed some escapers to survive and arrested development at a later stage (Fig. 2C). Nervous system specific DMarf-depleted individuals could not develop into adults, but died as pupae. As expected, mitochondria clusterized in neuronal cell bodies (Fig. S4), and were absent in the NMJs of muscles 6 and 7. The muscular phenotypes caused by ubiquitous Marf knockdown were confirmed in Mef2-

Gal4/UAS-*DMarf*-RNAi larvae. Again, mitochondria were massively clumped around nuclei and their organization in sarcomeric bands was lost (Fig. 2G). In conclusion, ubiquitous as well as tissue specific depletion of DMarf affects development and tissue organization. While the neuronal phenotype might appear prominent, depletion of DMarf in the muscle is sufficient for lethality, calling for a deeper analysis of the alterations caused by the lack of DMarf.

DMarf knockdown alters ER morphology in *Drosophila* larvae

One of the main functional difference between Mfn1 and Mfn2 is the ability of the latter to regulate ER morphology and tether it to mitochondria (de Brito and Scorrano, 2008b). Our data indicate that also DMarf can complement the ER defect of *Mfn2*$^{-/-}$ cells. Thus, an analysis of the role of DMarf in ER morphology *in vivo* was required and to this end we turned to an UAS-ERGFP reporter line that was crossed with the conditional *DMarf*-RNAi flies. Notably, when we inspected by confocal microscopy the architecture of the sarcoplasmic reticulum (SR) in muscles from Tub-Gal4, UAS-ERGFP/ UAS-*DMarf*-RNAi we found it profoundly distorted (Fig 3A). In control muscles, the signal of the ERGFP was distributed along the sarcomeric bands and was retrieved as expected in the nuclear membrane, whereas DMarf depletion resulted in alteration of this ER organization, with punctae of ERGFP randomly localized in the muscle architecture. To exclude that these changes were epiphenomena of a dysfunctional neuromuscular junction leading to muscle degeneration, SR morphology was analysed also in individuals where DMarf was specifically depleted in muscle. In Mef2-Gal4, UAS-ERGFP/ UAS-*DMarf*-RNAi larvae the SR was disorganized exactly as in larvae where DMarf was ablated ubiquitously (Fig 3B), thereby excluding that the phenotype depends on the muscular degeneration secondary to dysfunction of the NMJ. In accordance, the ER was also

altered, with clumps and fragments evident in ganglion cell bodies where DMarf was selectively ablated (Fig. 3C). Thus, systemic and tissue specific depletion of DMarf alters not only mitochondrial, but also ER shape.

Overexpression of hMfns in *Drosophila* differentially affects development and mitochondrial and ER morphology.

Can the developmental and structural defects of DMarf deficient flies be complemented by higher vertebrate Mfns? Can we exploit this complementation assay to address the phylogenesis of mammalians Mfns? To address these questions we needed to generate transgenic lines that overexpressed hMfns. We elected to produce the transgenic lines UAS-hMFN1, UAS-hMFN2 and UAS-hMFN2^{R94Q}, carrying one of the most frequent mutations associated with Charcot-Marie-tooth type IIA (CMT2A) peripheral neuropathy (Zuchner et al., 2004) for which mouse models already exist (Detmer et al., 2008;Cartoni et al., 2010). This mutation is particularly interesting since it dissociated complementation of mitochondrial from ER morphology, being able to correct the former but not the latter in *Mfn2*$^{-/-}$ cells (Detmer and Chan, 2007;de Brito and Scorrano, 2008b). Efficient ubiquitous expression of all UAS-hMFNs was lethal, arresting development at pupa stage (Fig. 4A). All hMfns caused aggregation of mitochondria in neuronal cell bodies and hyperelongated or clumped organelles inside axons (Fig. 4B). Phenotype was more severe in mutant hMfn2 individuals, where the mitochondrial network was completely lost in neuronal cell bodies. However, when we turned to the analysis of NMJs we found that hMfn1, hMfn2 and hMfn2^{R94Q} expression had completely different effects. Mitochondrial organization in muscle 6 and 7 was altered in all the three cases, but less severely in hMfn1 expression (Fig 4B, left panel). Moreover, while NMJs of hMfn2 and hMfn2^{R94Q} overexpressing individuals were depleted of mitochondria,

hMfn1 expression did not alter organelles distribution in the nervous system and mitochondria were retained inside junctions, despite the clumping observed in cell bodies. Finally, ER organization in muscles was not affected in wild-type hMfns expressing larvae. On the contrary, hMfn2^{R94Q} expression altered SR distribution, especially in the perinuclear regions. Thus, despite the fact that all three overexpressants are lethal at the pupa stage, hMfn1 does not alter SR morphology nor reduces mitochondrial content in the NMJs, calling for a more detailed analysis of the effect of tissue specific overexpression of the human Mfns in the fly. Nervous system Elav-Gal4 and muscle Mef2-Gal4 driven expression of all the three UAS-insertions tested allowed individuals to develop into adults, albeit tissue specific expression of mutated Mfn2 gave rise to a more severe phenotype with many individuals dying at pupa when expressed in the muscle, or at larva when expressed in the nervous system (Fig. 4A). In line with the more severe developmental phenotype, the alterations in mitochondrial morphology in hMfn2^{R94Q} overexpressing flies were generally more pronounced than those observed in flies overexpressing wild type Mfns. The analysis of the tissue specific overexpression of wt hMfn1 and 2 and of hMfn2^{R94Q} showed: (i) that mitochondria clumped in the neuronal cell bodies in all the lines tested, but were still retrieved in the NMJs of hMfn1 overexpressing flies (Fig 4C, upper panels); (ii) that ER morphology was conserved in neuronal cell bodies upon nervous system specific expression of hMfn1 and 2, but not of hMfn2^{R94Q} (Fig 4C, lower panels); (iii) that in the case of muscle specific expression of hMfn2^{R94Q} perinuclear aggregation of mitochondria is prominent while it is intermediate in the case of hMfn2 and even less evident for hMfn1. Similarly, ER organization was lost in the case of hMfn2^{R94Q} expression, but not hMfn2 (Fig. 4D, lower panel). In conclusion, the ectopic expression of hMfns in *Drosophila* leads to a complex picture: for example, the expression of hMfn1 and hMfn2 in the nervous

system is not lethal, yet mitochondria clump in neuronal bodies and in the case of hMfn2 are not retrieved in NMJs. Neuronal expression of hMfn2^{R94Q} reproduces the same mitochondrial alterations that Mfn2, but is lethal for the fly. Muscle expression of the transgenes yielded similar results of neuronal expression as for lethality and derangement of mitochondrial and ER structure, expression of hMfn2^{R94Q} being the only lethal one and the one that affects not only mitochondrial but also ER architecture. In conclusion, the outcome in terms of viability of flies expressing hMfns can not be predicted only from their effect on mitochondrial shape and distribution. Their effect on ER morphology should also be taken into account, since its derangement seems to correlate better with lethality. In any case, we could take advantage of the lack of lethality in the case of muscle and neuron specific overexpression of hMfns, using these flies to complement the Marf-depleted ones.

Selective rescue of DMarf depleted *D. melanogaster* by hMfn2.

Muscle and nervous system specific depletion of DMarf is lethal. To verify if mammalian Mfns could rescue Marf depletion, we generated recombinant UAS-*DMarf*-RNAi and UAS-hMFNs-Myc lines. Levels of the expressed Mfns in the brain of the transgenic larvae was efficient, as judged by immunoblotting for the Myc-tag (Fig. S3B). Simultaneous expression of hMFN2 and *DMarf*-RNAi transgenes partially rescued the lethality due to Marf depletion, allowing survival to adulthood of approx. 40% of the individuals (Fig. 5A). In contrast, individuals simultaneously expressing Mfn1 or Mfn2^{R94Q} and DMarf-RNAi in the nervous system or muscle tissues died as pupae, thus displaying a phenotype indistinguishable from that of *DMarf*-RNAi alone. We also checked whether hMfns expressions could ameliorate the impaired locomotory performance of DMarf depleted flies. To this end we turned to the weaker promoter MHC-Gal4 lines, which allowed muscle specific expression of all transgenic

lines we mated, without affecting their viability (not shown); and used a climbing test that is routinely used to measure locomotory and sensory performance in *D. melanogaster* (Orso *et al.*, 2005). MHC-Gal4/+;UAS-*DMarf*-RNAi/+ flies displayed reduced climbing performance compared to control flies starting from day 12. Simultaneous expression of *DMarf*-RNAi and hMfn2 but not of hMfn1 or hMfn2^{R94Q} climbing performance indistinguishable from that of control flies. In conclusion, hMfn2 corrects muscle specific DMarf-deficient flies developmentally and functionally. Recent data indicate conversely that in the hearth both human Mfns are able to correct the cardiomyopathy caused by the lack of DMarf, albeit Mfn2 seems more powerful (Dorn et al., 2011). When we examined the role of DMarf in the heart, we mainly recorded an increased level of arrithmias that was corrected again only by hMfn2 (VD and LS, manuscript in preparation), further corroborating the findings reported here.

What is the morphological counterpart of the DMarf complementation by hMfn2? To answer to this question we turned to the reporter lines described above and inspected both mitochondrial and ER morphology in the transgenic larvae. Mitochondrial morphology was only slightly recovered, maybe because the levels of overexpressed hMfns outbalanced the downregulation of DMarf. hMfn1 and hMfn2 only slightly ameliorated the clumped mitochondria in neuronal cell bodies and axons found in to *DMarf*-RNAi alone (Fig. 5C). Conversely, simultaneous expression of *DMarf*-RNAi and hMfn2^{R94Q} resulted in massive clusterization of mitochondria, a phenotype even more severe than that observed in DMarf-RNAi flies. The mitochondrial network was disorganized in muscles 6 and 7, with perinuclear organelle aggregation in all the genotypes analyzed, except that in hMfn2 rescued individuals (Fig. 5C, lower panel and 5G). We analyzed also mitochondrial distribution in NMJs: when ubiquitously or neuronally expressed, hMfns were not able

to rescue the depletion of NMJ mitochondria of the DMarf RNAi flies (Fig 5C, lower panel and 5D, upper panel). Therefore, rescue of lethality exerted by hMfn2 expression can not be ascribed to a recovery of mitochondrial shape and distribution. Conversely, when we assessed ER organization in individuals simultaneously expressing DMarf-RNAi and hMfns, we found that the loss of SR organization of *DMarf*-RNAi larvae was aggravated by concomitant expression of hMfn2^{R94Q} (Fig. 5D and H). While hMfn1 had no effect on SR alteration caused by DMarf knockdown, hMfn2 expression recovered the SR architecture in muscle when its expression was driven both by the Tub-Gal4 and the Mef2-Gal4 promoter. Similarly, the recovery of ER shape was also observed in the neuronal cell bodies upon Elav-Gal4 driven expression of the hMfn2, but not of the hMfn2^{R94Q} or the hMfn1 transgenes (Fig. 5F). In conclusion, complementation of DMarf is associated with recovery of ER shape by hMfn2, further substantiating this role of Mfn2 *in vivo*.

The genetic analysis reported here shows that the invertebrate *Drosophila* Mfn is complemented both developmentally and functionally only by hMfn2. Interestingly, ER alterations that were observed in mouse cells lacking Mfn2 (mitochondrial and ER network disruption) (de Brito and Scorrano, 2008b) are reproduced in several tissues of the fly upon selective or global ablation of DMarf, and are corrected only by functional hMfn2. Thus, our results substantiate *in vivo* a model in which Mfns are not functionally equivalent, Mfn2 displaying a broader spectrum of action and being more closely related to the ancestral Mfn. Our data therefore contribute to delineate the functional orthology among the Mfns, crucial mediators of mitochondrial fusion. According to our results, *Drosophila* can be considered the evolutionary turning point from a single to a double Mfn set. Interestingly, in *Drosophila* like in mammals the ablation of DMarf affects the shape of the ER, resembling the effects of the ablation

of the large GTPase atlastin (Orso et al., 2009). While we can not exclude that the ER disruption is secondary to mitochondrial dysfunction- a phenotype observed in mammalian cells from different neuromuscular diseases (Irwin et al., 2003)- it is tempting to speculate that atlastin and DMarf can cooperate in the maintenance of the shape of the ER. A global crosstalk is indeed emerging by which the shape of the two organelles is intimately linked and changes in the shape of one are linked to rearrangements of the shape of the other (Friedman et al., 2010).

The selective ablation of Mfn in the muscle of *D. melanogaster* allows genetic experiments aimed at testing genetic interactors that can rescue or aggravate the phenotype. Moreover, the generation of a fly that carries the CMT IIa allele in a DMarf null background is in principle a perfect tool to investigate drugs that can alleviate the locomotor phenotype described here. The *Drosophila* model might result more versatile than the mouse models already available (Detmer et al., 2008;Cartoni et al., 2010), for which the long breeding times represent a clear limitation. Given the lack of therapy for CMTIIa this could represent an important step towards the definition of genetic and pharmacological modulators of the tissue dysfunction that arises upon expression of mutant Mfn2.

Acknowledgements

L.S. is a Senior Telethon Scientist of the Dulbecco-Telethon Institute. This research was supported by Telethon Italy S02016, AIRC Italy, Swiss National Foundation SNF 31-118171. We thank S. Piccolo, J. Nunnai, D. Chan for reagents.

Materials and Methods

Molecular biology

Mitochondrial yellow fluorescent protein (mtYFP), ER-targeted yellow fluorescent protein (ERYFP), mitochondrial red fluorescent protein (mtRFP), pcB6-Myc-Mfn1, and pcB6-Myc-Mfn2 have been described previously (Cipolat et al., 2004;de Brito and Scorrano, 2008b).

Total RNA from adult *Drosophila* heads was purified with Trizol (Invitrogen). The *Marf* full-length complementary DNA was obtained by RT–PCR performed on total head RNA. The *Fzo1p* cDNA was a kind gift from Jodi Nunnari. The *XMfn1* and *XMfn2* full-length cDNA were obtained by PCR on total cDNA from *X. laevis* embryos (a gift from Stefano Piccolo). The full-length cDNA of each Mfn was first cloned in pDONR221 (invitrogen) and then into pcDNA3.2/V5-DEST by Gateway cloning (Invitrogen).

Generation of Anti- DMarf antibody

pGEX expression vector was used to produce a synthetic peptide corresponding to the first 367 amino acid residues of DMarf protein sequence. The immunization of rabbits for antibody production was performed by Davids Biotechnology.

Cell culture

Mfn1$^{-/-}$ and *Mfn2*$^{-/-}$ mouse embryonic fibroblasts (MEFs) were cultured as described before (Chen et al., 2003;Chen et al., 2005). Transfection was performed using Transfectin (Biorad) according to the manufacturer's instructions.

S2R+ cells were cultured in Schneider's medium (Invitrogen) supplemented with 5% FCS (Sigma) and 1% penicillin–streptomycin (Invitrogen-Gibco).

RNAi Treatment

Double-stranded RNAs (dsRNAs) were prepared using the MEGA script kit T7 (Ambion). Primers used to generate two dsRNAs targeted to *Marf* transcript sequence are the following: 5′-TTAATACGACTCACTATAGGGAGATACGCTACTTC-3′ and 5′-TTAATACGACTCACTATAGGGAGATTGACAGGGAGATTGACACCTTCTCCTCCACCTCCTC-3′; 5′-TTAATACGACTCACTATAGGGAGATGAGCAAATACCCCCAAAAG-3′ and 5′-TTAATACGACTCACTATAGGGAGAGATCTGGAGCGGTGATTTGT-3′. S2R+ cells (1.2 x10^6) were plated on 24 mm round coverslips and treated daily with 10 µg of each dsRNA probe in serum-free medium. Two hours after probe treatment, complete medium was added to the cells.

Tetramethyl rhodamine methyl ester staining

S2R+ cells (1x10^6) were plated on 24 mm round coverslips and loaded with 20 nM tetramethyl methyl ester (TMRM) dissolved in Hanks' balanced salt solution (HBSS) supplemented for 30 min at 25℃. Cells were then placed on the stage of an Olympus IMT-2 inverted microscope (Melville, NY) equipped with a CellR imaging system. Cells were excited using a 525/20 BP excitation filter, and emitted light was acquired using a 570/LP filter. Images were then deconvolved using the Convolve function of ImageJ (NIH, Bethesda) and a custom 9x9 matrix (available upon request).

Immunofluorescence

Mfn2$^{-/-}$ MEFs (2x10^4) grown on 24 mm round coverslips were transfected as indicated and after 24h fixed with 4% formaldehyde in PBS (pH 7.4) at RT for 30 min,

permeabilized with 0.01% Igepal (Nonidet P-40, Sigma) in PBS for 20 min and blocked with 0.5% BSA in PBS at RT for 15 min. Incubation with mouse anti-V5 (Invitrogen) at concentration 1:200 was then performed for 1 hour.

Imaging

For confocal imaging, cells seeded onto 24-mm round glass coverslips, incubated in Hanks balanced salt solution (HBSS) supplemented with 10 mM Hepes were placed on the stage of a Nikon Eclipse TE300 inverted microscope equipped with a spinning-disk PerkinElmer Ultraview LCI confocal system, a piezoelectric *z*-axis motorized stage (Pifoc, Physik Instrumente, Germany), and a Orca ER 12-bit charge-coupled device camera (Hamamatsu Photonics, Japan). Cells expressing ERYFP or mtYFP or mtRFP were excited using the 488 nm or the 543 nm line of the HeNe laser (PerkinElmer) with exposure times of 50 msec by using a 60x 1.4 NA Plan Apo objective (Nikon). For confocal *z*-axis stacks, stacks of 50 images separated by 0.2 μm along the *z*-axis were acquired. Total acquisition time for each stack was 1.1 sec to minimize reconstruction artifacts caused by movement of ER. 3D reconstruction and volume rendering of the stacks were performed with the appropriate plugins of ImageJ (NIH, Bethesda).

Confocal images of larvae were acquired using a Nikon C1 confocal microscope equipped with a 60X, 1.4NA CFI Plan Apochromat Nikon objective or a Leica laser scanning microscope (TCS SP5) using the LasAF software (Leica), a 63X, 1.4NA objective and the 488 nm laser line. Images were analysed using ImageJ (NIH, Bethesda).

Morphometric Analysis

Morphometric analysis was performed with Imagetool 3.0 (University of Texas Health Science Center, San Antonio). Images of cells expressing mtYFP or ERYFP were thresholded by using the automatic threshold function. For morphometric analysis of mitochondria, the major axis length and the roundness index of each identified object were calculated. Cells were scored with elongated mitochondria when >50% of the objects in the image (*i.e.*, mitochondria) displayed a major axis longer than 3 μm and a roundness index below 0.3 (maximum value is 1). For morphometric analysis of ER, major axis length and the elongation index of each identified object were calculated. Cells were scored with reticular ER when major axis was longer than 5 μm and the elongation index was above 4 of more than 50% of the identified objects.

Cell lysates for immunobloting

Twenty-four hours after transfection, cells were harvested and disrupted in RIPA buffer (150 mM NaCl, 1% Nonidet P-40/0, 0.25% deoxycholate, 1 mM EDTA, 50 mM Tris, pH 7.4) in the presence of complete protease-inhibitor mixture (Sigma).

Immunoblotting

Extracted proteins (50 μg) were separated by 4-12% SDS-PAGE (NuPAGE, Invitrogen), transferred onto polyvinylidene difluoride (PVDF, BioRad) or nitrocellulose membranes (Amersham). Membranes were probed using the following antibodies: anti-actin (1:2000, Chemicon); anti-Myc (1:1000, BDPharmingen or 1:1000, Roche); anti-V5 (1:1000, Invitrogen); anti-DMarf (1:500) ;anti-Fzo1p (1:1000, a kind gift from Jodi Nunnari).

***Drosophila* genetics**

To obtain transgenic lines, Myc-MFN1, Myc-Mfn2 and Myc-hMfn2^{R94Q} cDNAs were subcloned in the pUAST trasformation vector and the microinjection of *Drosophila* embryos was performed by BestGene Inc. Several transgenic lines for each construct were generated. Transgenic lines were then characterized and balanced to obtain a stable transgenic line. The *Drosophila* strains used were: Elav-Gal4; Tubulin-Gal4, (Bloomington); UAS-*DMarf*-RNAi (VDRC); Mef2-Gal4, MHC-GAL4; pUASp:Lys-GFP-KDEL (UAS-ERGFP); UAS-mtGFP (a kind gift from W. Saxton). Control genotypes varied depending on individual experiments, but always included promoter-Gal4/+ and UAS-transgene/+ individuals.

Immunohistochemistry

Wandering third instar larvae were raised at 25℃. After harvesting larvae, they were dissected dorsally in standard saline and fixed in 4% paraformaldehyde for 10 min and then washed in PBS containing 0.3% Triton-X. and incubated with primary anti horseradish peroxidase HRP (1:500; Molecular Probes, Eugene OR) antibody overnight at 4℃, while secondary antibodies (Cy5 and Cy3 anti mouse, 1:xxx Jackson laboratories) were incubated for 2 hr at RT. Antibody dilutions and sources are:, secondary antibodies for immunofluorescence.

Climbing Activity

Adult climbing test was used to measure *Drosophila* locomotor function. For each genotype tested, 15 individual flies, maintained at 28℃, were collected and placed into an empty vial with a line drawn 2 cm from the bottom of the tube. After a 1-hour recovery period from anesthesia (saturating CO_2), flies were gently tapped to the bottom of the tube, and the number of flies that successfully climbed above the 2-cm mark after 20 seconds was recorded. Fifteen separate and consecutive trials were performed, and the results were averaged. At least 240 flies were tested for each genotype.

Figure legends

Figure 1. Lower eukaryotes Mfns correct mitochondrial morphology in *Mfn1*$^{-/-}$ and *Mfn2*$^{-/-}$ MEFs.

(A) Equal amounts of proteins (50 µg) from MEFs cells of the indicated genotype transfected as indicated were separated by SDS–PAGE and immunoblotted using the indicated antibodies.

(B) Representative confocal images of MEFs of the indicated genotype co-transfected with mtYFP and the indicated plasmid. Scale bar, 15 µm.

(C) and (D) Mean±SE (n=4 independent experiments) of morphometric analysis of mitochondrial morphology in the indicated cell lines. Experiments were as in (B).

(E) Representative three-dimensional reconstructions of ER from *Mfn2*$^{-/-}$ MEFs co-transfected with ER-YFP and the indicated plasmid. Scale bar, 15 µm. Morphometric analysis of ER morphology is shown in the lower right panel. Data represent mean± SE of 4 independent experiments.

Figure 2. Ubiquitous, neuron- or muscle-specific ablation of Marf is lethal and alters mitochondrial morphology and distribution.

(A) Equal amounts of protein (50 µg) from S2R+ cells transfected as indicated for 96 hrs were separated by SDS-PAGE and immunoblotted with the indicated antibodies.

(B) Surface rendered 3D reconstruction of confocal z-stacks of S2R+ cells transfected with the indicated dsRNA for 96 hrs and stained with 20 nM tetramethylrhodamine methyl ester (TMRM). Scale bar, 10 µm.

(C) Distribution among developmental stages (larvae, pupae and adults) of the indicated strains of flies For each experiment, driver-Gal4/ TM6 (tm6) individuals were used as control. Data are presented as percentage of he total individuals analyzed (n=450).

(D) Representative confocal images of Tub-Gal4, UAS-mtGFP/+ larval ventral ganglion. Higher-magnifications of the boxed neuronal cell bodies (upper) and axons located in the proximity of the ventral ganglion (lower) from Tub-Gal4, UAS-mtGFP/+ (W^{1118}) and Tub-Gal4, UAS-mtGFP/ UAS-*DMarf*-RNAi ($DMarf^{RNAi}$) larvae are shown. Scale bar 10 μm.

(E) 3D-renderings of NMJs on muscles 6 and 7 labeled with α-HRP (red) of Tub-Gal4, UAS-mtGFP/+ (W^{1118}) and Tub-Gal4, UAS-mtGFP/ UAS-*DMarf*-RNAi ($DMarf^{RNAi}$) larvae. Scale bar 20 μm.

(F) 3D-renderings of NMJ on muscles 6 and 7 labeled with α-HRP (red) of UAS-mtGFP/+;Elav-Gal4/+ (W^{1118}) and UAS-mtGFP/+; Elav-Gal4/UAS-*DMarf*-RNAi ($DMarf^{RNAi}$) larvae. Scale bar 10 μm.

(G) Confocal images of body wall muscles of Mef2-Gal4, UAS-mtGFP/+ (W^{1118}) and Mef2-Gal4, UAS-mtGFP/ UAS-*DMarf*-RNAi ($DMarf^{RNAi}$) larvae. Scale bar 20 μm.

Figure 3. Ablation of *DMarf* disrupts ER morphology in larva

(A) Confocal images of neuronal cell bodies of Elav-Gal4/+;; UAS-ERGFP/+ (W^{1118}) and Elav-Gal4/+;;UAS-ERGFP/UAS-*DMarf*-RNAi ($DMarf^{RNAi}$) larvae. Scale bar 10 μm.

(B) Confocal images of NMJs on muscles 6 and 7 labeled with α-HRP (red) of Tub-Gal4, UAS-ERGFP/+ (W^{1118}) and Tub-Gal4, UAS-ERGFP/UAS-*DMarf*-RNAi ($DMarf^{RNAi}$) larvae. Scale bar 20 μm.

(C) Confocal images of NMJs on muscles 6 and 7 labeled with α -HRP (red) of Mef2-Gal4, UAS-ERGFP/+ (W^{1118}) and Mef2-Gal4, UAS-ERGFP/UAS-*DMarf*-RNAi ($DMarf^{RNAi}$) larvae. Scale bar 20 μm.

Figure 4. Overexpression of hMfns in Drosophila alters mitochondrial and ER morphology

(A) Distribution among developmental stages (larvae, pupae and adults) of individual of the indicated genotype. In each experiment, driver-Gal4/ TM6 (tm6) individuals were used as control.

(B) Tub-Gal4, mtGFP: representative confocal images of Tub-Gal4, UAS-mtGFP/TM6 mated to UAS-hMfns larvae. Muscles 6 and 7 labeled with α -HRP (red, left panel), neuronal cell bodies and axons located in the proximity of the ventral ganglion (top left and lower left panels) are shown. Tub-Gal4, ERGFP: representative confocal images of muscles 6 and 7 labeled with α -HRP (red) of Tub-Gal4, UAS-ERGFP/TM6 mated to UAS-hMfns larvae. . Genotypes of crossed flies are: UAS-hMfn1 (hMfn1), UAS-hMfn2 (hMfn2) and UAS-hMfn2^{R94Q} (hMfn2 ^{R94Q}). Scale bar are 20 μm in the case of muscle images and 10 μm for neuronal cell bodies and axons.

(C) Representative confocal images of neuronal cell bodies (left and lower panel) and 3D renderings of NMJs on muscles 6 and 7 labeled with α-HRP (red, right upper panel). UAS-mtGFP/CyO; Elav-Gal4 /TM6 line was used to analyse mitochondrial morphology and distribution (upper panel) and Elav-Gal4/+;; UAS-ERGFP/+ flies were used for ER morphology analyses (lower panel). Genotypes of crossed flies are: UAS-hMfn1 (hMfn1), UAS-hMfn2 (hMfn2) and UAS-hMfn2^{R94Q} (hMfn2 ^{R94Q}). Scale bar are 20 μm for NMJs and 10 μm for neuronal cell bodies.

(D) Representative confocal images of body wall muscles (upper panel) and NMJs on muscles 6 and 7 labeled with α-HRP (red, lower panel). Mef2-Gal4, UAS-mtGFP/TM6 and Mef2-Gal4, UAS-ERGFP/TM6 were used to visualize mitochondria (upper panel) and ER (lower panel). Genotypes of crossed flies are: UAS-hMfn1 (hMfn1), UAS-hMfn2 (hMfn2) and UAS-hMfn2^{R94Q} (hMfn2 ^{R94Q}). Scale bar 20 μm.

Figure 5. hMfn2, but not hMfn1 or hMfn2^{R94Q}, rescues Marf depletion in *D. melanogaster*.

(A) The indicated flies were mated to lines homozygous for the indicated *UAS*-insertion and viability was measured by determining the number of non-TM6 (A) and non-TM3 (B) flies relative to TM6 and TM3 flies. Data are expressed as percentage and represent mean ± SEM of 3 independent matings.

(B) MHC-Gal4 homozygous flies were mated to lines homozygous for the indicated UAS- insertion. Climbing performance was measured as described. Data are mean ±SEM of 3 independent experiments.

(C) Representative confocal images of larvae from Tub-Gal4, UAS-mtGFP/TM6 mated to UAS-*DMarf*-RNAi and recombinant UAS-*DMarf*-RNAi, UAS-hMfns flies. Neuronal cell bodies and axons located in the proximity of the ventral ganglion (top panels) and larval NMJs on muscles 6 and 7 labeled with α -HRP (red, bottom panels) are shown. UAS-insertion of hMfns for each recombinant are specified in every image whereas images on the left of each panel refer to expression of Marf-RNAi alone. Scale bars, 20 μm for NMJs and 10 μm for neuronal cell bodies and axons images.

(D) Representative confocal images of muscles 6 and 7 labeled with α -HRP (red) of larvae from Tub-Gal4, UAS-ERGFP/TM6 mated to UAS-*DMarf*-RNAi and recombinant UAS-*DMarf*-RNAi, hMfns flies. UAS-insertion of hMfns for each recombinant are specified. Images on the left of each panel refer to expression of Marf-RNAi alone. Scale bars, 20 μm.

(E) representative 3D-renderings from confocal stacks of NMJs (top) labelled with α–HRP (red) and confocal images of neuronal cell bodies (bottom) from UAS-mtGFP/+; Elav-Gal4 /UAS-*DMarf*-RNAi (left panels), UAS-mtGFP/+; Elav-Gal4 /UAS-DMarf-RNAi, hMfn1 (, hMfn1), UAS-mtGFP/+; Elav-Gal4 /UAS-DMarf-RNAi, hMfn2 (,

hMfn2) and UAS-mtGFP/+; Elav-Gal4 /UAS-DMarf-RNAi, UAS-hMfn2^{R94Q} (, hMfn2 ^{R94Q}) larvae. Scale bars are 20 μm for NMJs and 10 μm for neuronal cell bodies.

(F) Representative confocal images of neuronal cell bodies from Elav-Gal4;; UAS-ERGFP/UAS-*DMarf*-RNAi (left panel), Elav-Gal4;;UAS-ERGFP/UAS-*DMarf*-RNAi, hMfn1 (, hMfn1), Elav-Gal4;;UAS-ERGFP/UAS-*DMarf*-RNAi, hMfn2 (, hMfn2) and Elav-Gal4;;UAS-ERGFP/UAS-*DMarf*-RNAi, hMfn2 ^{R94Q}(, hMfn2 ^{R94Q}) larvae. Scale bar 10 μm.

(G) Confocal images of body wall muscles of Mef2-Gal4, UAS-mtGFP/ UAS-*DMarf*-RNAi (left), Mef2-Gal4, UAS-mtGFP/ UAS-*DMarf*-RNAi, hMfn1 (, hMfn1), UAS-mtGFP/ UAS-*DMarf*-RNAi, hMfn2 (, hMfn2), Mef2-Gal4, UAS-mtGFP/ UAS-*DMarf*-RNAi, hMfn2 ^{R94Q} (, hMfn2 ^{R94Q}) larvae. Scale bar are 20 μm.

(H) representative confocal images of muscles 6 and 7 labeled with α -HRP (red) of larvae from Mef2-Gal4, UAS-ERGFP/TM6 flies mated to UAS-*DMarf*-RNAi and recombinant UAS-*DMarf*-RNAi, hMfns flies. UAS-insertion of hMfns for each recombinant is specified. Left images, DMarf-RNAi alone. Scale bars, 20 μm.

References

1. Bach D, Naon D, Pich S, Soriano FX, Vega N, Rieusset J, Laville M, Guillet C, Boirie Y, Wallberg-Henriksson H, Manco M, Calvani M, Castagneto M, Palacin M, Mingrone G, Zierath JR, Vidal H, and Zorzano A (2005) Expression of Mfn2, the Charcot-Marie-Tooth neuropathy type 2A gene, in human skeletal muscle: effects of type 2 diabetes, obesity, weight loss, and the regulatory role of tumor necrosis factor alpha and interleukin-6. *Diabetes,* **54,** 2685-2693.

2. Baloh RH, Schmidt RE, Pestronk A, and Milbrandt J (2007) Altered axonal mitochondrial transport in the pathogenesis of Charcot-Marie-Tooth disease from mitofusin 2 mutations. *J Neurosci,* **27,** 422-430.

3. Breckenridge DG, Kang BH, Kokel D, Mitani S, Staehelin LA, and Xue D (2008) Caenorhabditis elegans drp-1 and fis-2 regulate distinct cell-death execution pathways downstream of ced-3 and independent of ced-9. *Mol Cell,* **31,** 586-597.

4. Campello S and Scorrano L (2010) Mitochondrial shape changes: orchestrating cell pathophysiology. *EMBO Rep,* **11,** 678-684.

5. Cartoni R, Arnaud E, Medard JJ, Poirot O, Courvoisier DS, Chrast R, and Martinou JC (2010) Expression of mitofusin 2(R94Q) in a transgenic mouse leads to Charcot-Marie-Tooth neuropathy type 2A. *Brain,* **133,** 1460-1469.

6. Chen H, Chomyn A, and Chan DC (2005) Disruption of fusion results in mitochondrial heterogeneity and dysfunction. *J Biol Chem,* **280,** 26185-26192.

7. Chen H, Detmer SA, Ewald AJ, Griffin EE, Fraser SE, and Chan DC (2003) Mitofusins Mfn1 and Mfn2 coordinately regulate mitochondrial fusion and are essential for embryonic development. *J Cell Biol,* **160,** 189-200.

8. Chen H, McCaffery JM, and Chan DC (2007) Mitochondrial fusion protects against neurodegeneration in the cerebellum. *Cell,* **130,** 548-562.

9. Chen KH, Guo X, Ma D, Guo Y, Li Q, Yang D, Li P, Qiu X, Wen S, Xiao RP, and Tang J (2004) Dysregulation of HSG triggers vascular proliferative disorders. *Nat Cell Biol,* **6,** 872-883.

10. Cipolat S, de Brito OM, Dal Zilio B, and Scorrano L (2004) OPA1 requires mitofusin 1 to promote mitochondrial fusion. *Proc Natl Acad Sci U S A,* **101,** 15927-15932.

11. de Brito OM and Scorrano L (2008a) Mitofusin 2: a mitochondria-shaping protein with signaling roles beyond fusion. *Antioxid Redox Signal,* **10,** 621-633.

12. de Brito OM and Scorrano L (2008b) Mitofusin 2 tethers endoplasmic reticulum to mitochondria. *Nature,* **456,** 605-610.

13. Deng H, Dodson MW, Huang H, and Guo M (2008) The Parkinson's disease genes pink1 and parkin promote mitochondrial fission and/or inhibit fusion in Drosophila. *Proc Natl Acad Sci U S A,* **105,** 14503-14508.

14. Detmer SA and Chan DC (2007) Complementation between mouse Mfn1 and Mfn2 protects mitochondrial fusion defects caused by CMT2A disease mutations. *J Cell Biol,* **176,** 405-414.

15. Detmer SA, Vande VC, Cleveland DW, and Chan DC (2008) Hindlimb gait defects due to motor axon loss and reduced distal muscles in a transgenic mouse model of Charcot-Marie-Tooth type 2A. *Hum Mol Genet,* **17,** 367-375.

16. Dorn GW, Clark CF, Eschenbacher WH, Kang MY, Engelhard JT, Warner SJ, Matkovich SJ, and Jowdy CC (2011) MARF and Opa1 control mitochondrial and cardiac function in Drosophila. *Circ Res,* **108,** 12-17.

17. Friedman JR, Webster BM, Mastronarde DN, Verhey KJ, and Voeltz GK (2010) ER sliding dynamics and ER-mitochondrial contacts occur on acetylated microtubules. *J Cell Biol,* **190,** 363-375.

18. Hales KG and Fuller MT (1997) Developmentally regulated mitochondrial fusion mediated by a conserved, novel, predicted GTPase. *Cell,* **90,** 121-129.

19. Hermann GJ, Thatcher JW, Mills JP, Hales KG, Fuller MT, Nunnari J, and Shaw JM (1998) Mitochondrial fusion in yeast requires the transmembrane GTPase Fzo1p. *J Cell Biol,* **143,** 359-373.

20. Hwa JJ, Hiller MA, Fuller MT, and Santel A (2002) Differential expression of the Drosophila mitofusin genes fuzzy onions (fzo) and dmfn. *Mech Dev,* **116**.

21. Irwin WA, Bergamin N, Sabatelli P, Reggiani C, Megighian A, Merlini L, Braghetta P, Columbaro M, Volpin D, Bressan GM, Bernardi P, and Bonaldo P (2003) Mitochondrial dysfunction and apoptosis in myopathic mice with collagen VI deficiency. *Nat Genet,* **35,** 367-371.

22. Liesa M, Palacin M, and Zorzano A (2009) Mitochondrial dynamics in mammalian health and disease. *Physiol Rev,* **89,** 799-845.

23. Olichon A, Emorine LJ, Descoins E, Pelloquin L, Brichese L, Gas N, Guillou E, Delettre C, Valette A, Hamel CP, Ducommun B, Lenaers G, and Belenguer P (2002) The human dynamin-related protein OPA1 is anchored to the mitochondrial inner membrane facing the inter-membrane space. *FEBS Lett,* **523,** 171-176.

24. Orso G, Martinuzzi A, Rossetto MG, Sartori E, Feany M, and Daga A (2005) Disease-related phenotypes in a Drosophila model of hereditary spastic paraplegia are ameliorated by treatment with vinblastine. *J Clin Invest,* **115,** 3026-3034.

25. Orso G, Pendin D, Liu S, Tosetto J, Moss TJ, Faust JE, Micaroni M, Egorova A, Martinuzzi A, McNew JA, and Daga A (2009) Homotypic fusion of ER membranes requires the dynamin-like GTPase atlastin. *Nature,* **460,** 978-983.

26. Park J, Lee G, and Chung J (2009) The PINK1-Parkin pathway is involved in the regulation of mitochondrial remodeling process. *Biochem Biophys Res Commun,* **378,** 518-523.

27. Rapaport D, Brunner M, Neupert W, and Westermann B (1998) Fzo1p is a mitochondrial outer membrane protein essential for the biogenesis of functional mitochondria in Saccharomyces cerevisiae. *J Biol Chem,* **273,** 20150-20155.

28. Santel A, Frank S, Gaume B, Herrler M, Youle RJ, and Fuller MT (2003) Mitofusin-1 protein is a generally expressed mediator of mitochondrial fusion in mammalian cells. *J Cell Sci,* **116,** 2763-2774.

29. Santel A and Fuller MT (2001) Control of mitochondrial morphology by a human mitofusin. *J Cell Sci,* **114,** 867-874.

30. Smirnova E, Griparic L, Shurland DL, and van der Bliek AM (2001) Dynamin-related protein Drp1 is required for mitochondrial division in mammalian cells. *Mol Biol Cell,* **12,** 2245-2256.

31. Westermann B (2010) Mitochondrial dynamics in model organisms: what yeasts, worms and flies have taught us about fusion and fission of mitochondria. *Semin Cell Dev Biol,* **21,** 542-549.

32. Ziviani E, Tao RN, and Whitworth AJ (2010) Drosophila parkin requires PINK1 for mitochondrial translocation and ubiquitinates mitofusin. *Proc Natl Acad Sci U S A,* **107,** 5018-5023.

33. Zuchner S, Mersiyanova IV, Muglia M, Bissar-Tadmouri N, Rochelle J, Dadali EL, Zappia M, Nelis E, Patitucci A, Senderek J, Parman Y, Evgrafov O, Jonghe PD, Takahashi Y, Tsuji S, Pericak-Vance MA, Quattrone A, Battologlu E, Polyakov AV, Timmerman V, Schroder JM, and Vance JM (2004) Mutations in the mitochondrial GTPase mitofusin 2 cause Charcot-Marie-Tooth neuropathy type 2A. *Nat Genet,* **36,** 449-451.

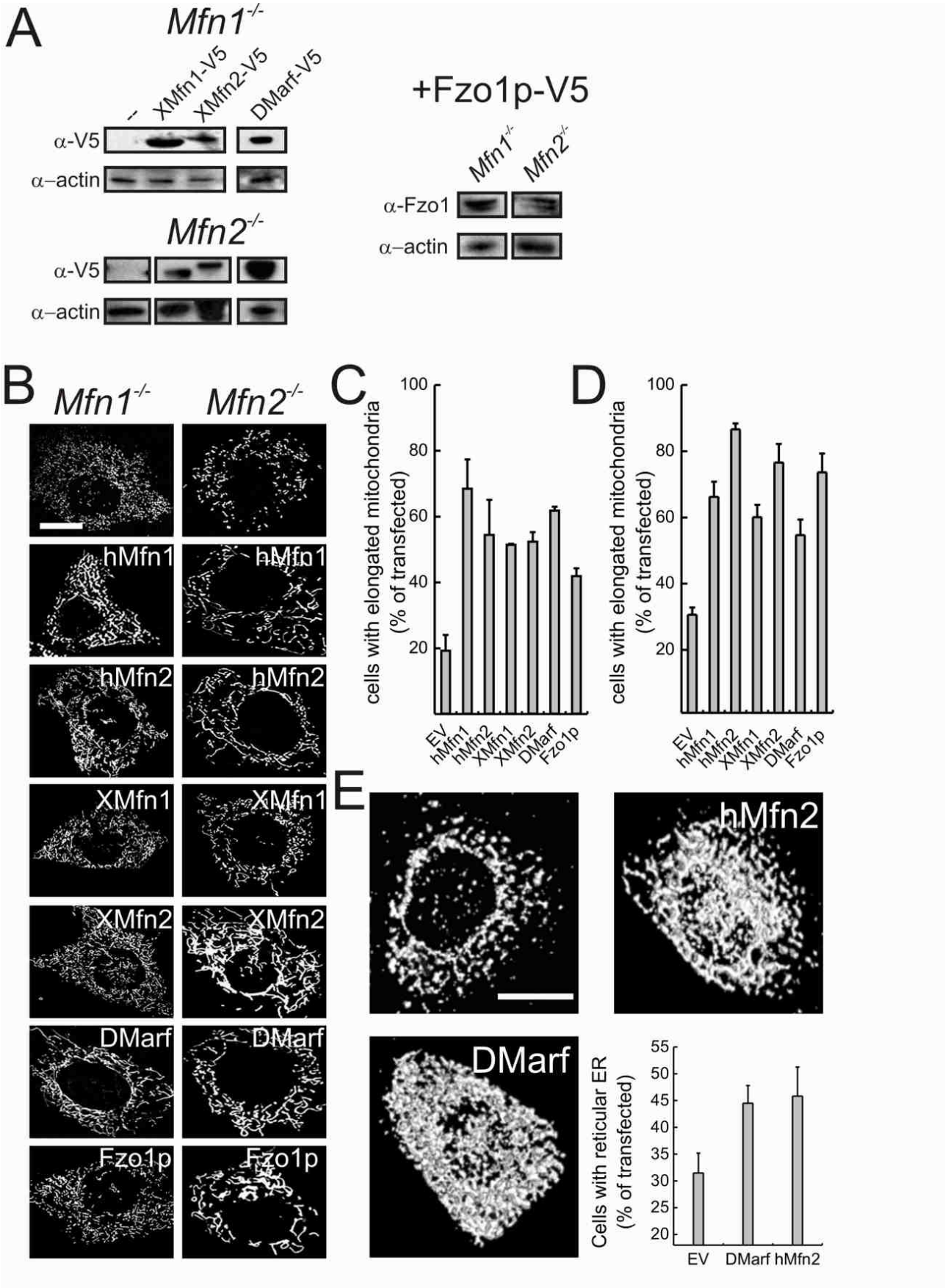
A
Mfn1-/-
–
XMfn1-V5
XMfn2-V5
DMarf-V5
α-V5
α–actin
Mfn2-/-
α-V5
α–actin
+Fzo1p-V5
Mfn1-/-
Mfn2-/-
α-Fzo1
α–actin
B
Mfn1-/-
Mfn2-/-
hMfn1
hMfn2
XMfn1
XMfn2
DMarf
Fzo1p
C
cells with elongated mitochondria (% of transfected)
100
80
60
40
20
EV
hMfn1
hMfn2
XMfn1
XMfn2
DMarf
Fzo1p
D
cells with elongated mitochondria (% of transfected)
100
80
60
40
20
EV
hMfn1
hMfn2
XMfn1
XMfn2
DMarf
Fzo1p
E
hMfn2
DMarf
Cells with reticular ER (% of transfected)
55
50
45
40
35
30
25
20
EV
DMarf
hMfn2

Fig. 1

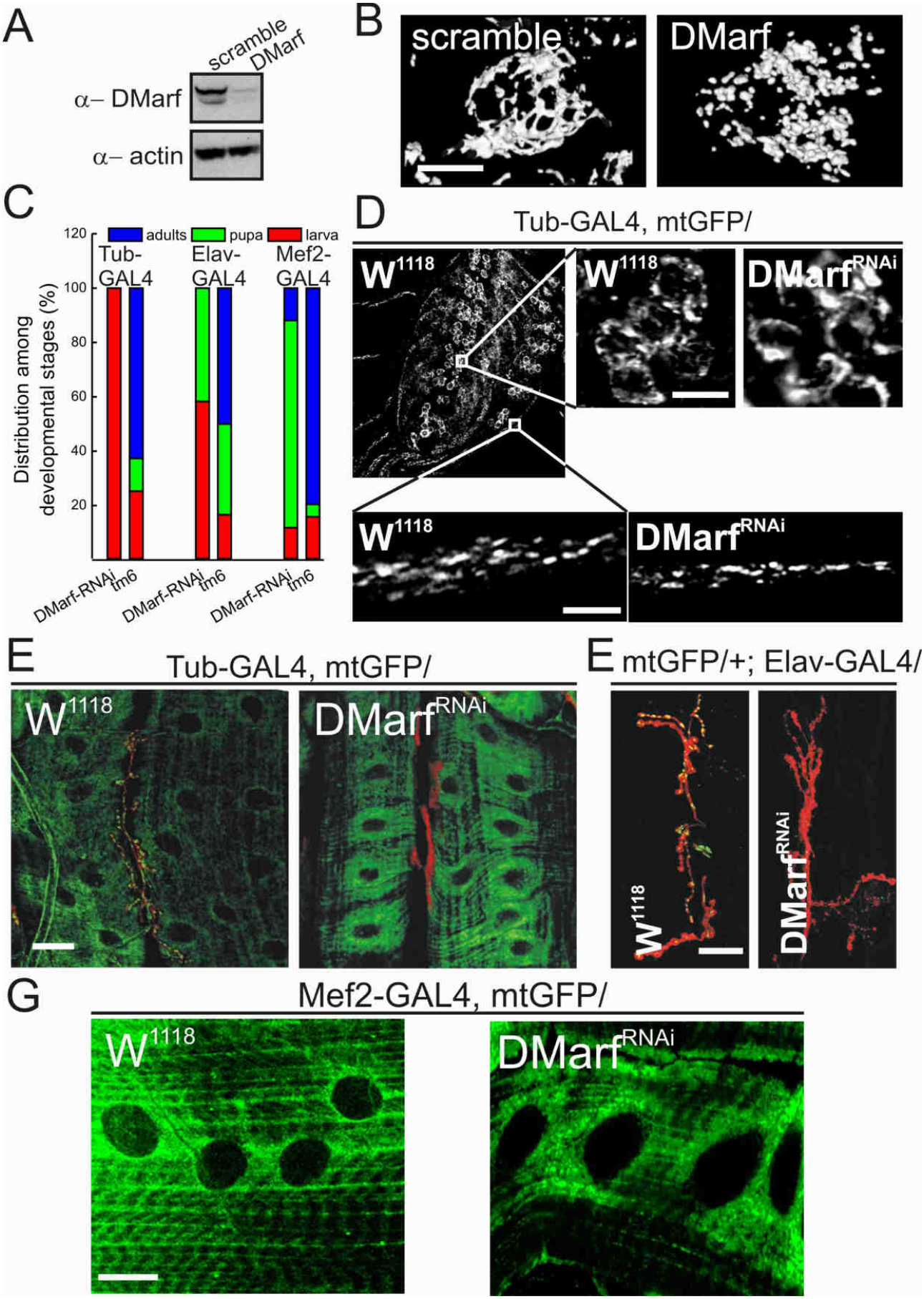
A
scramble
DMarf
α– DMarf
α– actin
B
scramble
DMarf
C
adults
pupa
larva
Distribution among developmental stages (%)
120
100
80
60
40
20
Tub-GAL4
Elav-GAL4
Mef2-GAL4
DMarf-RNAi
tm6
D
Tub-GAL4, mtGFP/
W1118
DMarfRNAi
E
Tub-GAL4, mtGFP/
E
mtGFP/+; Elav-GAL4/
G
Mef2-GAL4, mtGFP/

Fig. 2

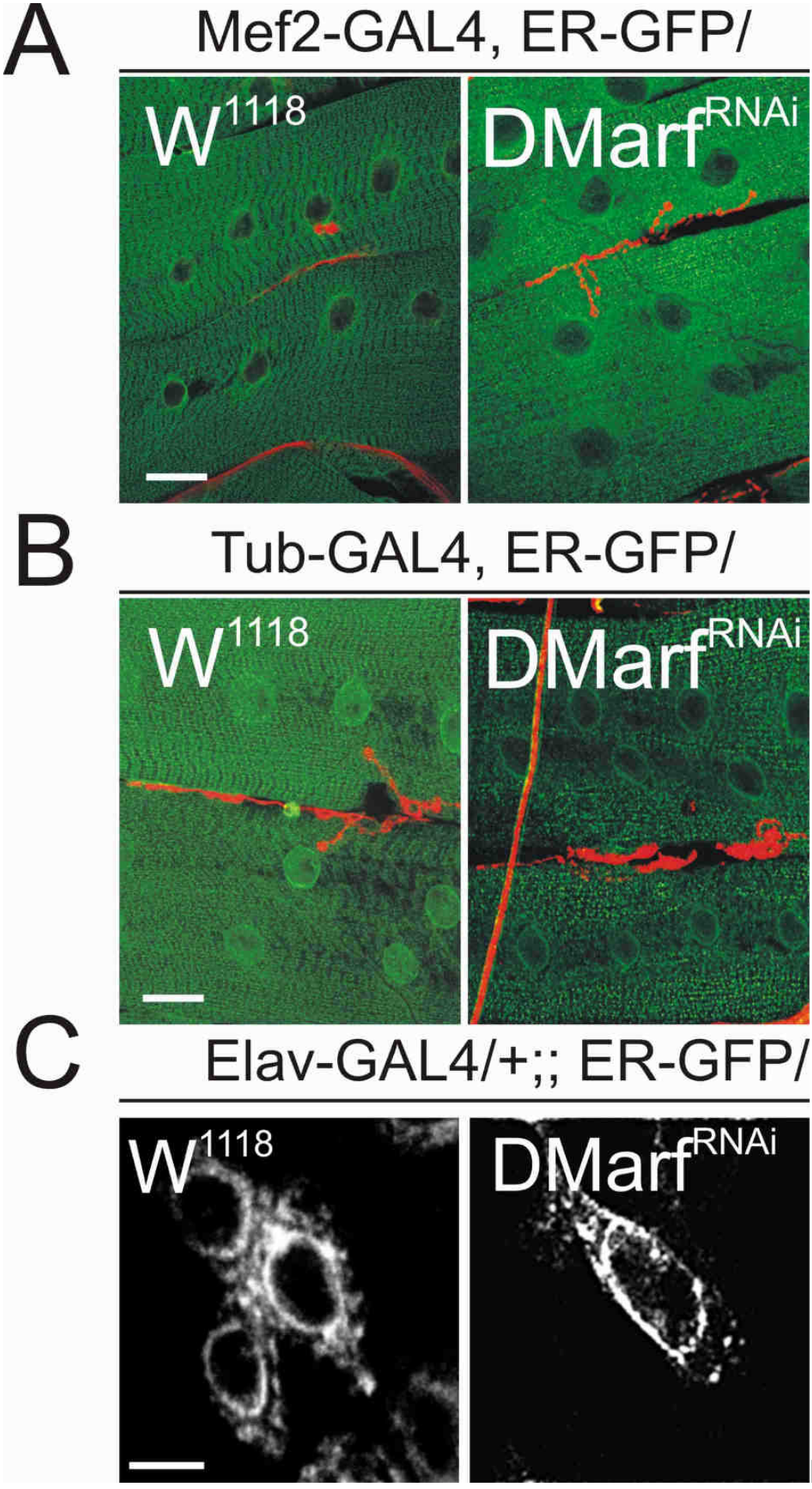
A
Mef2-GAL4, ER-GFP/
W1118
DMarfRNAi
B
Tub-GAL4, ER-GFP/
W1118
DMarfRNAi
C
Elav-GAL4/+;; ER-GFP/
W1118
DMarfRNAi

Fig3

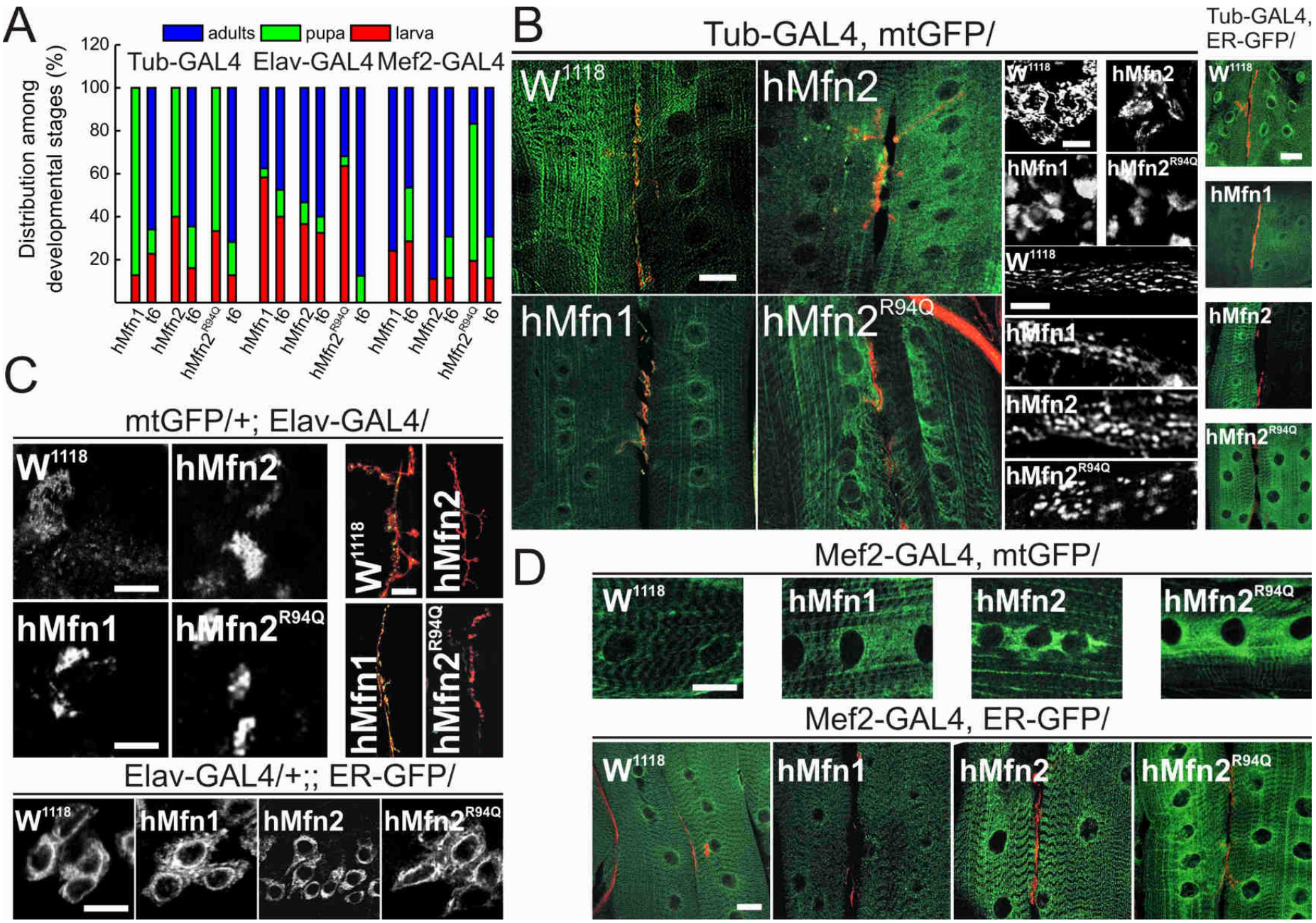
A
adults
pupa
larva
Distribution among developmental stages (%)
120
100
80
60
40
20
Tub-GAL4
Elav-GAL4
Mef2-GAL4
hMfn1
t6
hMfn2
t6
hMfn2R94Q
t6
B
Tub-GAL4, mtGFP/
W1118
hMfn2
hMfn1
hMfn2R94Q
Tub-GAL4, ER-GFP/
C
mtGFP/+; Elav-GAL4/
Elav-GAL4/+;; ER-GFP/
D
Mef2-GAL4, mtGFP/
Mef2-GAL4, ER-GFP/

Fig.4

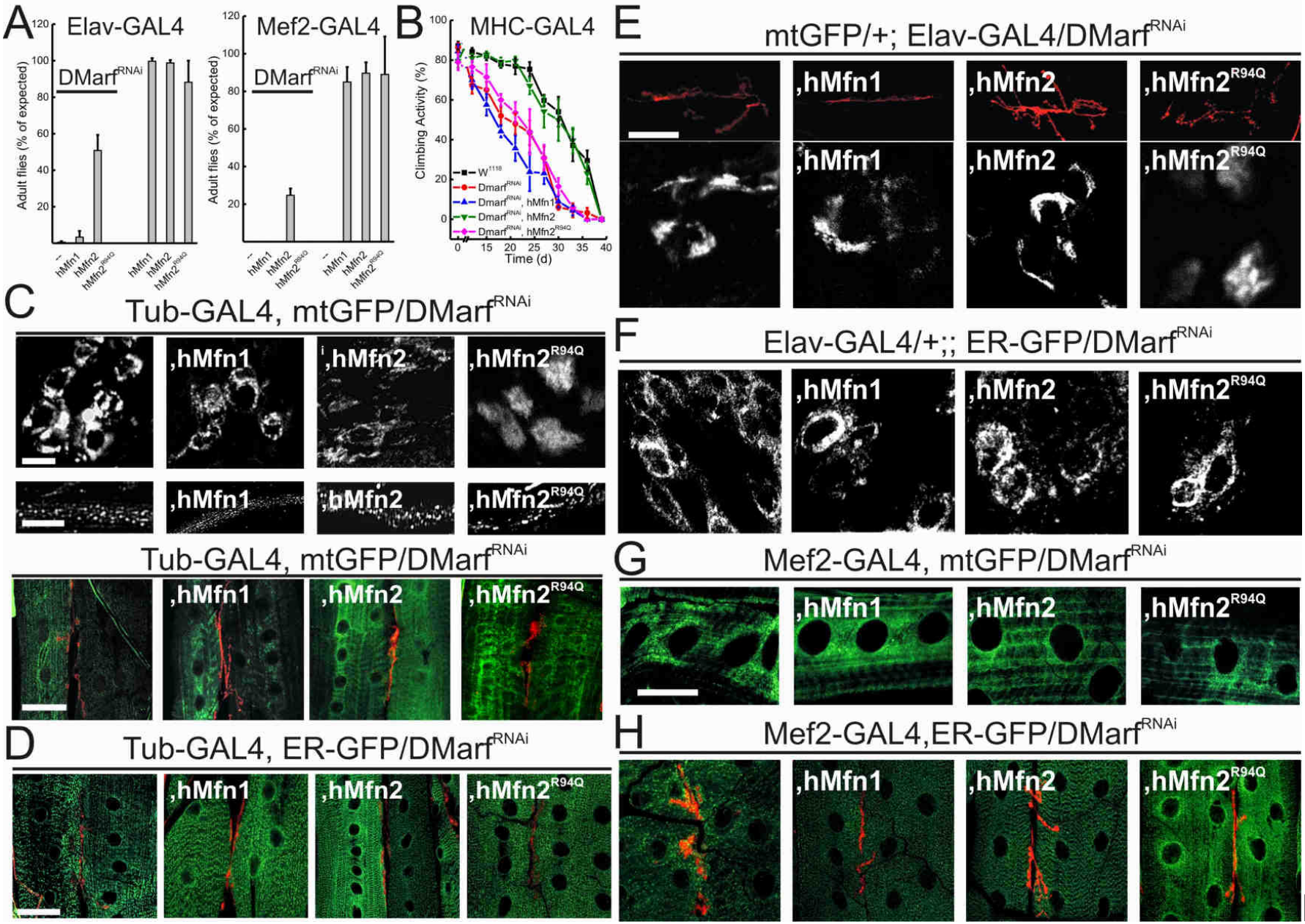
A
Elav-GAL4
DMarf^RNAi
Adult flies (% of expected)
Mef2-GAL4
DMarf^RNAi
Adult flies (% of expected)
–
hMfn1
hMfn2
hMfn2^R94Q
B
MHC-GAL4
Climbing Activity (%)
Time (d)
W^1118
Dmarf^RNAi
Dmarf^RNAi, hMfn1
Dmarf^RNAi, hMfn2
Dmarf^RNAi, hMfn2^R94Q
C
Tub-GAL4, mtGFP/DMarf^RNAi
,hMfn1
,hMfn2
,hMfn2^R94Q
Tub-GAL4, mtGFP/DMarf^RNAi
,hMfn1
,hMfn2
,hMfn2^R94Q
D
Tub-GAL4, ER-GFP/DMarf^RNAi
,hMfn1
,hMfn2
,hMfn2^R94Q
E
mtGFP/+; Elav-GAL4/DMarf^RNAi
,hMfn1
,hMfn2
,hMfn2^R94Q
,hMfn1
,hMfn2
,hMfn2^R94Q
F
Elav-GAL4/+;; ER-GFP/DMarf^RNAi
,hMfn1
,hMfn2
,hMfn2^R94Q
G
Mef2-GAL4, mtGFP/DMarf^RNAi
,hMfn1
,hMfn2
,hMfn2^R94Q
H
Mef2-GAL4,ER-GFP/DMarf^RNAi
,hMfn1
,hMfn2
,hMfn2^R94Q

Fig.5

Marf, the single mitofusin of *D. melanogaster,* is selectively complemented by Mitofusin 2.

Valentina Debattisti, Diana Pendin, Maria Giovanna Rossetto, Andrea Daga and Luca Scorrano

Supplementary online material

Supplementary online Methods

***Drosophila* lysates for immunoblotting**

20 brains from larvae, or 10 heads from adults or 5 whole larvae for each genotype were used for protein extraction as indicated in figure legends. Samples were rinsed in extraction buffer (100mM KCl, 20 mM Hepes, 5% glycerol, 0.1% Triton-X, 1 mM Dithiothreitol, 10mM EDTA) added with protease-inhibitor mixture (La Roche). Samples were then spinned at 13000rpm for 2 minutes; supernatants were collected and boiled for 5 minutes in Laemmly buffer (4% sodium dodecyl sulphate, 20% glycerol, 10% 2-mercaptoethanol, blue bromophenol).

Legends to supplementary figures

Figure S1.

(A) Protein sequence alignment between hMfn1 homologues. Sequences are indicated: human mitofusin 1 (hMfn1), Mfn1 from *Xenopus laevis* (XMfn1), *Drosophila* mitofusin (DMarf), mitofusin from *S.cerevisae* (Fzo1p).

(B) Protein sequence alignment between hMfn2 homologues. Sequences are indicated: human mitofusin 2 (hMfn2), Mfn2 from *Xenopus laevis* (XMfn2), *Drosophila* mitofusin (DMarf), mitofusin from *S.cerevisae* (Fzo1p). Homologous and identical regions are highlighted in grey and black.

Figure S2. Marf partially colocalize into ER in *Mfn2*$^{-/-}$ MEFs

Mfn2$^{-/-}$ MEFs were cotransfected with ERYFP (green), mtRFP (red) and DMarf-V5 (blue). After 24 hrs cells were fixed and representative confocal images acquired.

Figure S3. Efficiency of *DMarf*-RNAi and overexpression of hMfns in *Drosophila* larvae

(A) Tub-Gal4/+ (W^{1118}) and Tub-Gal4/UAS-*DMarf*-RNAi (RNAi) whole larvae were lysed. Equal amounts of protein (50 µg) were separated by SDS-PAGE and immunoblotted using the indicated antibodies.

(B) Larval brains were lysed from Elav-Gal4/+ (W^{1118}), Elav-Gal4/UAS-hMfn1 (hMfn1) and Elav-Gal4/UAS-hMfn2 (hMfn2). Equal amounts of protein (50 µg) were separated by SDS-PAGE and immunoblotted using the indicated antibodies.

(C) Adults heads were lysed from Elav-Gal4/+ (W^{1118}), Elav-Gal4/UAS-hMfn1 (hMfn1), Elav-Gal4/UAS-hMfn2 (hMfn2) and Elav-Gal4/UAS-hMfn2^{R94Q}(hMfn2 ^{R94Q}). Equal amounts of protein were separated by SDS-PAGE and immunoblotted using the indicated antibodies.

Figure S4. Nervous system-specific DMarf knockdown causes clusterization of mitochondria of neuronal cell bodies.

Confocal images of neuron cell bodies from UAS-mtGFP/+; Elav-Gal4/+ (W^{1118}) and UAS-mtGFP/+; Elav-Gal4/ UAS-*DMarf*-RNAi larvae. Bar 10 µm.

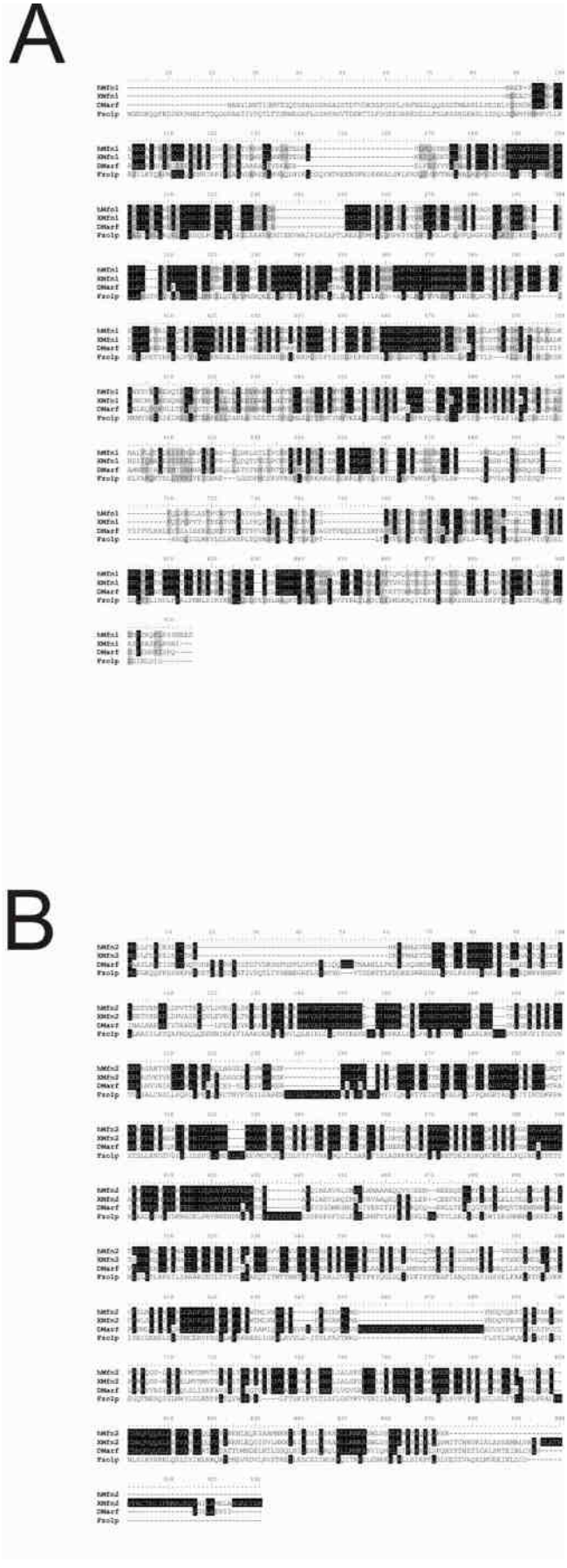

Fig. S1

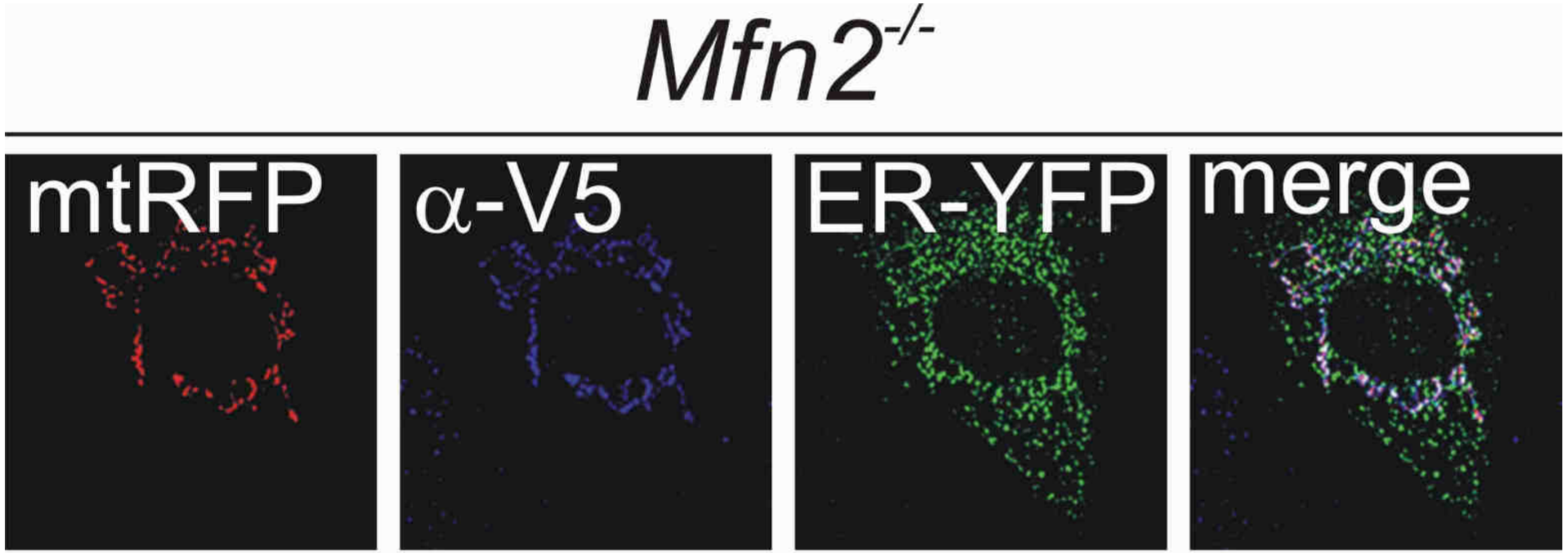

Fig. S2

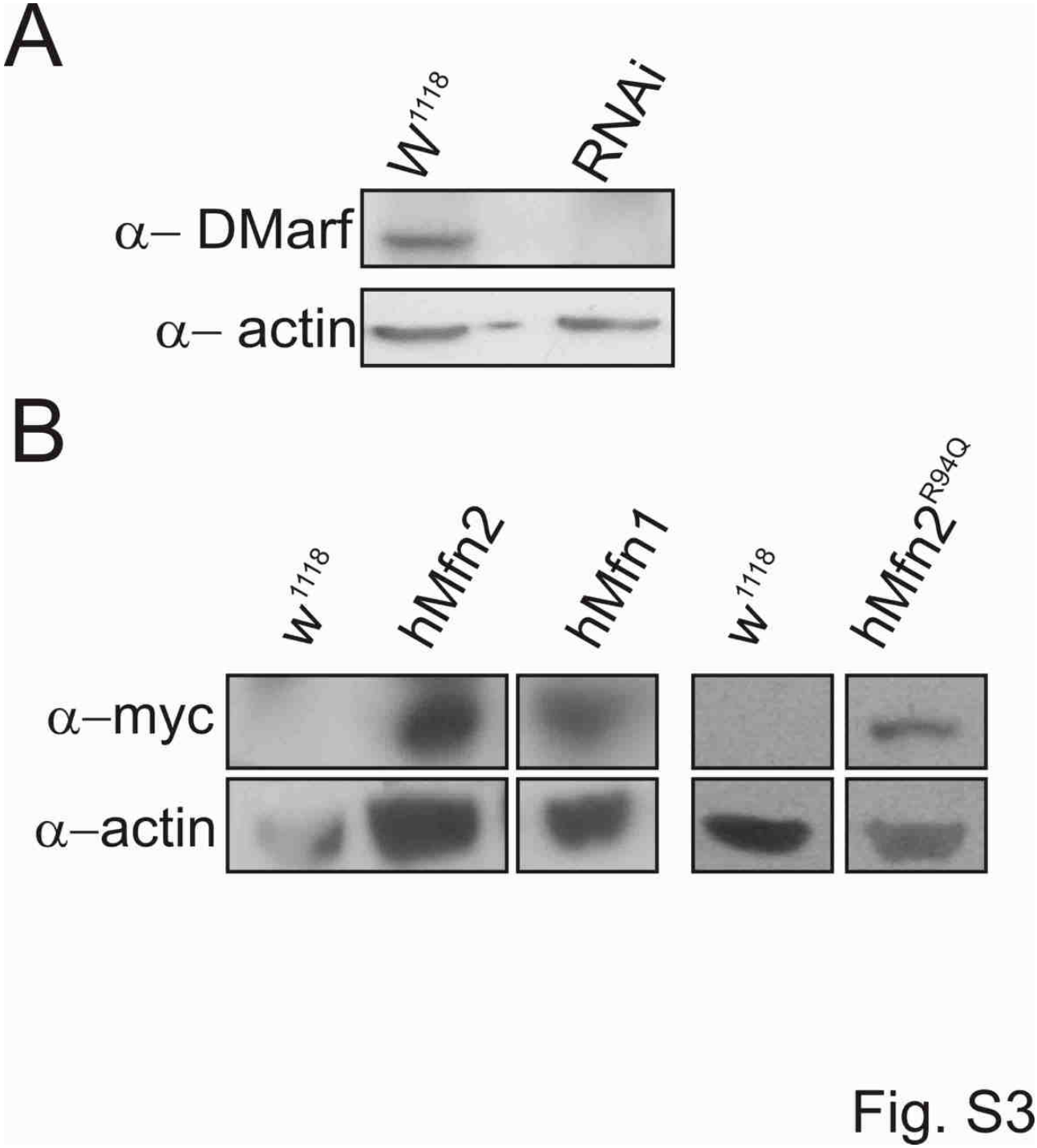
A
w^{1118}
RNAi
α– DMarf
α– actin
B
w^{1118}
hMfn2
hMfn1
w^{1118}
hMfn2^{R94Q}
α–myc
α–actin

Fig. S3

mtGFP/+; Elav-GAL4/

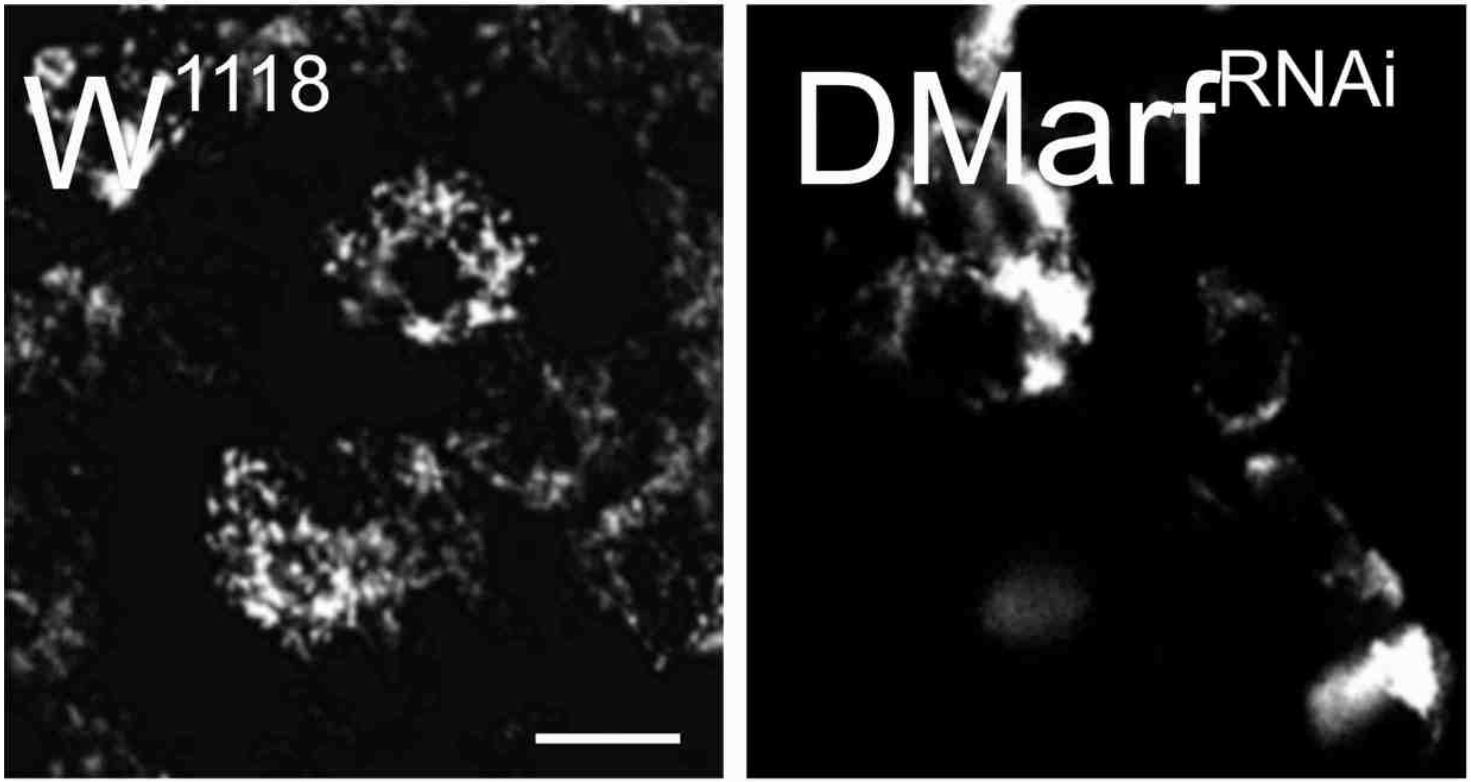

Fig. S4

5. Conclusions

The work presented in this Thesis reports the phylogenetic analysis of mitofusins (Mfns), resulting in a working model where *Drosophila* DMarf represents the ancestor of mammalian Mfn2. All vertebrates possess two mitofusins which are regulators of mitochondrial fusion. In the past, the presence of two mitofusins raised the question of their functional divergence. Nowadays many findings support the idea that Mfn1 and 2 do not display redundant functions (Bach, 2005a; Chen, 2004a; de Brito, 2008c). However, until now there was not much knowledge about the appearance of 2 mitofusins during evolution from invertebrates to vertebrates. Invertebrates have only one Mfn homologue, with the exception of *D.melanogaster,* which possesses Fzo and DMarf. Compared to Fzo, DMarf shares a higher percentage of sequence homology to mammalian mitofusins and has a broader pattern of expression: for this reason we focused our analysis on DMarf.

We tried to understand to which extent DMarf could complement mammalian mitofusins. To obtain a wider phylogenetic view, we extended our analysis to Mfns 1 and 2 from the vertebrate *Xenopus laevis* (XMfn1 and XMfn2) and on the Mfn homologue from the yeast *S.cerevisiae* (Fzo1p). We demonstrated that XMfn1 and XMfn2, DMarf and Fzo1p were able to rescue mitochondrial morphology in *Mfn1*$^{-/-}$ and *Mfn2*$^{-/-}$ MEFs and could therefore substitute for both mitofusins.

Unlikely *Mfn1*$^{-/-}$ MEFs, *Mfn2*$^{-/-}$ MEFs have altered ER morphology (de Brito, 2008b), which is recovered after re-expression of Mfn2. DMarf was able to rescue ER shape in *Mfn2*$^{-/-}$, showing a strong functional correlation with Mfn2.

In vivo, we found that *DMarf*-RNAi in *Drosophila* was lethal and caused mitochondrial clumping in central nervous system and muscle tissues and depletion of mitochondria inside neuromuscular junctions.

Given that Mfn2 can regulate ER morphology (de Brito and Scorrano, 2008g), we investigated whether DMarf could play a similar role in *Drosophila*. DMarf downregulation resulted in alteration of ER architecture in muscle tissues. In control muscles, ER distributes itself along the sarcomeric bands. On the contrary, DMarf depletion caused alteration of this ER organization and resulted in punctae of ER randomly localized.

Therefore, both mitochondrial morphology and distribution defects and ER shape alteration may contribute to lethal phenotype of DMarf-RNAi.

Increasing mitochondrial fusion by expressing hMfns in *Drosophila*, caused mitochondrial clusterization in both neuronal cell bodies and muscles. A main difference between hMfn1 and hMfn2 expression emerged analyzing mitochondrial distribution in the nervous system. While expression of hMfn2 and hMfn2^{R94Q} resulted in absence of mitochondria in neuromuscular junction, hMfn1 NMJs still retained mitochondria, again suggesting that mitochondrial transport is not affected by Mfn1 and therefore supporting earlier results (Misko, 2010a). Interestingly, ER morphology was found altered only in muscle tissues expressing hMfn2^{R94Q}, an aspect that has never been investigated in Charcot-Marie-Tooth pathogenesis. In CMT2A, the amino acid residue at position 94 of the Mfn2 protein displays a mutation rate much higher than any other site. This mutant Mfn2 preserves mitochondrial fusion activity (Detmer, 2007); therefore, impairment of mitochondrial dynamics seemed not to play a major role in the onset of the disease, pointing to other functions of the protein. We showed that ER morphology is compromised after expression of hMfn2^{R94Q}; thus, alterations of the ER morphology may be one of the factors contributing to pathogenesis of CMT2A.

Given that DMarf was able to complement both Mfns in mitochondrial morphology and Mfn2 in ER shape regulation, we tried to understand to which extent hMfn1 and -2 could supply for mitofusin absence in *Drosophila*.

In vivo experiments showed that hMfn2, but not hMfn1 or hMfn2 ^{R94Q} rescued the lethal phenotype of DMarf knock-down in *Drosophila melanogaster* in either nervous system or muscle tissues. HMfn2 was also able to recover locomotory impairment of DMarf muscle-specific depleted flies. We therefore investigated whether hMfn2 was able to specifically recover mitochondrial and endoplasmic reticulum alteration caused by DMarf absence. Mitochondrial clusters were still present in neuronal cell bodies and muscle tissues in individuals simultaneously expressing *DMarf*-RNAi and hMfn2. Moreover, any of the three Mfns tested was able to restore mitochondrial localization in NMJs. Thus, although Mfn2 rescued DMarf depletion lethality, this could not be ascribed to the recovery of mitochondrial morphology and distribution.

The loss of ER organization in muscle tissues depleted of DMarf was instead fully rescued by expression of hMfn2, while hMfn1 and hMfn2 ^{R94Q} do not. In individuals simultaneously expressing DMarf and hMfn2, ER was well organized and showed the ordinary distribution along sarcomeric bands. We can therefore speculate that recovery of ER organization is the main factor contributing to the rescue by hMfn2.

The R94Q mutant failed to restore ER morphology in *Drosophila* individuals confirming previous data reported by our lab (de Brito, 2008a); additionally, concomitant expression of *DMarf*-RNAi and hMfn2 ^{R94Q} aggravate ER alteration. This phenotype was more severe than single expression of either of two transgenes, showing an additional effect of DMarf downregulation and expression of CMT2A hMfn2 mutation on ER disorganization.

Taken together, our findings support the idea that DMarf represents the evolutionary ancestor of mammalian Mfn2, sharing with this mitofusin not only the mitochondrial

fusion function, but also its role in the regulation of ER morphology. According to this view, *Drosophila* represents evolutionary turning point between one and two mitofusins.

6. Reference List

Alavi,M.V., Bette,S., Schimpf,S., Schuettauf,F., Schraermeyer,U., Wehrl,H.F., Ruttiger,L., Beck,S.C., Tonagel,F., Pichler,B.J., Knipper,M., Peters,T., Laufs,J., and Wissinger,B. (2007). A splice site mutation in the murine Opa1 gene features pathology of autosomal dominant optic atrophy. Brain *130*, 1029-1042.
Aldridge,A.C., Benson,L.P., Siegenthaler,M.M., Whigham,B.T., Stowers,R.S., and Hales,K.G. (2007). Roles for Drp1, a dynamin-related protein, and milton, a kinesin-associated protein, in mitochondrial segregation, unfurling and elongation during Drosophila spermatogenesis. Fly. (Austin.) *1*, 38-46.
Alexander,C., Votruba,M., Pesch,U.E., Thiselton,D.L., Mayer,S., Moore,A., Rodriguez,M., Kellner,U., Leo-Kottler,B., Auburger,G., Bhattacharya,S.S., and Wissinger,B. (2000). OPA1, encoding a dynamin-related GTPase, is mutated in autosomal dominant optic atrophy linked to chromosome 3q28. Nat. Genet. *26*, 211-215.
Alirol,E., James,D., Huber,D., Marchetto,A., Vergani,L., Martinou,J.C., and Scorrano,L. (2006). The mitochondrial fission protein hFis1 requires the endoplasmic reticulum gateway to induce apoptosis. Mol. Biol. Cell *17*, 4593-4605.
Amati-Bonneau,P., Pasquier,L., Lainey,E., Ferre,M., Odent,S., Malthiery,Y., Bonneau,D., and Reynier,P. (2005a). Sporadic optic atrophy due to synonymous codon change altering mRNA splicing of OPA1. Clin. Genet. *67*, 102-103.
Andrews,R.M., Griffiths,P.G., Johnson,M.A., and Turnbull,D.M. (1999). Histochemical localisation of mitochondrial enzyme activity in human optic nerve and retina. Br. J. Ophthalmol. *83*, 231-235.
Ardail,D., Gasnier,F., Lerme,F., Simonot,C., Louisot,P., and Gateau-Roesch,O. (1993). Involvement of mitochondrial contact sites in the subcellular compartmentalization of phospholipid biosynthetic enzymes. J. Biol Chem. *268*, 25985-25992.
Ardail,D., Lerme,F., and Louisot,P. (1991). Involvement of contact sites in phosphatidylserine import into liver mitochondria. J. Biol Chem. *266*, 7978-7981.
Arnoult,D., Grodet,A., Lee,Y.J., Estaquier,J., and Blackstone,C. (2005). Release of OPA1 during apoptosis participates in the rapid and complete release of cytochrome c and subsequent mitochondrial fragmentation. J. Biol. Chem. *280*, 35742-35750.
Bach,D. (2005a). Expression of Mfn2, the Charcot-Marie-Tooth neuropathy type 2A gene, in human skeletal muscle: effects of type 2 diabetes, obesity, weight loss, and the regulatory role of tumor necrosis factor alpha and interleukin-6.
Bach,D., Naon,D., Pich,S., Soriano,F.X., Vega,N., Rieusset,J., Laville,M., Guillet,C., Boirie,Y., Wallberg-Henriksson,H., Manco,M., Calvani,M., Castagneto,M., Palacin,M., Mingrone,G., Zierath,J.R., Vidal,H., and Zorzano,A. (2005a). Expression of Mfn2, the Charcot-Marie-Tooth neuropathy type 2A gene, in human skeletal muscle: effects of type 2 diabetes, obesity, weight loss, and the regulatory role of tumor necrosis factor alpha and interleukin-6. Diabetes *54*, 2685-2693.
Bach,D., Pich,S., Soriano,F.X., Vega,N., Baumgartner,B., Oriola,J., Daugaard,J.R., Lloberas,J., Camps,M., Zierath,J.R., Rabasa-Lhoret,R., Wallberg-Henriksson,H., Laville,M., Palacin,M., Vidal,H., Rivera,F., Brand,M., and Zorzano,A. (2003b). Mitofusin-2 determines mitochondrial network architecture and mitochondrial metabolism. A novel regulatory mechanism altered in obesity. J. Biol. Chem. *278*, 17190-17197.

Bakeeva,L.E., Chentsov,Y.S., Jasaitis,A.A., and Skulachev,V.P. (1972). The effect of oncotic pressure on heart muscle mitochondria. Biochim. Biophys. Acta *275*, 319-332.
Bakeeva,L.E., Chentsov,Y.S., and Skulachev,V.P. (1981). Ontogenesis of mitochondrial reticulum in rat diaphragm muscle. Eur. J. Cell Biol *25*, 175-181.
Barinaga,M. (1999). Mutant fruit flies respond to Lorenzo's oil. Science *284*, 1899, 1901.
Bereiter-Hahn,J. and Voth,M. (1994a). Dynamics of mitochondria in living cells: shape changes, dislocations, fusion, and fission of mitochondria. Microsc. Res. Tech. *27*, 198-219.
Boehning,D., Patterson,R.L., Sedaghat,L., Glebova,N.O., Kurosaki,T., and Snyder,S.H. (2003). Cytochrome c binds to inositol (1,4,5) trisphosphate receptors, amplifying calcium-dependent apoptosis. Nat Cell Biol *5*, 1051-1061.
Bracker,C.E. and Grove,S.N. (1971). Continuity between cytoplasmic endomembranes and outer mitochondrial membranes in fungi. Protoplasma *73*, 15-34.
Bristow,E.A., Griffiths,P.G., Andrews,R.M., Johnson,M.A., and Turnbull,D.M. (2002). The distribution of mitochondrial activity in relation to optic nerve structure. Arch. Ophthalmol. *120*, 791-796.
Campello,S., Lacalle,R.A., Bettella,M., Manes,S., Scorrano,L., and Viola,A. (2006). Orchestration of lymphocyte chemotaxis by mitochondrial dynamics. J. Exp. Med. *203*, 2879-2886.
Carelli,V., Ross-Cisneros,F.N., and Sadun,A.A. (2004). Mitochondrial dysfunction as a cause of optic neuropathies. Prog. Retin. Eye. Res. *23*, 53-89.
Cartoni,R., Leger,B., Hock,M.B., Praz,M., Crettenand,A., Pich,S., Ziltener,J.L., Luthi,F., Deriaz,O., Zorzano,A., Gobelet,C., Kralli,A., and Russell,A.P. (2005a). Mitofusins 1/2 and ERRalpha expression are increased in human skeletal muscle after physical exercise. J. Physiol *567*, 349-358.
Cereghetti,G.M., Stangherlin,A., Martins de,B.O., Chang,C.R., Blackstone,C., Bernardi,P., and Scorrano,L. (2008). Dephosphorylation by calcineurin regulates translocation of Drp1 to mitochondria. Proc. Natl. Acad. Sci. U. S. A *105*, 15803-15808.
Chen,H., Chomyn,A., and Chan,D.C. (2005). Disruption of fusion results in mitochondrial heterogeneity and dysfunction. J. Biol. Chem. *280*, 26185-26192.
Chen,H., Detmer,S.A., Ewald,A.J., Griffin,E.E., Fraser,S.E., and Chan,D.C. (2003e). Mitofusins Mfn1 and Mfn2 coordinately regulate mitochondrial fusion and are essential for embryonic development. J. Cell Biol. *160*, 189-200.
Chen,H., McCaffery,J.M., and Chan,D.C. (2007b). Mitochondrial fusion protects against neurodegeneration in the cerebellum. Cell. *130*, 548-562.
Chen,K.H., Guo,X., Ma,D., Guo,Y., Li,Q., Yang,D., Li,P., Qiu,X., Wen,S., Xiao,R.P., and Tang,J. (2004b). Dysregulation of HSG triggers vascular proliferative disorders. Nat. Cell Biol. *6*, 872-883.
Cipolat,S., de Brito,O.M., Dal Zilio,B., and Scorrano,L. (2004b). OPA1 requires mitofusin 1 to promote mitochondrial fusion. Proc. Natl. Acad. Sci. U. S. A *101*, 15927-15932.
Csordas,G., Renken,C., Varnai,P., Walter,L., Weaver,D., Buttle,K.F., Balla,T., Mannella,C.A., and Hajnoczky,G. (2006). Structural and functional features and significance of the physical linkage between ER and mitochondria. J. Cell Biol. *174*, 915-921.
Davies,V.J., Hollins,A.J., Piechota,M.J., Yip,W., Davies,J.R., White,K.E., Nicols,P.P., Boulton,M.E., and Votruba,M. (2007). Opa1 deficiency in a mouse model of

autosomal dominant optic atrophy impairs mitochondrial morphology, optic nerve structure and visual function. Hum. Mol. Genet. *16*, 1307-1318.
de Brito,O.M. and Scorrano,L. (2010). An intimate liaison: spatial organization of the endoplasmic reticulum-mitochondria relationship. EMBO J *29*, 2715-2723.
de Brito,O.M. and Scorrano,L. (2008g). Mitofusin 2 tethers endoplasmic reticulum to mitochondria. Nature *456*, 605-610.
Delettre,C., Lenaers,G., Griffoin,J.M., Gigarel,N., Lorenzo,C., Belenguer,P., Pelloquin,L., Grosgeorge,J., Turc-Carel,C., Perret,E., Astarie-Dequeker,C., Lasquellec,L., Arnaud,B., Ducommun,B., Kaplan,J., and Hamel,C.P. (2000). Nuclear gene OPA1, encoding a mitochondrial dynamin-related protein, is mutated in dominant optic atrophy. Nat. Genet. *26*, 207-210.
Deng,H., Dodson,M.W., Huang,H., and Guo,M. (2008c). The Parkinson's disease genes pink1 and parkin promote mitochondrial fission and/or inhibit fusion in Drosophila. Proc. Natl. Acad. Sci. U. S. A. *105*, 14503-14508.
Detmer,S.A. (2008). Hindlimb gait defects due to motor axon loss and reduced distal muscles in a transgenic mouse model of Charcot-Marie-Tooth type 2A.
Detmer,S.A. (2007). Complementation between mouse Mfn1 and Mfn2 protects mitochondrial fusion defects caused by CMT2A disease mutations.
Dimmer,K.S. and Scorrano,L. (2006). (De)constructing mitochondria: what for? Physiology. (Bethesda.) *21*, 233-241.
Drummond,R.M., Mix,T.C., Tuft,R.A., Walsh,J.V., Jr., and Fay,F.S. (2000). Mitochondrial Ca2+ homeostasis during Ca2+ influx and Ca2+ release in gastric myocytes from Bufo marinus. J. Physiol *522 Pt 3*, 375-390.
Egner,A., Jakobs,S., and Hell,S.W. (2002). Fast 100-nm resolution three-dimensional microscope reveals structural plasticity of mitochondria in live yeast. Proc. Natl. Acad. Sci. U. S. A *99*, 3370-3375.
Eura,Y., Ishihara,N., Yokota,S., and Mihara,K. (2003). Two mitofusin proteins, mammalian homologues of FZO, with distinct functions are both required for mitochondrial fusion. J. Biochem. (Tokyo) *134*, 333-344.
Ferre,M., Amati-Bonneau,P., Tourmen,Y., Malthiery,Y., and Reynier,P. (2005b). eOPA1: an online database for OPA1 mutations. Hum. Mutat. *25*, 423-428.
Filippin,L., Magalhaes,P.J., Di Benedetto,G., Colella,M., and Pozzan,T. (2003). Stable interactions between mitochondria and endoplasmic reticulum allow rapid accumulation of calcium in a subpopulation of mitochondria. J. Biol. Chem. *278*, 39224-39234.
Frezza,C., Cipolat,S., Martins,d.B., Micaroni,M., Beznoussenko,G.V., Rudka,T., Bartoli,D., Polishuck,R.S., Danial,N.N., De Strooper,B., and Scorrano,L. (2006a). OPA1 Controls Apoptotic Cristae Remodeling Independently from Mitochondrial Fusion. Cell *126*, 177-189.
Frieden,M., James,D., Castelbou,C., Danckaert,A., Martinou,J.C., and Demaurex,N. (2004). Ca^{2+} homeostasis during mitochondrial fragmentation and perinuclear clustering induced by hFis1. J. Biol. Chem. *279*, 22704-22714.
Gaigg,B., Simbeni,R., Hrastnik,C., Paltauf,F., and Daum,G. (1995). Characterization of a microsomal subfraction associated with mitochondria of the yeast, Saccharomyces cerevisiae. Involvement in synthesis and import of phospholipids into mitochondria. Biochim. Biophys. Acta *1234*, 214-220.
Gallop,J.L., Jao,C.C., Kent,H.M., Butler,P.J., Evans,P.R., Langen,R., and McMahon,H.T. (2006a). Mechanism of endophilin N-BAR domain-mediated membrane curvature. EMBO. J. *25*, 2898-2910.
Gallop,J.L. and McMahon,H.T. (2005). BAR domains and membrane curvature: bringing your curves to the BAR. Biochem. Soc. Symp. 223-231.

Gandre-Babbe,S. and van der Bliek,A.M. (2008). The novel tail-anchored membrane protein Mff controls mitochondrial and peroxisomal fission in mammalian cells. Mol. Biol. Cell *19*, 2402-2412.
Garnier,A., Fortin,D., Zoll,J., N'Guessan,B., Mettauer,B., Lampert,E., Veksler,V., and Ventura-Clapier,R. (2005). Coordinated changes in mitochondrial function and biogenesis in healthy and diseased human skeletal muscle. FASEB J. *19*, 43-52.
Griparic,L., van der Wel,N.N., Orozco,I.J., Peters,P.J., and van der Bliek,A.M. (2004a). Loss of the intermembrane space protein Mgm1/OPA1 induces swelling and localized constrictions along the lengths of mitochondria. J. Biol. Chem. *279*, 18792-18798.
Hales,K.G. and Fuller,M.T. (1997a). Developmentally regulated mitochondrial fusion mediated by a conserved, novel, predicted GTPase. Cell *90*, 121-129.
Hermann,G.J., Thatcher,J.W., Mills,J.P., Hales,K.G., Fuller,M.T., Nunnari,J., and Shaw,J.M. (1998). Mitochondrial fusion in yeast requires the transmembrane GTPase Fzo1p. J. Cell Biol. *143*, 359-373.
Hinshaw,J.E. (1999a). Dynamin spirals. Curr. Opin. Struct. Biol *9*, 260-267.
Hwa,J.J., Hiller,M.A., Fuller,M.T., and Santel,A. (2002). Differential expression of the Drosophila mitofusin genes fuzzy onions (fzo) and dmfn. Mech Dev *116*.
Ishihara,N., Eura,Y., and Mihara,K. (2004a). Mitofusin 1 and 2 play distinct roles in mitochondrial fusion reactions via GTPase activity. J. Cell Sci. *117*, 6535-6546.
James,D.I., Parone,P.A., Mattenberger,Y., and Martinou,J.C. (2003). hFis1, a novel component of the mammalian mitochondrial fission machinery. J. Biol. Chem. *278*, 36373-36379.
Jones,B.A. and Fangman,W.L. (1992b). Mitochondrial DNA maintenance in yeast requires a protein containing a region related to the GTP-binding domain of dynamin. Genes. Dev. *6*, 380-389.
Jouaville,L.S., Pinton,P., Bastianutto,C., Rutter,G.A., and Rizzuto,R. (1999). Regulation of mitochondrial ATP synthesis by calcium: evidence for a long-term metabolic priming. Proc. Natl. Acad. Sci. U. S. A. *96*, 13807-13812.
Karbowski,M., Jeong,S.Y., and Youle,R.J. (2004). Endophilin B1 is required for the maintenance of mitochondrial morphology. J. Cell Biol. *166*, 1027-1039.
Karbowski,M., Lee,Y.J., Gaume,B., Jeong,S.Y., Frank,S., Nechushtan,A., Santel,A., Fuller,M., Smith,C.L., and Youle,R.J. (2002). Spatial and temporal association of Bax with mitochondrial fission sites, Drp1, and Mfn2 during apoptosis. J. Cell Biol. *159*, 931-938.
Karbowski,M., Norris,K.L., Cleland,M.M., Jeong,S.Y., and Youle,R.J. (2006). Role of Bax and Bak in mitochondrial morphogenesis. Nature *443*, 658-662.
Kay,B.K., Williamson,M.P., and Sudol,M. (2000). The importance of being proline: the interaction of proline-rich motifs in signaling proteins with their cognate domains. FASEB. J. *14*, 231-241.
Kijima,K., Numakura,C., Izumino,H., Umetsu,K., Nezu,A., Shiiki,T., Ogawa,M., Ishizaki,Y., Kitamura,T., Shozawa,Y., and Hayasaka,K. (2005). Mitochondrial GTPase mitofusin 2 mutation in Charcot-Marie-Tooth neuropathy type 2A. Hum. Genet. *116*, 23-27.
Kjer,B., Eiberg,H., Kjer,P., and Rosenberg,T. (1996). Dominant optic atrophy mapped to chromosome 3q region. II. Clinical and epidemiological aspects. Acta. Ophthalmol. Scand. *74*, 3-7.
Koch,A., Schneider,G., Luers,G.H., and Schrader,M. (2004). Peroxisome elongation and constriction but not fission can occur independently of dynamin-like protein 1. J. Cell Sci. *117*, 3995-4006.

Koch,A., Thiemann,M., Grabenbauer,M., Yoon,Y., McNiven,M.A., and Schrader,M. (2003). Dynamin-like protein 1 is involved in peroxisomal fission. J. Biol. Chem. *278*, 8597-8605.
Koshiba,T., Detmer,S.A., Kaiser,J.T., Chen,H., McCaffery,J.M., and Chan,D.C. (2004a). Structural basis of mitochondrial tethering by mitofusin complexes. Science *305*, 858-862.
Labrousse,A.M., Zappaterra,M.D., Rube,D.A., and van der Bliek,A.M. (1999). C. elegans dynamin-related protein DRP-1 controls severing of the mitochondrial outer membrane. Mol. Cell *4*, 815-826.
Lawson,V.H., Graham,B.V., and Flanigan,K.M. (2005a). Clinical and electrophysiologic features of CMT2A with mutations in the mitofusin 2 gene. Neurology. *65*, 197-204.
Lee,Y.J., Jeong,S.Y., Karbowski,M., Smith,C.L., and Youle,R.J. (2004b). Roles of the mammalian mitochondrial fission and fusion mediators Fis1, Drp1, and Opa1 in apoptosis. Mol. Biol. Cell *15*, 5001-5011.
Lee,Y.J., Jeong,S.Y., Karbowski,M., Smith,C.L., and Youle,R.J. (2004a). Roles of the mammalian mitochondrial fission and fusion mediators Fis1, Drp1, and Opa1 in apoptosis. Mol. Biol. Cell *15*, 5001-5011.
Legros,F., Lombes,A., Frachon,P., and Rojo,M. (2002). Mitochondrial fusion in human cells is efficient, requires the inner membrane potential, and is mediated by mitofusins. Mol Biol Cell *13*, 4343-4354.
Lewis,J.A. and Tata,J.R. (1973). Heterogeneous distribution of glucose 6-phosphatase in rat liver microsomal fractions as shown by adaptation of a cytochemical technique. Biochem. J. *134*, 69-78.
Li,X. and Gould,S.J. (2003). The dynamin-like GTPase DLP1 is essential for peroxisome division and is recruited to peroxisomes in part by PEX11. J. Biol. Chem. *278*, 17012-17020.
Li,Z., Okamoto,K., Hayashi,Y., and Sheng,M. (2004b). The importance of dendritic mitochondria in the morphogenesis and plasticity of spines and synapses. Cell *119*, 873-887.
Liesa,M., Palacin,M., and Zorzano,A. (2009). Mitochondrial dynamics in mammalian health and disease. Physiol Rev. *89*, 799-845.
Lodi,R., Tonon,C., Valentino,M.L., Iotti,S., Clementi,V., Malucelli,E., Barboni,P., Longanesi,L., Schimpf,S., Wissinger,B., Baruzzi,A., Barbiroli,B., and Carelli,V. (2004). Deficit of in vivo mitochondrial ATP production in OPA1-related dominant optic atrophy. Ann. Neurol. *56*, 719-723.
Madesh,M. and Hajnoczky,G. (2001). VDAC-dependent permeabilization of the outer mitochondrial membrane by superoxide induces rapid and massive cytochrome c release. J. Cell Biol. *155*, 1003-1015.
Mannella,C.A. (2000). Introduction: our changing views of mitochondria. J. Bioenerg. Biomembr. *32*, 1-4.
Marchbank,N.J., Craig,J.E., Leek,J.P., Toohey,M., Churchill,A.J., Markham,A.F., Mackey,D.A., Toomes,C., and Inglehearn,C.F. (2002). Deletion of the OPA1 gene in a dominant optic atrophy family: evidence that haploinsufficiency is the cause of disease. J. Med. Genet. *39*, e47.
Meeusen,S., McCaffery,J.M., and Nunnari,J. (2004). Mitochondrial fusion intermediates revealed in vitro. Science. *305*, 1747-1752.
Mendes,C.C., Gomes,D.A., Thompson,M., Souto,N.C., Goes,T.S., Goes,A.M., Rodrigues,M.A., Gomez,M.V., Nathanson,M.H., and Leite,M.F. (2005). The type III inositol 1,4,5-trisphosphate receptor preferentially transmits apoptotic Ca2+ signals into mitochondria. J. Biol Chem. *280*, 40892-40900.

Mingrone,G., Manco,M., Calvani,M., Castagneto,M., Naon,D., and Zorzano,A. (2005). Could the low level of expression of the gene encoding skeletal muscle mitofusin-2 account for the metabolic inflexibility of obesity? Diabetologia *48*, 2108-2114.
Misaka,T., Miyashita,T., and Kubo,Y. (2002). Primary structure of a dynamin-related mouse mitochondrial GTPase and its distribution in brain, subcellular localization, and effect on mitochondrial morphology. J. Biol. Chem. *277*, 15834-15842.
Misko,A. (2010b). Mitofusin 2 is necessary for transport of axonal mitochondria and interacts with the Miro/Milton complex.
Neuspiel,M., Zunino,R., Gangaraju,S., Rippstein,P., and McBride,H.M. (2005). Activated Mfn2 signals mitochondrial fusion, interferes with Bax activation and reduces susceptibility to radical induced depolarization. J. Biol. Chem. *280*, 25060-25070.
Oakley,M.G. and Hollenbeck,J.J. (2001). The design of antiparallel coiled coils. Curr. Opin. Struct. Biol *11*, 450-457.
Olichon,A., Baricault,L., Gas,N., Guillou,E., Valette,A., Belenguer,P., and Lenaers,G. (2003b). Loss of OPA1 perturbates the mitochondrial inner membrane structure and integrity, leading to cytochrome c release and apoptosis. J. Biol. Chem. *278*, 7743-7746.
Palade,G.E. (1952). The fine structure of mitochondria. Anat. Rec. *114*, 427-451.
Park,J., Lee,G., and Chung,J. (2009). The PINK1-Parkin pathway is involved in the regulation of mitochondrial remodeling process. Biochem. Biophys. Res. Commun. *378*, 518-523.
Pawlikowska,P., Gajkowska,B., and Orzechowski,A. (2007). Mitofusin 2 (Mfn2): a key player in insulin-dependent myogenesis in vitro. Cell Tissue Res. *327*, 571-581.
Pelloquin,L., Belenguer,P., Menon,Y., Gas,N., and Ducommun,B. (1999). Fission yeast Msp1 is a mitochondrial dynamin-related protein. J. Cell. Sci. *112 (Pt 22)*, 4151-4161.
Pesch,U.E., Leo-Kottler,B., Mayer,S., Jurklies,B., Kellner,U., Apfelstedt-Sylla,E., Zrenner,E., Alexander,C., and Wissinger,B. (2001). OPA1 mutations in patients with autosomal dominant optic atrophy and evidence for semi-dominant inheritance. Hum. Mol Genet. *10*, 1359-1368.
Petit,P.X., Goubern,M., Diolez,P., Susin,S.A., Zamzami,N., and Kroemer,G. (1998). Disruption of the outer mitochondrial membrane as a result of large amplitude swelling: the impact of irreversible permeability transition. FEBS Lett. *426*, 111-116.
Pich,S., Bach,D., Briones,P., Liesa,M., Camps,M., Testar,X., Palacin,M., and Zorzano,A. (2005). The Charcot-Marie-Tooth type 2A gene product, Mfn2, up-regulates fuel oxidation through expression of OXPHOS system. Hum. Mol. Genet. *14*, 1405-1415.
Pitts,K.R., Yoon,Y., Krueger,E.W., and McNiven,M.A. (1999). The dynamin-like protein DLP1 is essential for normal distribution and morphology of the endoplasmic reticulum and mitochondria in mammalian cells. Mol Biol Cell *10*, 4403-4417.
Pizzo,P. and Pozzan,T. (2007). Mitochondria-endoplasmic reticulum choreography: structure and signaling dynamics. Trends Cell Biol. *17*, 511-517.
Poole,A.C., Thomas,R.E., Andrews,L.A., McBride,H.M., Whitworth,A.J., and Pallanck,L.J. (2008). The PINK1/Parkin pathway regulates mitochondrial morphology. Proc. Natl. Acad. Sci. U. S. A *105*, 1638-1643.
Rapaport,D., Brunner,M., Neupert,W., and Westermann,B. (1998). Fzo1p is a mitochondrial outer membrane protein essential for the biogenesis of functional mitochondria in Saccharomyces cerevisiae. J. Biol. Chem. *273*, 20150-20155.

Rapizzi,E., Pinton,P., Szabadkai,G., Wieckowski,M.R., Vandecasteele,G., Baird,G., Tuft,R.A., Fogarty,K.E., and Rizzuto,R. (2002). Recombinant expression of the voltage-dependent anion channel enhances the transfer of Ca2+ microdomains to mitochondria. J Cell Biol *159*, 613-624.
Reiter,L.T., Potocki,L., Chien,S., Gribskov,M., and Bier,E. (2001). A systematic analysis of human disease-associated gene sequences in Drosophila melanogaster. Genome Res. *11*, 1114-1125.
Rizzuto,R., Bernardi,P., and Pozzan,T. (2000). Mitochondria as all-round players of the calcium game. J. Physiol. *529 Pt 1:37-47.*, 37-47.
Rizzuto,R., Brini,M., Murgia,M., and Pozzan,T. (1993). Microdomains with high Ca2+ close to IP3-sensitive channels that are sensed by neighboring mitochondria. Science *262*, 744-747.
Rizzuto,R., Pinton,P., Carrington,W., Fay,F.S., Fogarty,K.E., Lifshitz,L.M., Tuft,R.A., and Pozzan,T. (1998a). Close contacts with the endoplasmic reticulum as determinants of mitochondrial Ca2+ responses. Science *280*, 1763-1766.
Rojo,M., Legros,F., Chateau,D., and Lombes,A. (2002a). Membrane topology and mitochondrial targeting of mitofusins, ubiquitous mammalian homologs of the transmembrane GTPase Fzo. J. Cell Sci. *115*, 1663-1674.
Rong,Y.S. and Golic,K.G. (2000). Gene targeting by homologous recombination in Drosophila. Science *288*, 2013-2018.
Ruby,J.R., Dyer,R.F., and Skalko,R.G. (1969). Continuities between mitochondria and endoplasmic reticulum in the mammalian ovary. Z. Zellforsch. Mikrosk. Anat. *97*, 30-37.
Rusinol,A.E., Cui,Z., Chen,M.H., and Vance,J.E. (1994). A unique mitochondria-associated membrane fraction from rat liver has a high capacity for lipid synthesis and contains pre-Golgi secretory proteins including nascent lipoproteins. J Biol Chem. *269*, 27494-27502.
Santel,A. (2006). Get the balance right: mitofusins roles in health and disease. Biochim. Biophys. Acta *1763*, 490-499.
Santel,A., Frank,S., Gaume,B., Herrler,M., Youle,R.J., and Fuller,M.T. (2003). Mitofusin-1 protein is a generally expressed mediator of mitochondrial fusion in mammalian cells. J. Cell Sci. *116*, 2763-2774.
Santel,A. and Fuller,M.T. (2001). Control of mitochondrial morphology by a human mitofusin. J. Cell Sci. *114*, 867-874.
Satoh,M., Hamamoto,T., Seo,N., Kagawa,Y., and Endo,H. (2003). Differential sublocalization of the dynamin-related protein OPA1 isoforms in mitochondria. Biochem. Biophys. Res. Commun. *300*, 482-493.
Schmidt,A., Wolde,M., Thiele,C., Fest,W., Kratzin,H., Podtelejnikov,A.V., Witke,W., Huttner,W.B., and Soling,H.D. (1999b). Endophilin I mediates synaptic vesicle formation by transfer of arachidonate to lysophosphatidic acid. Nature *401*, 133-141.
Shahrestani,P., Leung,H.T., Le,P.K., Pak,W.L., Tse,S., Ocorr,K., and Huang,T. (2009). Heterozygous mutation of Drosophila Opa1 causes the development of multiple organ abnormalities in an age-dependent and organ-specific manner. PLoS. ONE. *4*, e6867.
Simmen,T., Aslan,J.E., Blagoveshchenskaya,A.D., Thomas,L., Wan,L., Xiang,Y., Feliciangeli,S.F., Hung,C.H., Crump,C.M., and Thomas,G. (2005). PACS-2 controls endoplasmic reticulum-mitochondria communication and Bid-mediated apoptosis. EMBO J *24*, 717-729.
Smirnova,E., Griparic,L., Shurland,D.L., and van der Bliek,A.M. (2001). Dynamin-related protein Drp1 is required for mitochondrial division in mammalian cells. Mol. Biol. Cell *12*, 2245-2256.

Spinazzi,M., Cazzola,S., Bortolozzi,M., Baracca,A., Loro,E., Casarin,A., Solaini,G., Sgarbi,G., Casalena,G., Cenacchi,G., Malena,A., Frezza,C., Carrara,F., Angelini,C., Scorrano,L., Salviati,L., and Vergani,L. (2008). A novel deletion in the GTPase domain of OPA1 causes defects in mitochondrial morphology and distribution, but not in function. Hum. Mol. Genet. *17*, 3291-3302.
Stojanovski,D., Koutsopoulos,O.S., Okamoto,K., and Ryan,M.T. (2004). Levels of human Fis1 at the mitochondrial outer membrane regulate mitochondrial morphology. J. Cell Sci. *117*, 1201-1210.
Sugioka,R., Shimizu,S., and Tsujimoto,Y. (2004). Fzo1, a protein involved in mitochondrial fusion, inhibits apoptosis. J. Biol. Chem. *279*, 52726-52734.
Suzuki,M., Jeong,S.Y., Karbowski,M., Youle,R.J., and Tjandra,N. (2003). The solution structure of human mitochondria fission protein Fis1 reveals a novel TPR-like helix bundle. J. Mol. Biol. *334*, 445-458.
Szabadkai,G., Bianchi,K., Varnai,P., De,S.D., Wieckowski,M.R., Cavagna,D., Nagy,A.I., Balla,T., and Rizzuto,R. (2006). Chaperone-mediated coupling of endoplasmic reticulum and mitochondrial Ca2+ channels. J. Cell Biol. *175*, 901-911.
Szabadkai,G., Simoni,A.M., Chami,M., Wieckowski,M.R., Youle,R.J., and Rizzuto,R. (2004). Drp-1-Dependent Division of the Mitochondrial Network Blocks Intraorganellar Ca(2+) Waves and Protects against Ca(2+)-Mediated Apoptosis. Mol. Cell *16*, 59-68.
Thomson,M. (2003). Does cholesterol use the mitochondrial contact site as a conduit to the steroidogenic pathway? Bioessays *25*, 252-258.
Tondera,D., Czauderna,F., Paulick,K., Schwarzer,R., Kaufmann,J., and Santel,A. (2005). The mitochondrial protein MTP18 contributes to mitochondrial fission in mammalian cells. J Cell Sci *118*, 3049-3059.
Tondera,D., Santel,A., Schwarzer,R., Dames,S., Giese,K., Klippel,A., and Kaufmann,J. (2004). Knockdown of MTP18, a novel phosphatidylinositol 3-kinase-dependent protein, affects mitochondrial morphology and induces apoptosis. J Biol Chem *279*, 31544-31555.
Vance,J.E. (1990). Phospholipid synthesis in a membrane fraction associated with mitochondria. J Biol Chem. *265*, 7248-7256.
Verstreken,P., Ly,C.V., Venken,K.J., Koh,T.W., Zhou,Y., and Bellen,H.J. (2005). Synaptic mitochondria are critical for mobilization of reserve pool vesicles at Drosophila neuromuscular junctions. Neuron. *47*, 365-378.
Vettori,A., Bergamin,G., Moro,E., Vazza,G., Polo,G., Tiso,N., Argenton,F., and Mostacciuolo,M.L. (2011). Developmental defects and neuromuscular alterations due to mitofusin 2 gene (MFN2) silencing in zebrafish: a new model for Charcot-Marie-Tooth type 2A neuropathy. Neuromuscul. Disord. *21*, 58-67.
Voehringer,D.W., Hirschberg,D.L., Xiao,J., Lu,Q., Roederer,M., Lock,C.B., Herzenberg,L.A., Steinman,L., and Herzenberg,L.A. (2000). Gene microarray identification of redox and mitochondrial elements that control resistance or sensitivity to apoptosis. Proc. Natl. Acad. Sci. U. S. A *97*, 2680-2685.
Voelker,D.R. (2003). New perspectives on the regulation of intermembrane glycerophospholipid traffic. J. Lipid Res. *44*, 441-449.
Votruba,M., Moore,A.T., and Bhattacharya,S.S. (1997a). Genetic refinement of dominant optic atrophy (OPA1) locus to within a 2 cM interval of chromosome 3q. J. Med. Genet. *34*, 117-121.
Wang,H.J. (2000). Calcium regulates the association between mitochondria and a smooth subdomain of the endoplasmic reticulum.

Wang,L., Dong,J., Cull,G., Fortune,B., and Cioffi,G.A. (2003). Varicosities of intraretinal ganglion cell axons in human and nonhuman primates. Invest. Ophthalmol. Vis. Sci. *44*, 2-9.
Waterham,H.R., Koster,J., van Roermund,C.W., Mooyer,P.A., Wanders,R.J., and Leonard,J.V. (2007). A lethal defect of mitochondrial and peroxisomal fission. N. Engl. J. Med. *356*, 1736-1741.
White-Cooper,H., Schafer,M.A., Alphey,L.S., and Fuller,M.T. (1998). Transcriptional and post-transcriptional control mechanisms coordinate the onset of spermatid differentiation with meiosis I in Drosophila. Development *125*, 125-134.
Wong,W. and Scott,J.D. (2004). AKAP signalling complexes: focal points in space and time. Nat Rev Mol Cell Biol *5*.
Yang,Y., Ouyang,Y., Yang,L., Beal,M.F., McQuibban,A., Vogel,H., and Lu,B. (2008). Pink1 regulates mitochondrial dynamics through interaction with the fission/fusion machinery. Proc. Natl. Acad. Sci. U. S. A. *105*, 7070-7075.
Yoon,Y., Krueger,E.W., Oswald,B.J., and McNiven,M.A. (2003). The mitochondrial protein hFis1 regulates mitochondrial fission in mammalian cells through an interaction with the dynamin-like protein DLP1. Mol. Cell Biol. *23*, 5409-5420.
Youn,H.D., Sun,L., Prywes,R., and Liu,J.O. (1999). Apoptosis of T cells mediated by Ca2+-induced release of the transcription factor MEF2. Science *286*, 790-793.
Ziviani,E., Tao,R.N., and Whitworth,A.J. (2010). Drosophila parkin requires PINK1 for mitochondrial translocation and ubiquitinates mitofusin. Proc. Natl. Acad. Sci. U. S. A *107*, 5018-5023.
Zuchner,S., Mersiyanova,I.V., Muglia,M., Bissar-Tadmouri,N., Rochelle,J., Dadali,E.L., Zappia,M., Nelis,E., Patitucci,A., Senderek,J., Parman,Y., Evgrafov,O., Jonghe,P.D., Takahashi,Y., Tsuji,S., Pericak-Vance,M.A., Quattrone,A., Battologlu,E., Polyakov,A.V., Timmerman,V., Schroder,J.M., and Vance,J.M. (2004b). Mutations in the mitochondrial GTPase mitofusin 2 cause Charcot-Marie-Tooth neuropathy type 2A. Nat. Genet. *36*, 449-451.
Zuchner,S., Mersiyanova,I.V., Muglia,M., Bissar-Tadmouri,N., Rochelle,J., Dadali,E.L., Zappia,M., Nelis,E., Patitucci,A., Senderek,J., Parman,Y., Evgrafov,O., Jonghe,P.D., Takahashi,Y., Tsuji,S., Pericak-Vance,M.A., Quattrone,A., Battologlu,E., Polyakov,A.V., Timmerman,V., Schroder,J.M., and Vance,J.M. (2004d). Mutations in the mitochondrial GTPase mitofusin 2 cause Charcot-Marie-Tooth neuropathy type 2A. Nat. Genet. *36*, 449-451.
Zuchner,S. and Vance,J.M. (2006). Mechanisms of disease: a molecular genetic update on hereditary axonal neuropathies. Nat. Clin. Pract. Neurol. *2*, 45-53.